2-23-2021 10:30 AM

Motion Intention Estimation using sEMG-ACC Sensor Fusion

Jose Alejandro Lopez, *The University of Western Ontario*

Supervisor: Ana Luisa Trejos, *The University of Western Ontario*

A thesis submitted in partial fulfillment of the requirements for the Master of Engineering Science degree in Biomedical Engineering

Motion Intention Estimation using sEMG-ACC Sensor Fusion

José Alejandro López Molina

M.E.Sc. Thesis, 2020

School of Biomedical Engineering

The University of Western Ontario

Abstract

Musculoskeletal injuries can severely impact the ability to produce and control body motion. In order to regain function, rehabilitation is often required. Wearable smart devices are currently under development to provide therapy and assistance for people with impaired arm function. Electromyography (EMG) signals are used as an input to pattern recognition systems to determine intended movements. However, there is a gap between the accuracy of pattern recognition systems in constrained laboratory settings, and usability when used for detecting dynamic unconstrained movements. Motion factors such as limb position, interaction force, and velocity, are known to have a negative impact on the pattern recognition. A possible solution lies in the use of data from other sensors along with the EMG signals, such as signals from accelerometers (ACC), in the training and use of classifiers in order to improve classification accuracy. The objectives of this study were to quantify the impact of motion factors on ACC signals, and to use these ACC signals along with EMG signals for classifying categories of motion factors. To address these objectives, a dataset containing EMG and ACC signals while individuals performed unconstrained arm motions was studied. Analyses of the EMG and accelerometer signals and their use in training classification models to predict characteristics of intended motion were completed.

The results show that the combination of EMG and ACC provided a statistically significant improvement in the performance of motion intention detection. Prediction of movement (stationary and movement) ranged from 75.80 to 91.01% during elbow flexion–extension motion.

Future work should expand on motion factors and EMG–ACC sensor fusion to identify interactions between a person and the environment, in order to guide tuning of control models working towards controlling wearable mechatronic devices during dynamic movements.

Keywords: wearable mechatronic devices,motion classification, motion characteristics, dynamic movements, interaction forces, arm position, joint velocity, electromyography, sensor fusion.

Lay Summary

Injuries to the bones, muscles and/or connective tissues of the body can severely limit the ability to perform daily life activities, such as dressing or pouring water into a glass. Rehabilitation is often required to recover from these injuries. Technology has been under development to provide solutions that help with the treatment. Wearable robotic devices offer a potential tool for providing physical therapy to the arm without the need of going to the clinic. These devices are controlled by measuring the electrical signals of the muscles in order to predict the subject's intention to move the arm. However, these devices suffer from the limitation of not performing well when used during complex movements. Several factors, including the speed of the movement and external forces (for example, the increased weight when carrying a bag) decrease the capability to predict movement intention. One important suggestion is to incorporate signals from other sensors, such as accelerometers (devices that measure acceleration), that may provide additional information for the prediction. This work provides an analysis of accelerometer signals obtained during complex arm movements and demonstrates an increased prediction rate when using both muscle activity and acceleration information to predict arm movement intention. Motion intention could be distinguished between stationary and moving during arm movement with less than 10% error. This could be used to further improve the control of a wearable robotic device.

Acknowledgements

First and foremost, I would like to congratulate Dr. Ana Luisa Trejos. I feel extremely honoured to have had the opportunity to work under her supervision. She has provided me with constant support and guidance, and it is because of her that I have been able to do a Masters degree. Thank you for inviting me to join the Wearable Biomechatronics Laboratory. There I have found not just great colleagues, but also good friends. I am hoping to stay in touch. Big thanks to each member that is, and has been, part of this wonderful and talented team. Special thanks to Jake and Memo for their advice with statistics and machine learning topics. Another person I would also like to thank in particular is Taylor Stanbury, for allowing me to use part of her research material, as I was not able to perform any data collection during the current pandemic situation.

Next, I must express my gratitude to my family for their constant love and support. Thanks to my mother, Dr. María Elena Molina Ayala, for encouraging me to pursue a Masters degree. Thanks to my dad, José López, my grandma María Elena, aunt Elizabeth, aunt Veronica and uncle Luis Fernando, and my cousins María Fernanda and Mariana. I love you all so much and I dedicate this milestone to you. Finally, I am very thankful with all the kind friends that I have met at Western University. I will definitely miss going to Global Cafe or the Grad Club with you.

This work was supported by the Natural Sciences and Engineering Research Council (NSERC) of Canada under grant RGPIN-2014-03815; by the Canadian Foundation for Innovation (CFI); and by the Ontario Research Fund (ORF). Thanks to the Mexican National Council of Science and Technology (CONACYT) for funding my studies.

Contents

List of Figures

List of Tables

Nomenclature and Acronyms

Acronyms

ACC	Accelerometer
AD	Anterior Deltoid
ADL	Activity of Daily Living
ANN	Artificial Neural Network
AR	Auto-Regressive
BBL	Biceps Brachii Long Head
BBS	Biceps Brachii Short Head
BRA	Brachialis
BRD	Brachioradialis
DT	Decision Tree
ECR	Extensor Carpi Radialis
ECRB	Extensor Carpi Radialis Brevis
ECU	Extensor Carpi Ulnaris
EMG	Electromyography
FCR	Flexor Carpi Radialis
FCU	Flexor Carpi Ulnaris
FIM	Functional Impedance Measure

ISPI	Infraspinatus
K-NN	K-Nearest Neighbours
LD	Lateral Deltoid
LDA	Linear Discriminant Analysis
LOSO	Leave-One-Subject-Out
MAV	Mean Absolute Value
MDF	Median Frequency
MNF	Mean Frequency
MSK	Musculoskeletal
MUAP	Motor Unit Action Potential
MVC	Maximum Voluntary Contraction
PCA	Principal Component Analysis
PD	Posterior Deltoid
PSR	Power Spectrum Ratio
QDA	Quadratic Discriminant Analysis
RMS	Root Mean Square
ROM	Range of Motion
sEMG	Surface Electromyography
SMA	Signal Magnitude Area
SMV	Signal Vector Magnitude
SPSS	Statistical Package for Social Sciences
SSC	Slope Sign Changes
SVM	Support Vector Machine
TRILAT	Triceps Brachii Lateral Head
TRILO	Triceps Brachii Long Head

TRIM	Triceps Brachii Medial Head
VRE	Virtual Reality Environment
WAMP	Wilson Amplitude
WL	Waveform Length
WMFT	Wolf Motor Function Test
ZC	Zero Crossings

Variables

a	Acceleration signal
a_k	Autoregressive coefficient
E1	Frequency constant 1
E2	Frequency constant 2
f	Frequency
F1	Force 1
F2	Force 2
F3	Force 3
i	Signal segment
j	Frequency bin
l	Integral limit
M	Length of the frequency bin
n	Order of the AR model
N	Length of the signal
P	Power spectrum
P1	Position 1
P2	Position 2

P3	Position 3
V1	Velocity 1
V2	Velocity 2
V3	Velocity 3
w_i	White noise
x	EMG Signal

Units

Hz	Hertz
kg	Kilograms
mm	Millimetres
ms	Milliseconds
N	Newton
s	Seconds
°	Degrees

Chapter 1

Introduction

Musculoskeletal (MSK) conditions are disorders or injuries that affect bones, joints, muscles and/or connective tissues of the body. They negatively impact the ability to produce and control motion. These conditions are a leading cause of long-term disability, affecting over 1.2 billion people worldwide [1] and 11 million Canadians annually [2]. In order to recover, assistance is needed. Professional care may be required from a few weeks up to years. Consequently, MSK conditions cause long-term physical, psychological and financial burdens [3]. MSK disorders are estimated to cost the Canadian economy over $22 billion per year, and MSK injuries contribute to an additional $15 billion each year [2]. Direct costs including health professional visits, drugs and other expenditures related to rehabilitation represent 20% of the total cost while over 80% of the cost is due to absence from work and loss of productivity. Moreover, with obesity anticipated to rise over the coming decade and an aging population, the incidence of MSK conditions is expected to increase worldwide [4]. By 2031, an estimated 15 million Canadians will be affected annually by MSK conditions [2]. Innovative strategies must be developed to restrict the impact of these conditions on the economy, health care and social care systems. In this regard, technological advancements can assist in rehabilitation, working towards the goal of improved mobility and quality of life.

1.1 Motivation

When this type of accidents happen, the patient can recover with the aid of rehabilitative therapy, a process that allows the patient to improve muscle strength and relearn the best possible use of their limbs [5]. Conventional rehabilitative therapy involves a series of repetitive exercises executed by the patient with the aid of a therapist, who may manually assist the patient to move or provide resistance during the training [6]. When the patient is not in the therapy session, orthotic braces are often used to progressively increase joint range of motion and prevent stiffness that occurs after trauma, as well as prevent further injury [7]. However, poor adherence to rehabilitation programs, including not attending the therapy sessions or not performing home-based exercises, poses a barrier to health improvement [8]. Technology has been under development to provide solutions that aid with the treatment of MSK conditions. Mechatronic devices, made from mechanical structures with electrical and computational components, have recently emerged as an alternative of their purely mechanical predecessors [9]. These devices can be used to guide repetitive exercises and reduce manual labour, allowing therapists to focus on other aspects of the patient's rehabilitation. Rehabilitative mechatronic devices have been under clinical evaluation for the better part of two decades and have shown that they can provide motion assistance equivalent to that of a therapist [10, 11] . Wearable versions of these devices have also been launched, showing promise when used in rehabilitation programs for stroke survivors [12, 13]. These devices can accomplish even higher accuracy and repeatability of motion patterns than expert therapists if programmed and controlled properly [14]. However, in order to control these devices, it is necessary to detect the intended motions of the user. There are currently challenges in accurately detecting intended motions during unconstrained dynamic movements [18].

1.2 General Problem Statement

Currently, research groups are working on developing wearable smart devices to provide therapy and assistance for people with impaired arm function [14]. Wearable mechatronic devices allow for the rehabilitation of specific groups of muscles by applying different torques at certain joints of the upper limb [5]. Such devices can interface with the patients by measuring EMG (electromyography)

signals, which allow the device to track muscle activity [15]. Based on the EMG signals, pattern recognition models are used to classify intended motion. Once intended motions are identified, wearable devices can be commanded to assist with these motions and provide therapeutic training [16]. There is a significant body of research describing the use of pattern recognition of EMG signals to control assistive devices. However, EMG signals are very sensitive to both physical and physiological variations [17] and it has been noted that there is a gap between the accuracy of pattern recognition systems in constrained laboratory settings, and usability in unconstrained daily activities [18]. On the other hand, body-worn accelerometers have become popular tools for measuring physical activity [19–23]. A possible solution then lies in the use of data from other sensors along with the EMG signals, such as signals from accelerometers, in the training and use of classifiers, in order to improve classification accuracy [18]. This work aims to evaluate the effect of motion characteristics on accelerometer signals to inform the development of better motion classification models.

1.3 Research Objectives and Scope

The main goal of this thesis is to assess the feasibility of classifying categories of motion characteristics, such as position or force, using electromyography and accelerometer data, working towards a smart wearable elbow brace. To achieve this objective, the work has focused on the following specific objectives:

1. To analyse EMG and dynamic data from subjects performing diverse movements while interacting with the environment in order to extract meaningful features.

2. To train several pattern recognition algorithms using the sets of extracted features and then evaluate their classification performance.

1.4 Overview of the Thesis

The structure of this thesis is summarized in the outline below:

Chapter 1 Introduction: The introductory chapter.

Chapter 2 Literature Review: Presents a review of elbow rehabilitation, elbow biomechanics, rehabilitation robotics, myoelectric control of assistive devices, and challenge issues in EMG control systems.

Chapter 3 Experimental protocol, Pre-Processing and Statistical Analysis: Outlines the measurement systems and methods of data collection of the dataset utilized for feature extraction. Describes the process of extracting relevant features from EMG and accelerometer signals. Features with statistical significance related to motion characteristics are discussed.

Chapter 4 Motion Characteristic Classification and Applications: Presents the results of the training of pattern recognition models to classify motion characteristics using EMG and accelerometer signal inputs and explains their significance.

Chapter 5 Conclusions and Future Work: Emphasizes the contributions of this work and provides recommendations for future work.

Appendix A MATLAB Code: Describes the MATLAB code used for data analysis.

Appendix B Statistical Analysis Tables: Includes the consolidated statistical analyses of ACC signals.

Appendix C Ethics Permissions and Approvals: Includes ethics permission and approval.

Chapter 2

Literature Review

2.1 Introduction

To provide a knowledge base for the remainder of this thesis, this chapter presents a review of the literature in the areas of elbow rehabilitation, robot assisted therapy, elbow biomechanics and motion.

2.2 Elbow Rehabilitation

A non-functional elbow extremely hinders the ability to perform activities of daily living (ADLs) [24], which are common movements performed repeatedly during daily life. They are goal oriented, performed with the purpose of completing a task, for example dressing, pouring water into a glass, and picking up a coin. During rehabilitation, clinicians work with patients to regain functional ability [25]. The specific rehabilitation practices and exercises to perform depend on the type of injury to the elbow and on the stages of healing [7]. A general guideline includes four overlapping phases: immediate motion, an intermediate phase, advanced strengthening, and return to activity. In the first phase, pain and edema are managed [7, 26] since the elbow tissues undergo an inflammatory phase. Mobilization of the elbow is important to prevent joint stiffness [7, 27]. The intermediate phase focuses on restoring typical elbow function and range of motion (ROM) [7, 26, 28]. Next, the advanced strengthening stage introduces strengthening exercises to reduce

muscle weakness [7]. Muscle weakness due to pain, soft tissue injury, and/or immobilization is a common problem following an elbow fracture. It can persist up to 6 months following injury, long after bone healing has occurred [26]. Strengthening exercises should begin when the ROM is complete and painless [7]. The muscles are strengthened progressively, for example, via resistance training [29]. Return to normal activity is achieved gradually, by increasing intensity of activities and joint use [6].

2.2.1 Rehabilitative Braces

There are several types of braces that may be required during elbow trauma rehabilitation [30], as follows:

1. Immobilization braces are used to protect the limb by completely restricting its movement. Their use is indicated at the beginning of treatment when early movement cannot be allowed.

2. Restriction braces allow a controlled ROM. After trauma, this type of brace enables early movement that can be adjusted according to the type of lesion, or surgery performed.

3. Mobilization braces are used to maintain or increase the ROM. They exert distractive forces on the soft tissues, exploiting their viscous-elastic properties.

2.2.2 Elbow Rehabilitation Challenges

As mentioned, professionals in rehabilitation are focused on returning patient's function lost to impairments, so that they improve their independence in the performance of ADLs. Some challenges for traditional rehabilitative approaches persist, including a lack of patient adherence to therapy, and the lack of evidence-based methods and objective outcome measures.

2.2.3 Adherence to Therapy

In order to achieve a therapeutic result, patient adherence to therapy is required. It is well recognized that non-adherence can reduce the effectiveness of the treatment, increase the risk of disability and bias assessment of treatment efficacy. Mutual collaboration between the patient and therapist reduces the risks of non-adherence and improves the patient's healthcare outcomes

[31]. Social determinants of health, such as poverty, unemployment or lack of social support, and the cost of travel and treatment are associated with factors that affect adherence to long-term therapies [32].

2.2.4 Assessment and Outcome Measures

Clinical assessments used by therapists assist in diagnosing problems, tracking patient progress over time (monitoring), and predicting therapeutic outcomes [25]. Assessments generally comprise a defined set of questions, tasks, objects, and/or instructions that are quantified according to specific scales or metrics. Most clinical assessments evaluate ADLs or closely related tasks involving movement. These tests convey a measure of patient's independence in ADLs and/or the quality of their performance [25]. A subset of measures to assess movement include the Functional Independence Measure, the Barthel Index, the Arm Motor Ability Test, the Fugl-Meyer assessment, and the Wolf Motor Function Test [33]. In addition, tests may be tailored to specific patient populations and injuries. For example, the Wolf Motor Function Test has repeatedly been used to study chronic stroke patients [34]. The current clinical outcome measures are self-reported or observer-reported and often depend on the therapist's perspective. For example, the Patient Rated Elbow Evaluation allows patients to rate pain, and their ability to perform 32 activities on an 11 point scale, while the American Shoulder and Elbow Surgeons elbow scale consists of a patient questionnaire and an assessment from the physician [35]. Subjective outcome measures pose difficulties for accurately assessing the effectiveness of therapy. As well, observer-rated measures are time-consuming for the caregiver to perform [36].

2.2.5 Robotic Rehabilitation

Robot-assisted therapy, used as a complementary method to conventional rehabilitation techniques, has the potential to achieve significant improvements in the rehabilitation outcomes [37]. Thanks to technological advances, two forms of robotic assistive devices, capable of providing consistent training [38], have become popular over the last few decades: the end-effector robot and the robotic exoskeleton. The former is based on the use of a robotic manipulator, with an end effector that is attached to an extremity of the patient, for example the hand. It produces motion through

a series of joints and links and assists the user when needed to complete tasks [39]. Due to their large size, these systems are mounted on rigid surfaces such as the floor or a wall. The effectiveness of these robots comes from their large workspace that enables to practice various ADLs. Many research projects have led to the development of end-effector robots for rehabilitation purposes, including popular systems such as MIT-MANUS [40], GENTLE/s [41], and Rehabrob [42]. One major concern is the inability of these systems to control the user's joints independently. Rehabilitative therapy usually begins by retraining joint motion separately until the patient is capable of completing more complex multi-joint tasks. However, end-effector robots in general, can only provide multi-joint motion therapy.

Due to an increased level of ability to assist with the production of motion compared to end-effector robots, robotic exoskeletons have become the most common form of assistive devices. Exoskeleton-based systems originated in 1883 with the purpose of complementing the ability of the human limb [16]. Their joints and links correspond to the human joints and limbs respectively, and robot axes are aligned with the anatomical axes of the human limb. Upper limb exoskeletons aiding with musculoskeletal rehabilitation tasks have shown a similar level of effectiveness compared to the same amount of exercise performed by trained therapists [10, 11]. However, the size and cost of end-effector robots and robotic exoskeletons limit where they can be used. The large size of the systems requires the patients to travel to the clinic to reap the benefits, and only medical centers with large budgets can afford to purchase these expensive systems. Consequently, research and industrial sectors are now moving towards the development of wearable assistive devices to benefit a larger portion of society. A comparison on rehabilitative systems was made in 2014, revealing the shift towards wearable devices [43]. Examples of assistive devices are shown in Figure 2.1.

Wearable assistive devices, designed so that their joints match those of the user, combine the advantages of the leading robotic technologies, such as high accuracy of motions and high repeatability, while maintaining independence from the clinical environment. They allow for rehabilitation of specific groups of muscles by applying torques at certain joints of the upper limb [5]. For the wearable devices to work properly, it is necessary to apply effective control strategies, which, on top of the intrinsic mechanical behaviour of the devices, will dictate the human–robot interactions [44]. Different kinds of control modalities have been used during robot-assisted therapies, as

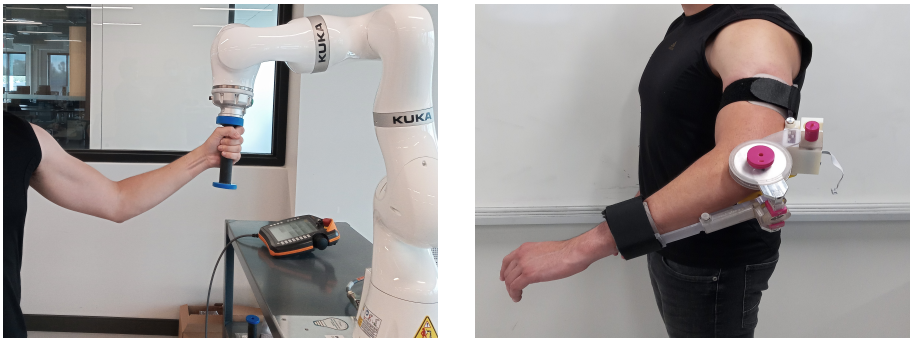

Figure 2.1: Example of robotic devices that can be used during upper limb rehabilitation. The KUKA LBR, an end-effector robot (Left), and an elbow wearable powered brace (Right).

summarized in Table 2.1.

Table 2.1: Control modalities used during robot-assisted therapy [45]

Modality	**Specifications**
Assistive	The subject's voluntary activity is required during the entire movement. The robot can assist providing forces to the impaired limb to complete the task.
Active	The robot is only used as a measurement device, without providing any force to the subject's limb.
Passive	The robot moves the impaired limb without the need for the patient to start the action.
Passive-mirrored	The robot mimics the behaviour of the healthy limb to synchronously drag the impaired limb.
Active-assistive	Assistance towards task completion is provided only when the subject has not been able to perform actively.
Corrective	The robot is only active when the patient is not performing the intended motion in a correct manner.
Path guidance	The robot guides the subject when deviating from a pre-defined trajectory.
Resistive	The robot provides forces opposing the movement.

The human elbow is a popular choice for developing wearable assistive systems due to the availability of the major muscles that move the elbow and the large area for placement of components. Thus, many devices are aimed at assisting with elbow motion [12, 46–50]. An understanding of

elbow motion is required for developing assistive devices [24].

2.2.6 Elbow Motion

The elbow is a complex structure acting as the mechanical link in the upper limb between the wrist and shoulder. Its main function is to position the hand in a stable manner relative at varying shoulder positions while allowing flexion and extension as well as pronation and supination [51]. Such stability is derived from a contribution of bony, soft tissue and dynamic stabilizers. The bony anatomy consists of 3 articulations: the humeroulnar and humeroradial joints and the proximal radioulnar articulation [52]. During the flexion–extension movement, the hinged articulation formed by the humeroulnar joint moves through a centerline of rotation [51]. Flexion increases the angle of the joint, while extension decreases the angle of the joint, as shown in Figure 2.2.

Figure 2.2: An elbow joint fully extended (Left), and flexed 90° (Right).

For their part, the proximal radioulnar and humeroradial joints are pivoting joints that allow forearm rotation (pronation–supination), as shown in Figure 2.3.

Other portions of the upper limb anatomy are involved in radial–ulnar deviation of the wrist, as shown in Figure 2.4. Major shoulder motions, adduction–abduction and flexion–extension, are shown in Figure 2.5.

Many muscles are attached to the elbow joint. They act as the dynamic stabilizers of the elbow, by reducing the forces that the elbow is experiencing [51], and oversee joint movement. Groups of muscles are often activated to contribute to a particular movement [53]; for example, the biceps and brachioradialis, acting synergistically, are the main muscles in charge of elbow flexion [54].

Figure 2.3: A forearm at 90° pronation (Top), neutral position (Middle), and at 90° supination (Bottom).

Figure 2.4: Wrist radial deviation (Left) and ulnar deviation (Right).

Thus, muscles are often classified according to the main function they perform, such as flexors, extensors or stabilizers [52]. However, human motion is complex, and muscles do not always fall into these strict categories. During ADLs, where motions are used to perform a task, several muscles are coordinated and motions from multiple joints may be included at the same time to cause a resultant movement.

Motions can be divided into isometric movements and dynamic movements with muscles in different kinds of contraction, which are defined by the changes in length of the muscle. During isometric contractions, the joint angle and muscle length stay constant. During dynamic movements, the joint angle and muscle length may vary. There are two kinds of dynamic movements: concentric and eccentric. If the activated muscle is shortening, working to move the joint in the direction of the motion, the muscle is performing concentric contractions. On the other hand, if the muscle is lengthening, resisting the direction of joint movement, the muscle is performing

Figure 2.5: Shoulder adduction–abduction and flexion–extension.

eccentric contractions.

Arm movements are caused by a coordination of muscle groups. When performing or attempting to perform a motion or muscle contraction, electromyography can be used to detect levels of muscle activation.

With regards to arm rehabilitation, the muscles described in Table 2.2 and shown in Fig. 2.6 are commonly measured using EMG to detect intended arm motions and control devices [57, 61–67].

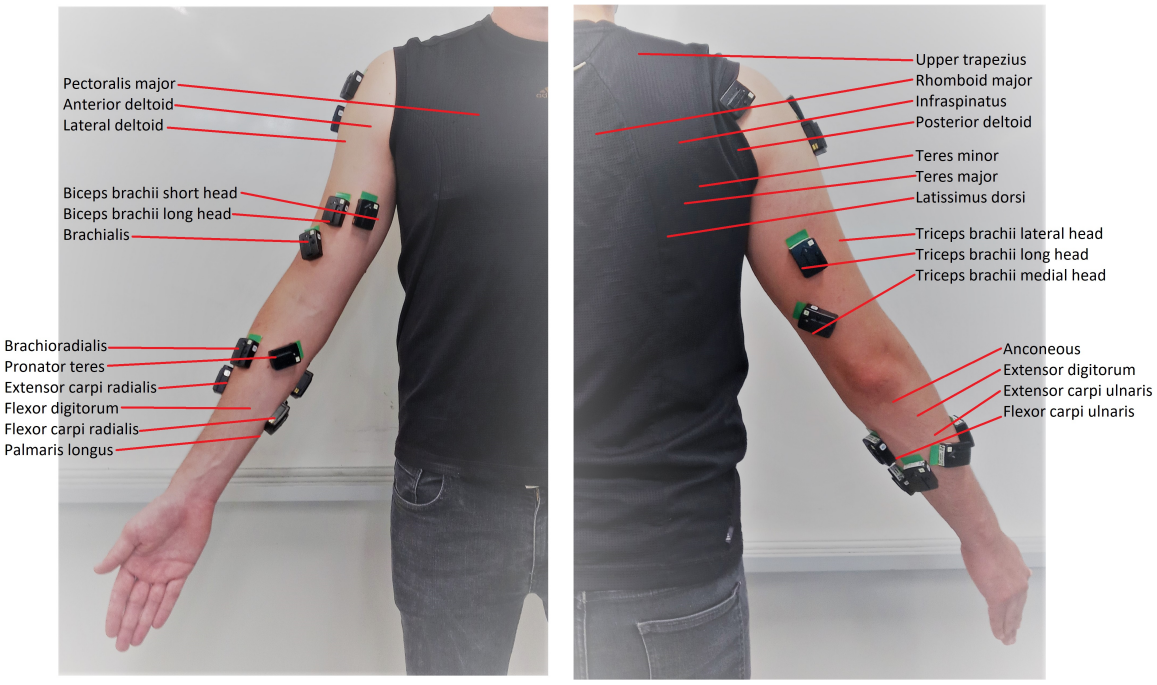

Figure 2.6: Upper extremity muscles commonly measured using sEMG, anterior view *(Left)* and posterior view *(Right)*.

Table 2.2: Muscles commonly measured to control assistive devices.

Muscle	**Main function** [68–70]
Biceps brachii short head	Flexor of elbow, forearm supinator, involved in flexing shoulder
Biceps brachii long head	Flexor of elbow, supinator
Brachialis	Flexor of elbow
Brachioradialis	Flexor of elbow, pronator
Pronator teres	Elbow extension, forearm pronator
Infraspinatus	Shoulder rotator, stabilizer in rotator cuff
Latissimus dorsi	Involved in adduction, extension and internal rotation of the arm at the shoulder
Upper trapezius	Depresor of shoulder
Rhomboid major	Assists to fix scapula
Pectoralis major	Shoulder rotation and transversal adduction
Anterior deltoid	Shoulder vertical and horizontal flexion, shoulder rotation
Lateral deltoid	Shoulder abduction
Posterior deltoid	Shoulder vertical and horizontal extension, shoulder rotation
Teres major	Adducts and internally rotates the arm
Teres minor	Provides stability to the shoulder joint
Triceps brachii long head	Elbow extension
Triceps brachii lateral head	Elbow extension
Triceps brachii medial head	Elbow extension
Extensor carpi ulnaris	Wrist extension
Flexor carpi ulnaris	Wrist flexion
Extensor carpi radialis	Wrist extension
Flexor carpi radialis	Wrist flexion
Palmaris longus	Wrist flexion
Anconeus	Extension of the forearm
Extensor digitorum	Wrist extension
Flexor digitorum	Wrist flexion

2.3 EMG signals

Electromyography (EMG) refers to the recording of electrical activity of the muscles. During muscle contractions, multiple motor units are activated, generating motor unit action potentials (MUAPs). MUAPs produce extracellular currents that extend from the cell membrane to the surface of the skin. Electrodes can be placed on the surface of the skin over the underlying muscles of interest, this is referred to as surface electromyography (sEMG). This way, the ionic

potentials generated by the muscles can be converted into voltages [55], which are measured on a millivolt scale. Electrodes can also penetrate the skin and muscle of interest with intramuscular EMG electrodes. This method allows for individual MUAPs to be recorded, but it is invasive and only useful in a clinical setting. sEMG sensors can vary in shape, size, material, inter-electrode distance, and construction. Electrode placement can vary with skin preparation, location and orientation of the electrodes, and fixation method. Hermens et al. have provided recommendations for best practices by looking at a variety of methods used and results [56]. By evaluating the signals recorded from the electrodes, information related to the muscle activation can be gathered. However, it should be noted that certain limitations exist.

2.3.1 Limitations of EMG signals

EMG signals are sensitive to both physical and physiological variations [17]. An important limiting factor is that there can be crosstalk between signals gathered from muscles close to each other. Specially when the muscle activation is measured on the surface of the skin, the signals can have interference from surrounding muscles. However, if the crosstalk remains somewhat constant, it can provide additional information [57]. Electrodes attached to the surface of the skin can also shift with respect to the muscle underneath, adding undesirable and difficult to remove signal variation [58]. Other factors affecting the quality of the EMG signals measured are altered skin conditions, temperature changes, sweat on the skin surface [59] and electrode impedance changes [60]. Even with these limitations, EMG signals have many applications, including their use in control of robotic assistive devices.

2.3.2 EMG Control of Assistive Devices

EMG signals have been introduced as inputs to the control systems of assistive devices to determine intended movements. Whenever a person intends to move a joint, different muscle fibers corresponding to the muscles of that joint, produce different patterns of contraction and relaxation. Motion intention detection works by identifying those patterns and classifying them into different categories. In turn, output commands are produced according to the classification stage and fed to the robot or assistive device [71]. Several studies have managed to utilize motion intention de-

tection as a sophisticated control method. For example, Ryser *et al.* developed a wearable robotic hand orthosis controlled using motion intention detection based on EMG signals [72]. The device detected patterns produced by the activation of different muscles while performing specific hand gestures and then, these patterns were utilized to control a wrist wearable mechatronic device. Other controllers not based on pattern recognition include proportional control, finite state machines, and onset analysis [59]. Finite state machines involve states, transitions, and commands. The transitions are associated with the input signals and the states are motion commands [60]. These controllers are simple and can be intuitive to use and implement, comparing EMG signal levels to set thresholds, but are limited in the number of commands that can be implemented. In general, the development of an EMG-based pattern recognition system follows the procedure summarized in Figure 2.7 [59, 71].

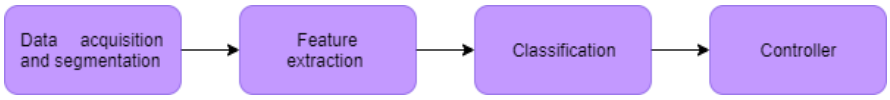

Figure 2.7: Stages for developing pattern recognition systems

2.3.3 EMG Data Pre-Processing

Once obtained, the EMG signal must be preprocessed. Since EMG signals are in the order of millivolts, the first preprocessing step consists of amplifying with a gain in the range of 1000 to 10000 [73]. After being amplified, the EMG signal is then filtered using a bandpass filter with cut off values between 10 or 20 Hz for the low frequency cut off and 500 Hz for the high frequency cut off [74]. Furthermore, a notch filter with a cut-off frequency of 60 Hz is also applied to remove power line interference.

2.3.4 EMG Data Segmentation

Following the amplification and filtering of the raw EMG signal, the next step of the pattern recognition process consists of segmenting the preprocessed signal so that it can be analyzed for real-time applications. Segmenting the EMG signal allows for the extraction of information from the active segments of the signal, i.e., segments where the motion is being performed. First, it is

necessary to detect the moment when the muscle goes from an idle or relaxed state to a contracted stat. This process is known as the EMG onset detection and is important because it can be used as the trigger to start the analysis. Typical EMG onset detection methods use threshold-based algorithms. These algorithms include single-threshold approaches [75], and double-threshold approaches [76]. While single-threshold based approaches rely on detecting the instant when the amplitude of the signal surpasses a predefined value, double-threshold approaches take this concept even further by ignoring false-alarm triggers. This is achieved by counting the number of consecutive samples in which the amplitude of the EMG signal is above a predefined threshold, after the first motion trigger event happens. For the information to be used in real-time applications, segments must be divided into windows, which may be either continuous or with overlap. From these windows, features used on the latest stages of the EMG pattern recognition are extracted. If the system were to work in real time, the length of the windows should account for the maximum tolerated delay (300 ms) between processing the information and controlling a myoelectric device [77]. Furthermore, depending on the application, a trade-off between classification accuracy and delay exists, which can affect the choice of the window length. In this sense, continuous windows with lengths of 200 ms provide better classification accuracies, while overlapped windows with lengths above 200 ms, and 150 ms of overlap, provide a faster response with a noticeable increase in the classification error [78].

2.3.5 EMG Feature Extraction

The feature extraction stage transforms the raw signal into a feature vector by highlighting important data. Three types of features are used in EMG control systems: time domain features, frequency domain features, and time-frequency domain features. Time domain features are the predominant features used in applications involving wearable mechatronic devices and most myoelectrical devices. Their popularity comes from their relatively fast computation due to not requiring any type of transformation [79]. On the other hand, frequency domain features are mostly used in applications that study muscle fatigue and are based on the signal's estimated power spectrum density (PSD) [71, 79]. Finally, time-frequency domain features are used to extract the signal's energy information in time and frequency simultaneously. However, both frequency and

time-frequency domain features require transformations that can be computationally expensive [71].

2.3.5.1 Time Domain Features

Some of the most used time domain features used in the literature are listed below [60, 79, 80]:

Mean Absolute Value (MAV) The MAV feature represents the mean absolute value of the signal amplitude, calculated as follows:

$$MAV = \frac{1}{N}\sum_{i=1}^{N}|x_i| \tag{2.1}$$

where N is the length of the signal, and x_i is the i^{th} sample of the signal.

Waveform Length (WL) This feature represents the accumulative length of the signal over a time segment [79], defined as follows:

$$WL = \sum_{i=1}^{N-1}|x_{i+1} - x_i| \tag{2.2}$$

where N is the length of the signal, and x_i is the i^{th} sample of the signal.

Slope Sign Changes (SSC) The SSC refers to the number of times the slope of the signal changes from positive to negative to positive, calculated as follows:

$$SSC = \sum_{i=2}^{N-1} f\left[(x_i - x_{i-1}) \times (x_i - x_{i+1})\right] \tag{2.3}$$

where the function $f(x)$ is defined as follows:

$$f(x) = \begin{cases} 1 & \text{if } x \geq threshhold \\ 0 & \text{otherwise} \end{cases} \tag{2.4}$$

Zero Crossings (ZC) ZC refers to the number of times the amplitude of the signal crossed zero. It is calculated as follows:

$$ZC = \sum_{i=1}^{N-1} f(x_i, x_{i+1}) \tag{2.5}$$

$$f(x,y) = \begin{cases} 1 & \text{if } (x \times y) < 0 \cap |x - y| \geq threshold \\ 0 & \text{otherwise} \end{cases} \tag{2.6}$$

Root Mean Square (RMS) RMS is found by squaring the signal amplitude values, taking the mean of these squares over a window, and then calculating the square root, as follows:

$$RMS = \sqrt{\frac{1}{N} \sum_{i=1}^{N} {x_i}^2} \tag{2.7}$$

Auto-regressive (AR) Coefficients An AR model represents each sample x_i of the EMG signal as the linear combination of each previous x_{i-k} samples and white noise w_i [79]. The AR model is defined as follows:

$$x_i = \sum_{k=1}^{n} a_k x_{i-k} + w_i \tag{2.8}$$

where n is the AR order and the coefficients a_k are used as the EMG features.

Wilson Amplitude (WAMP) For WAMP, the difference in EMG amplitude between two segments is found. WAMP is the number of times this difference exceeds a threshold, obtained as follows:

$$WAMP = \sum_{i=1}^{N-1} f(x_i - x_{i-1}) \tag{2.9}$$

where the function $f(x)$ is defined as follows:

$$f(x) = \begin{cases} 1 & \text{if } x \geq threshhold \\ 0 & \text{otherwise} \end{cases} \tag{2.10}$$

2.3.5.2 Frequency Domain Features

Although it has been found that frequency domain features are not well suited for EMG signal classification due to some of the features having the same discrimination as most time domain features while requiring more computational time [79], some features in the frequency domain do have the ability to provide useful information for EMG signal classification. Frequency domain features are described below.

Mean Frequency (MNF) The MNF is the average frequency of the EMG signal in the power spectrum, obtained as follows:

$$MNF = \sum_{j=1}^{M} f_j P_i \Big/ \sum_{i=0}^{M} P_j \tag{2.11}$$

where M is the length of the frequency bin, f_j is the frequency of the power spectrum at bin j, and P is the EMG power spectrum at frequency bin j.

Median Frequency (MDF) The MDF is the median frequency of the EMG signal in the power spectrum, calculated as follows:

$$\sum_{j=1}^{MDF} P_j = \sum_{j=MDF}^{M} P_j = \frac{1}{2} \sum_{j=1}^{M} P_j \tag{2.12}$$

where M is the length of the frequency bin, f_j is the frequency of the power spectrum at bin j, and P is the EMG power spectrum at frequency bin j.

Power Spectrum Ratio (PSR) The power spectrum ratio represents the ratio between the maximum value of the power spectrum and the whole energy of the power spectrum. The PSR is calculated as follows:

$$PSR = \frac{P_0}{P} = \sum_{i=f_0-l}^{f_0+l} P_i \Big/ \sum_{i=E_1}^{E_2} P_i \tag{2.13}$$

where P is the energy of the power spectrum, which can lie within the range of E_1=20 Hz and E_2=500 Hz. On the other hand, P_0 is the energy near the maximum value of the power spectrum, l is the integral limit, and f_0 is the frequency with the maximum power spectrum in a frequency bin of length M.

2.3.5.3 Dimensionality Reduction

Once the feature vector is obtained, it is necessary to reduce its dimensionality by eliminating the redundant data from it. The resulting vector is called reduced feature vector. There are two main strategies for dimensionality reduction [81]:

1. Feature selection: This strategy chooses the best subset of the original feature vector according to some criteria for deciding whether one subset is better than another.

2. Feature projection: This method tries to determine the best combination of the original features to form a new feature set. Principal component analysis (PCA) can be used as a feature projection technique. PCA aims to find a subset of features by projecting the original features along the directions of their greatest variances [82].

2.3.6 Classification Methods

Once the features have been extracted from the raw signal, and redundant information has been reduced, classifiers should be deployed to detect motion intention. This section reviews some of the common pattern recognition classification methods used for the control of wearable assistive devices.

2.3.6.1 Linear Discriminant Analysis (LDA)

First, Linear Discriminant Analysis (LDA) is a robust classifier that uses hyperplanes to separate the feature space into linear decision regions. It minimizes the distances between feature vectors

of the same class and maximizes the distances between different classes. It assumes that the observations within each class come from Gaussian distribution, and that the covariance of all classes is equal. The decision regions must be linearly separable, otherwise the LDA will not work [83]. LDA provides fast predictions and small memory usages. It has been applied to a variety of EMG classification problems [18].

2.3.6.2 Quadratic Discriminant Analysis (QDA)

Quadratic Discriminant Analysis (QDA) is an extension of LDA that provides non-linear quadratic decision boundaries. It is best for large data sets as it may overfit data sets with a low number of observations and high variance. In general, the performance of QDA is comparable to LDA [84, 85].

2.3.6.3 Support Vector Machines (SVM)

Linear models such as LDA and QDA are simple and fast but perform poorly if the relationships between features are non-linear or complex. Support Vector Machines (SVM) solve this issue by using kernel functions. These functions allow the data samples to be separated into hyperplanes, where similar data are grouped together. This allows to treat the classification problem as a linear classification problem. Commonly used kernel functions include the linear kernel, the polynomial kernel, and the Gaussian or radial basis function kernel [86]. If a hyperplane cannot be constructed to separate all classes, a margin can be tuned to allow for some violations.

The SVM typically allows for better classifications than LDA, but the prediction speeds and memory usage are worse. SVM classifiers have been used in many applications, including motion classification for the control of wearable devices [78, 87].

2.3.6.4 K-Nearest Neighbours Classification (K-NN)

The K-Nearest Neighbours (K-NN) classifier is another method that works well on data that are not linearly separable. K-NN is an unsupervised learning method that allows unlabeled data to be organized into “clusters.” Data samples are assigned to the clusters such that the the sum of the

squares of the distances of each data sample to the centre of the cluster is at a minimum. K-NN has been effectively used to distinguish between upper-limb motions [84].

2.3.6.5 Decision Trees (DT)

Decision Trees (DT) are simple models that can outperform classical approaches when classifying non-linear data [83]. The outcome of a single decision tree is determined by a series of splitting rules. However, a single decision tree is susceptible to a lack of robustness. In other words, a small change in the data can cause a large change in the final estimated tree [83]. The predictive performance can be substantially improved by aggregating many decision trees, using methods like bagging, random forests, and boosting [83]. These methods use trees as building blocks to construct more powerful prediction models. The tree bagging method builds hundreds to thousands of decision trees by taking repeated samples from the data set. The most common decision obtained from the trees is then used as the final output. The random forest algorithm is an improvement upon the tree bagging method. It applies a tweak that prevents the models from considering most of the available predictors at each split [88]. This ensures that decision trees will not be highly correlated due to the influence of very strong predictors. For its part, the boosting method works in a similar way to bagging, except that the trees are grown sequentially: decision trees grown using information from previously grown trees [83]. Each tree is fit on a modified version of the original data set. AdaBoost, short for Adaptive Boosting, is a boosting algorithm that creates a more powerful predictor by iteratively adding weak learners [89]. It obtains the combined classifier by means of a weighted majority voting scheme, given an ensemble of weak classifiers [90].

2.3.6.6 Artificial Neural Networks (ANN)

Another important classification method is the Artificial Neural Network (ANN) classification algorithm. It also works well with data that are not linearly separable, or when the classes of the training data are unknown. ANNs are designed to imitate the networks of neurons in the brain. The output is determined by a non-linear function of the sum of its inputs. ANNs have high generalization abilities over large datasets [91] and can meet real-time constraints, which are an important feature in control systems. ANN models have been used for the classification of motions

[92].

2.3.7 Evaluation of Classification Model Accuracy

After developing predictive classification models, as the ones presented above, it is necessary to evaluate their performance, that is, how good are the models in predicting the outcome of new observations. In order to estimate the model prediction accuracy and prediction errors, training sets and validation sets should be used [93]. The models are initially fit on a training set, and then they are used to predict the classes of the validation set.

k–fold cross-validation can be used to determine the classification error. It divides the data set into k groups, or folds. The first fold consists of the validation set and the remaining k–1 folds are the training set. This is repeated k times until the average of the classification error is obtained [83].

Another option, suitable for data sets with a low number of observations, is to use leave-one-subject-out (LOSO) cross-validation. In this case, a single observation is used as the validation set, and the remaining observations are used as the training set. The procedure is repeated until each observation has been used as the validation set, and the average of the classification error is obtained. With this method, the bias in determining the classification error is decreased [83].

2.3.8 Challenge Issues in EMG Control Systems

EMG-based control systems have a great potential for improving the quality of life of persons with limb deficiency. However, despite the huge amount of academic achievements regarding pattern recognition-based classification techniques, the clinical and commercial impact of assistive devices is still limited [94]. Training periods are required for the motion classifiers to associate EMG patterns with the motion classes. Current pattern recognition models are limited by long training periods and poor reliability that prevent them for being used in clinical situations, in which the signals are not conditioned as well as in research laboratories [95]. In laboratory settings, classification systems using EMG inputs generally have a higher accuracy than the same systems used in unconstrained daily activities [96]. Frequently, in training these systems, motions are very constrained, and variables are controlled, for example, body movements are performed at very

specific limb positions. In contrast, the functional movements of a limb involved for achieving a task are generally complex. Motion characteristics, such as limb position, joint velocity and interaction force can all have an impact in the accuracy of motion classification systems as demonstrated in a study performed by Stanbury et al. [97], where these factors significantly impacted the activation of a variety of arm and shoulder muscles, as seen in variations of up to 11 EMG feature values. In addition, analyzing signals gathered from different motion segments (static muscle activation vs. time-varying portions) and other noise factors may cause the accuracy of the systems to differ as well.

2.3.9 Factors

Many factors alter EMG signals, and in turn, affect the accuracy of motion classification algorithms. Some of the factors are external to the actual muscle performance, meaning that they can cause noise and drift or change the output signals when there are not real changes in the muscle activations [98]. Examples of these factors are the electrodes (type, material, style, electrode spacing, sweating, skin cleanliness), placement (position of electrodes over muscle bodies, shifting of electrode location during use, crosstalk mixing signals from surrounding muscles) and the recording system itself (amplification, filtering). In addition, they may only affect the signals intermittently. On the other hand, factors affecting the accuracy of motion classification algorithms that are related to the actual muscle performance and motion, include the limb position, joint velocity, interaction force and the training protocol. They are described further in the following sections.

2.3.9.1 Limb Position

In studies, EMG data are generally collected in very constrained laboratory settings. Participants are measured with their arms supported in specific positions, resulting in repeatable contractions [99]. Shoulder movements are restrained by fixing the upper arm to the body trunk and other body movements are avoided by sitting the participants in chairs and fixing their arms to measurement devices that restrict motion to a single DOF [100]. Whereas in task-oriented situations or activities of daily living, limbs take on a variety of changing postures during contractions [18]. Muscle

activations can change with limb posture and indirect joint angles [97]. This is reflected in the accuracies of pattern recognition of motion reducing with limb position variation [18]. Yang et al. reported that collecting EMG signals on dynamic arm postures influenced the classification rate of finger motions [96]. Khushaba et al. [17] studied the combined effect of muscle contraction and forearm orientation on the generalizability of the EMG pattern recognition and observed that changing the forearm orientation had a profound impact on the classification results. In addition, different limb positions can cause activations in muscles not usually involved in the motion of interest. For example, during trials of repetitive hand gripping while the arm was positioned with four shoulder flexion–extension angles and three elbow flexion–extension angles, EMG signal features of the extensor carpi radialis brevis (ECRB), which is located in the forearm and its main function is extending the wrist, were not significantly different for different positions except for one feature [101]. So, despite the ECRB not playing an active role in controlling elbow and shoulder joint angles, one of the EMG features was affected by those joint positions. Similarly, muscles may not be affected by position in the same way. Depending on the joint angles, muscles can play a larger or smaller role during motions and may need to activate to counteract several forces. In another study, the mean normalized sEMG envelope feature of the brachioradialis did not change with changes in elbow joint angles [99]. Systems using EMG with the arm in varying positions could use these signal changes as control inputs, or be designed to be robust and not affected by them.

EMG readings can also change with limb position without being caused by changes in true muscle activation. When limbs move dynamically, the muscles contract or stretch, changing shape, and shifting beneath the skin. The movement of muscles under the electrodes may alter the measurement conditions (such as distance from electrode to muscle), making electrode readings appear different even if the true muscle activation is not changing [58].

2.3.9.2 Force

Force is another factor that affects motion and EMG signals. In one study, a dramatic increase of classification error of an LDA model predicting hand actions based on EMG signals was observed when forces were introduced [60]. In order to cause movement or provide stabilization during

isometric contractions, activated muscles apply forces to the joints. Such forces are produced by increased recruitment of motor units and increase firing rate of those motor units [102]. Levels of muscle activation measured through sEMG can be related to force output, with higher signal amplitudes typically related to higher levels of force output [54]. However, it has been noted that this relationship is not always linear above force thresholds. For example, the shape of the force-sEMG relationship of the muscles controlling finger movement has more of a parabolic shape [102]. During controlled isometric contractions of the biceps, sEMG has been non-linearly related to force output at the wrist as well [54]. Changes in EMG signals with motion type at constant force values are consistent. Levels of muscle activation are higher during concentric motions, lower during isometric contractions, and lowest during eccentric motions [102]. An important example of the force-EMG relationship changing with motion is the dependence of force on changes in elbow joint angle [102]. External forces also have an impact on muscle activation. They can cause torques in the same direction of the joint rotation during movement or can oppose the joint motion, causing torques acting in the opposite direction of the intended joint motion. During activities of daily living, external forces acting on the limbs can also cause torques that are not necessarily aligned with the axis of rotation of the joints. In turn, these different loadings can cause changes in the muscle activations patterns. Understanding the relationships between sEMG signals and generated force can be used to predict intended force based on EMG signals and then control assistive devices to produce desired force levels. For example, Hashemi et al. [103] calibrated a parallel cascade identification model to estimate the force induced at the wrist during upper limb movements.

2.3.9.3 Velocity

In addition to position and force, varying motion activation patterns can be related to varying joint rotation velocities. The effects of velocity on muscle activation mostly depend on the specific muscle and the type of motion. For example, muscle activation of the biceps and brachioradialis has been observed to increase with increasing velocities during elbow flexion [99]. However, during fine-tuning tasks (extension of the elbow), muscle activation of the biceps decreased with increasing velocities, while the brachioradialis mean normalized sEMG envelope feature increased with

increasing angular velocity [99]. Changes in velocity can deteriorate the pattern recognition rate of EMG-based systems. The root mean square error of a parallel cascade identification model estimating forces at the wrist based on EMG inputs, increased from 8.3%, when forces and velocities were not varied, to 33.3%, when variation in forces and velocities were introduced [103]. Stanbury et al. [97] studied the combined effect of position, force and velocity on the motion characteristic classification accuracy and observed that velocity was the most difficult factor to classify during both flexion–extension arm movements and ADLs.

2.3.9.4 Fatigue

Pattern recognition rates are also degraded by muscular fatigue [104]. Muscle fatigue is a condition in which muscles fail to maintain the required or expected force after a sustained contraction, this is accompanied by changes in muscle electrical activity [105]. Changes in sEMG due to muscle fatigue are due to various factors that include the accumulation of lactic acid in the muscle, which causes a reduction in the action potential conduction velocity, the recruitment of fast twitch muscle fibers, synchronization of motor units with the onset of muscle fatigue, and nonlinear motor unit recruitment patterns in response to pain sensation [106, 107]. The overall effect of these factors on sEMG is the spectral shift towards low-frequency regions and increased amplitude in signals [54, 102]. In studies, rest periods are commonly given during trials between contractions, and motions are performed in randomized orders to minimize the effects of fatigue. For example, in one study, 60 second rest periods were given between 45 second contractions [99]. However, the reasoning behind why these durations are chosen is unclear. On the other hand, rest times for fatigue avoidance can greatly increase training periods when sets of contractions are performed to train systems for control of devices. In training an artificial neural network for prosthesis control, 5 minutes of rest allotted between 25 second contractions to avoid fatigue was presented as a limitation [57]. Robust pattern classifiers for human-machine interaction are currently under development to avoid muscular fatigue effects [104].

2.3.9.5 Training Protocol

While designing and testing EMG controlled devices, pattern recognition classifiers are usually trained for long periods of time in very controlled lab settings. However, during ADLs and functional tasks, the body is not constrained in the same way, with the previously discussed factors affecting the EMG signals and intended movements not exactly matching the movement profiles used in the training period. Improved training protocols are being studied to make pattern recognition control systems more generalizable to arm movements outside of laboratory settings [96]. Lorrain et al. [95] showed that EMG signals recorded during dynamic contractions could be accurately classified for the control of multi-function prostheses. They included data from dynamic portions of muscle contractions in the training protocol of LDA and SVM classifiers, instead of only static portions. In another study, it was found that SVM models trained with data from both dynamic arm positions and levels of muscle contractions performed better at classifying finger motions under a variety of conditions, including external disturbance forces [96]. An important suggestion for improving classification accuracy is to incorporate data from other sensors, such as accelerometers, in the training and use of classifiers [18]. This is known as sensor fusion. Blana et al. [108] demonstrated the use of sensor fusion for prosthesis control in a simulated virtual reality environment (VRE). They developed a controller based on two time-delayed artificial neural networks that combined EMG and kinematic signals from the proximal humerus to predict the movement of the forearm. However, the workspace was quite small, and the range of tasks examined, limited by the lack of interaction with the environment allowed by the VRE, did not represent functional tasks or ADLs. More research efforts should be directed to investigate whether sensor fusion could provide a reliable alternative or complementary medium for motor intention detection when the quality of EMG signals deteriorates [17].

2.4 Conclusion

This chapter reviewed methods of arm rehabilitation and functional assessments, the use of EMG pattern recognition in assistive devices, EMG control systems, and the motivation for incorporating additional data, such as signals from accelerometers, with the surface EMG signals in the training

and use of pattern recognition classifiers. In the following chapters, an accelerometer and EMG-based sensor fusion technique for motion intention detection will be explored.

Chapter 3

Data Collection and Processing

This chapter describes the procedures for processing EMG and accelerometer data. A database from a previous study, which investigated the impact of motion characteristics on EMG signals from several arm and shoulder muscles [97], was used. The database contains kinematic and sEMG data from the upper limb of 24 subjects, while performing various ADLs and unconstrained activities. The collected data were processed and statistical analyses were performed to inform the use of combined sensor modalities in detecting characteristics of intended motion. The following sections review the equipment used and experimental procedures of the previous study [97] and present a description of the data processing and statistical analyses performed in the current work. The experimental procedures were subject to approval by the Human Research Ethics Board at Western University. Refer to Appendix C for the Ethics Approval.

3.1 Experimental Procedures

3.1.1 Equipment

3.1.1.1 Acquisition System

Participants were asked to complete a series of isometric exercises, flexion–extension movements and ADL's in a simulated environment. Measurements were recorded using a commercial wireless myoelectric system (Trigno Wireless system, Delsys Inc., USA). The Trigno system includes a base

station that interfaces with 16 wireless radio frequency sensors (Figure 3.1). Each 27 × 37 × 15 mm sensor is composed of four silver bar electrodes and a triaxial (3 DOF) accelerometer. The EMG sampling frequency was 1925.93 Hz, and the accelerometer sampling frequency was 148.1 Hz. The sensors were affixed to the surface of the skin above the main bulky area of the muscles of

Figure 3.1: The Trigno wireless myoelectric system

interest using Trigno Sensor Skin Interface double-sided adhesive stickers, as shown in Figure 3.2. The use of a wireless system ensured for more natural movements and the use of silver electrodes eliminated the need for gel, which simplified the data acquisition process.

3.1.1.2 Data Recording and Analysis Software

The proprietary software provided by Delsys, EMGworks Acquisition, was utilized to collect and save the data. Afterwards, using EMGworks Analysis, the raw files were converted into comma-separated format to be easily accessed.

Figure 3.2: Trigno EMG sensors attached to the muscles of interest

3.1.1.3 Collaborative robot

A KUKA LBR iiwa collaborative robot (KUKA, Germany), shown in Figure 3.3, was used to implement and measure force levels during human movements. The KUKA LBR is a lightweight robot capable of safely interacting with humans. It has 6 joints with an extra turning flange, providing redundancy as it moves with 6 degrees of freedom (x, y, z translation, α, β, γ rotation). Torque sensors in each joint provide torque and force feedback [109]. The robot was programmed using the KUKA Sunrise Workbench software provided by the manufacturer. Three Cartesian Impedance Control Modes were configured [110] to simulate environment interaction. The code of the programs can be found in [97]. The data collected during runtime of the program were written to log files on the robot controller. A USB was inserted into the robot controller to access the files and transfer them to a computer.

Because the KUKA robot and the Trigno system were not connected at the time of the trials, data points from the separate systems were required to be synchronized offline after collection. Timestamps recorded by each system were used to match data points obtained from the different systems. When viewing the files in the Trigno software, a real world time timestamp for the beginnning of the measurement was available and recorded. In the case of the KUKA robot, each data point in the log files was labeled with an epoch timestamp to relate it to data collected with the Trigno system.

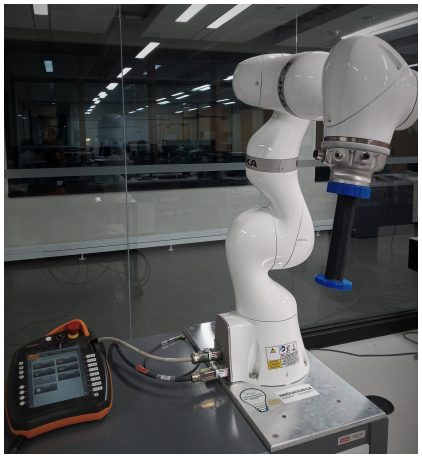

Figure 3.3: The KUKA LBR robot.

3.1.1.4 Participant Interface

A handle end effector was used as an interface between the user and equipment. The same handle was used by every participant during all the motion trials. No wrist braces were worn by the participants to constrict movements. Participants were merely instructed to hold their forearm and wrist in a constant neutral position.

3.1.2 Muscles Measured

The prime elbow flexion–extension muscles, as well as other muscles in the arm and shoulder area, were measured. Muscles involved with shoulder abduction and flexion were considered to study the effect of arm position. Effects of pronation and supination of the forearm were not investigated in detail. Thus, during most tasks the forearm was held in a neutral position. Nonetheless, it should be noted that forearm stabilization involves a variety of arm muscles, including those that are responsible for forearm rotation, which might also be activated during elbow flexion–extension [97]. For this reason, selected forearm muscles, including wrist flexors and extensors, were also measured. Table 3.1 lists the selected muscles for which measurements were studied.

Table 3.1: Studied muscles

Channel	**Muscle**	**Acronym**
1	biceps brachii short head	BBS
2	biceps brachii long head	BBL
3	brachialis	BRA
4	brachioradialis	BRD
5	triceps brachii long head	TRILO
6	triceps brachii lateral head	TRILAT
7	triceps medial head	TRIM
8	infraspinatus	ISPI
9	anterior deltoid	AD
10	lateral deltoid	LD
11	posterior deltoid	PD
12	extension carpi ulnaris	ECU
13	extensor carpi radialis	ECR
14	flexor carpi ulnaris	FCU
15	flexor carpi radialis	FCR

3.1.3 Motion Sets

In the experiment, muscle activation was measured and kinematic information was collected during isometric exercises and dynamic movements [97]. The dynamic movements were divided into simple elbow flexion–extension movements, and more complex activities of daily living (ADLs). Arm position, resistance force, and velocity were the observed movement factors. These factors were varied through multiple levels in multiple combinations during the motion trial movements.

3.1.3.1 Isometric Exercises

During isometric exercises, the participants were expected to hold their arm still. The elbow angle did not change during the muscle contraction; however, separate isometric contractions were held with the elbow fully extended, or the elbow flexed 90°. These contractions were held with the arm in three different positions (shoulder orientations), and three different forces were applied to the hand.

3.1.3.2 Maximum Voluntary Contractions

Maximum Voluntary Contraction (MVC) measurements were included as part of the isometric exercises. EMG signals are commonly measured in studies during maximum muscle contraction to allow for comparisons of EMG patterns between subjects, not only within subjects [111]. In this experiment, MVC was measured by holding the upper arm against the torso with the elbow flexed 90° while the hand gripped the handle of the robot (Fig 3.4). The robot was stiff, resisting movement, and the participants maximally contracted the arm for one trial, attempting to flex the elbow (raise the hand), and a second trial, attempting to extend the elbow (lower the hand), each for a 5 second duration.

3.1.3.3 Elbow Flexion–Extension

In the flexion–extension trials, the arm was held in the starting position with the elbow fully extended, the elbow joint was rotated to 90° flexion, then extended again. One repetition consisted of the full movement from extended elbow, to flexed elbow, and return to extended elbow. These

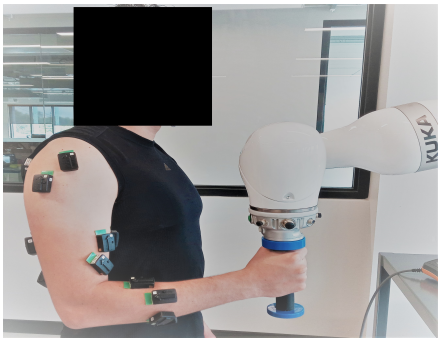

Figure 3.4: The MVC start position for a right-handed participant holding the robot handle interface.

flexion–extension movements expanded on the isometric contractions, by being performed with the arm held in the three corresponding arm positions (shoulder orientations), three force levels applied to the hand, and at two velocities (slow, fast).

3.1.3.4 Activities of Daily Living

Several ADLs were tested to consider more complex scenarios. As mentioned previously, various sets of ADLs are usually performed for the assessment of upper extremity kinematics, dynamics, and functionality. The specific ADLs included can vary. In this case, motions that produced variations in elbow flexion–extension were of interest. The following two activities of daily living (Figure 3.5) were selected as a sample of arm movements to measure: lowering and raising arm above horizontal (reaching above shoulder level in front of body) and moving the hand to mouth (simulating eating and drinking). Resistance force was varied between two levels and the velocity at which the motion was performed varied between two levels. The levels of the motion factors are described further in the following section.

3.1.4 Levels of Motion Factors

3.1.4.1 Arm Position

For isometric exercises and flexion–extension motions, the orientation of the upper arm was held in three different positions. P1 consisted on the arm placed down along the torso (0° abduction, 0° flexion). In P2, the arm was placed horizontal and stretched forwards (90° flexion). In P3, the arm

Figure 3.5: The ADL 1 and ADL 2 start positions for a right-handed participant holding the robot handle interface.

was also horizontal but stretched to side (90° abduction). The patients were instructed to remain stationary, but their shoulder and torso were not physically constrained. This allowed for some movement of the upper arm to occur naturally, which was reflective of how motions are performed during daily activities.

3.1.4.2 Resistance Force

The three force levels during isometric contractions and elbow flexion–extension, were 0 N, 22 N in the direction resisting elbow flexion, and 22 N resisting elbow extension. The value of 22 N was chosen to represent the weight felt to lift objects, such as a bag of potatoes or textbooks. During activities of daily living, two force levels (11 N and 22 N) were applied to the participant's hand. The 11 N or 22 N forces were applied directly downwards to simulate the force of gravity acting on objects a person may carry.

3.1.4.3 Velocity

Movements were performed at three different velocities: 0°/sec during isometric contractions, a slow quasi-static speed (approximately 11°/sec), and a faster speed (approximately 23°/sec). In order to perform the motions at two different speeds, participants were instructed to perform the slow trials in about 8 seconds (duration from full extension to 90° elbow flexion), and complete the motion segment in about 4 seconds for the faster speed.

3.1.4.4 Fatigue

Three repetitions of each trial were performed. To prevent extreme muscle fatigue and discomfort due to overworked muscles, rest periods were given between each repetition, and between each set. Ten seconds of rest were given between each repetition, and approximately 1 minute of rest was given between motion sets.

3.2 Pre-Processing and Statistical Analysis

The previous section reviewed the data collection procedures as described in [97]. The work presented in this thesis extends the results of the previous study by quantifying the impact of motion characteristics on accelerometer signals from arm and shoulder muscles. Data were processed offline, not in real time, using MATLAB R2020a (MathWorks, USA). The scripts of the computer programs used in this section are shown in Appendix A.

3.2.0.1 Filtering

Collected EMG data were filtered using a 60 Hz notch filter to remove power line interference, and a 4th order Butterworth band-pass filter with a lower boundary of 20 Hz and an upper boundary of 450 Hz to remove any motion artifact [112]. Accelerometer data were filtered using a 4th order Butterworth band-pass filter with cut-off frequencies of 0.2 Hz and 15 Hz to remove the effect of gross orientation changes from the signals as well as high frequency noise components affecting the data [113].

3.2.0.2 Segmenting Repetitions

Timestamps recorded from the KUKA robot, indicating the beginning and end of each repetition were identified and then synchronized to the EMG files. Accordingly, the EMG signals were segmented into separate repetitions. ACC data were upsampled so that the number of samples of these data were the same as the EMG data. Then, the previously obtained onset and offset indices of the EMG were matched to the upsampled data, and the ACC signals were segmented.

3.2.0.3 Normalizing EMG Signals

To allow comparison of the signals between participants and muscles, the filtered signals were normalized relative to the absolute maximum of the EMG signals gathered from the corresponding muscle during the maximum voluntary contraction exercises.

3.2.0.4 Choice of Feature Sets

Various features were investigated in this study to implement classification of motion characteristics. In order to extract the features, each active segment of the data was divided into windows of approximately 250 ms with an overlap of 125 ms, following the recommendations of Englehart and Hudgins, who stated that the maximum acceptable controller delay of upper-limb myoelectric devices should be 300 ms [80]. The effects of window size and overlap were not of interest in this study and thereby held constant. The first feature set consisted of a time domain multi-feature set, known as the Hudgins feature set, widely used for extracting information from EMG signals to be used as inputs to classifiers for motion classification [57, 79, 80]. This set includes the MAV, SSC, WL and ZC. A second group of time domain features, often seen in the literature [78, 114], consisted of RMS and AR. Additionally, two frequency domain features were extracted from the EMG data: the MNF and MDF. These were included to provide more frequency information than is represented in the SSC and ZC time domain features. A description of these features was provided as part of Chapter 2.

Finally, a feature set based on accelerometer data was computed. This set included the Signal Magnitude Area (SMA) and the Signal Vector Magnitude (here SMV to avoid confusion with the SVM classifier). We adopted the SMA to extract a feature quantity according to:

$$SMA = \frac{1}{N}\sum_{i=1}^{N}\left(|x_i| + |y_i| + |z_i|\right) \tag{3.1}$$

where x_i, y_i and z_i indicate the values of x axis, y axis, and z axis acceleration signals after preprocessing.

The SMA can indicate the fluctuation degree of the acceleration signal; the higher the value is, the more violent the fluctuation is [115]. It has been previously used as a basis for distinguishing

periods of activity and rest, in order to identify when the subject is undertaking activities and when they are immobile [21, 116]. This feature is related to the gross amount of activity and to energy expenditure [21, 117].

For its part, the SMV was calculated as follows:

$$SMV = \frac{1}{N}\sum_{i=1}^{N}\sqrt{{x_i}^2 + {y_i}^2 + {z_i}^2}, \tag{3.2}$$

where x_i, y_i and z_i again indicate the values of x axis, y axis, and z axis acceleration signals after preprocessing. The SMV indicates the degree of movement intensity [118], and has also been used to predict energy expenditure [21].

3.2.1 Statistical Analysis

Following the feature extraction procedures, the feature values were averaged over the entire repetitions of the corresponding movement, and then, the mean of the repetition averages were collected to give one value for the feature per movement. Data from flexion–extension motions and isometric exercises were grouped together. Similarly, motion trials for ADL1 were grouped together, as well as motion trials for ADL2. A statistical analysis was performed using the Statistical Package for Social Sciences v.24 (SPSS) software in order to assess if motion factor levels can be distinguished using the accelerometer features. A series of three-way repeated measures ANOVA, with a Bonferroni correction for multiple comparisons [119], were run to identify if there were significant differences among the means of the features for each of the motion factors. This procedure was completed for each subject. Each muscle and feature were analyzed separately. The results of all statistical analyses described are presented in the next section.

3.2.1.1 Flexion–Extension Statistical Results

For flexion–extension, there were many significant differences between all position levels, between all force levels, and between all velocity levels for both the SMA and SMV features, as ilustrated in Figure 3.6.

However, several muscles, including the BRD, TRILO, TRIM, ISPI, LD, PD, ECU, ECR, FCU

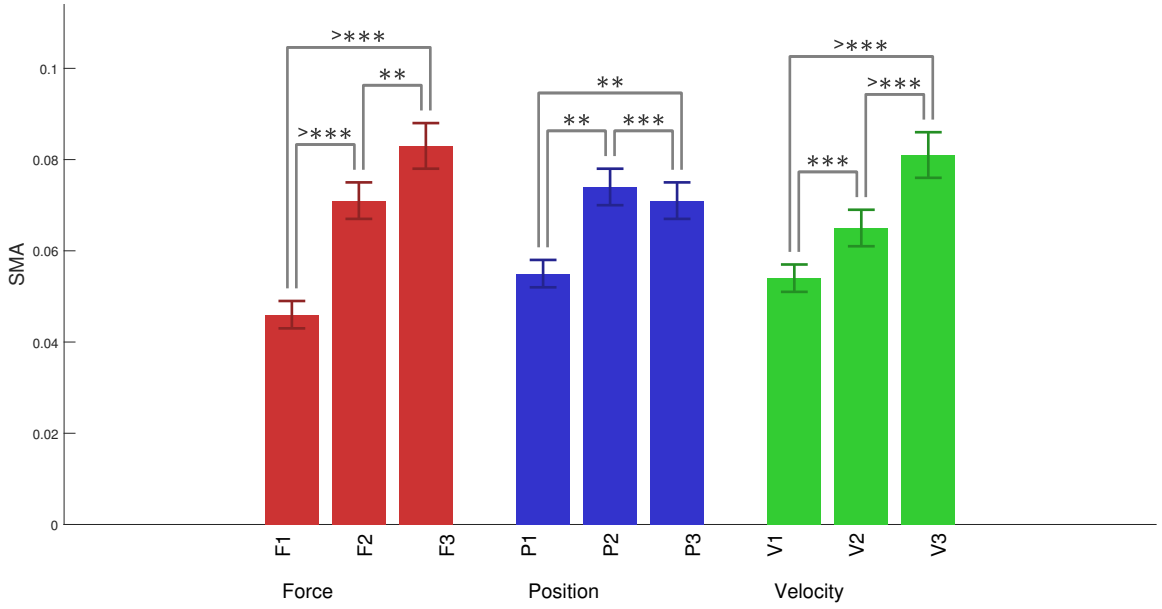

Figure 3.6: Comparisons among mean SMA values for the TRILO. Significant differences between all positions levels, all forces levels and all velocity levels were observed. Asterisks denote statistical significance (* p <0.05; ** p <0.01; *** p <0.001). Error bars represent standard deviation.

and FCR, did not show significant differences between P2 and P3, as ilustrated in Figure 3.7. The differences in arm position between P1, P2, and P3 were shoulder flexion angles and shoulder abduction angles. Motions in P2 and P3 were both performed with the arm horizontal. In terms of gross motion, the difference may have not been abrupt and thus it was not distinguished with the SMA and SMV features.

Similarly, some muscles, including the BBS, BBL, BRD, AD, ECU, ECR, FCU and FCR did not show significant differences between F2 and F3, as ilustrated in Figure 3.8. The levels of force applied in F2 and F3 were 22 N resisting elbow flexion, and 22 N resisting elbow extension. The main difference between F2 and F3 was the direction of the force applied. For the SMA and SMV features, absolute and squared values were calculated and the sign (representing direction) of the force was lost, which explains why the difference between F2 and F3 was not distinguished.

A full comparison of mean ACC feature values for each muscle, and significant differences in these values corresponding to varying levels of arm position, force, and velocity during the studied movements, is provided in Appendix B.

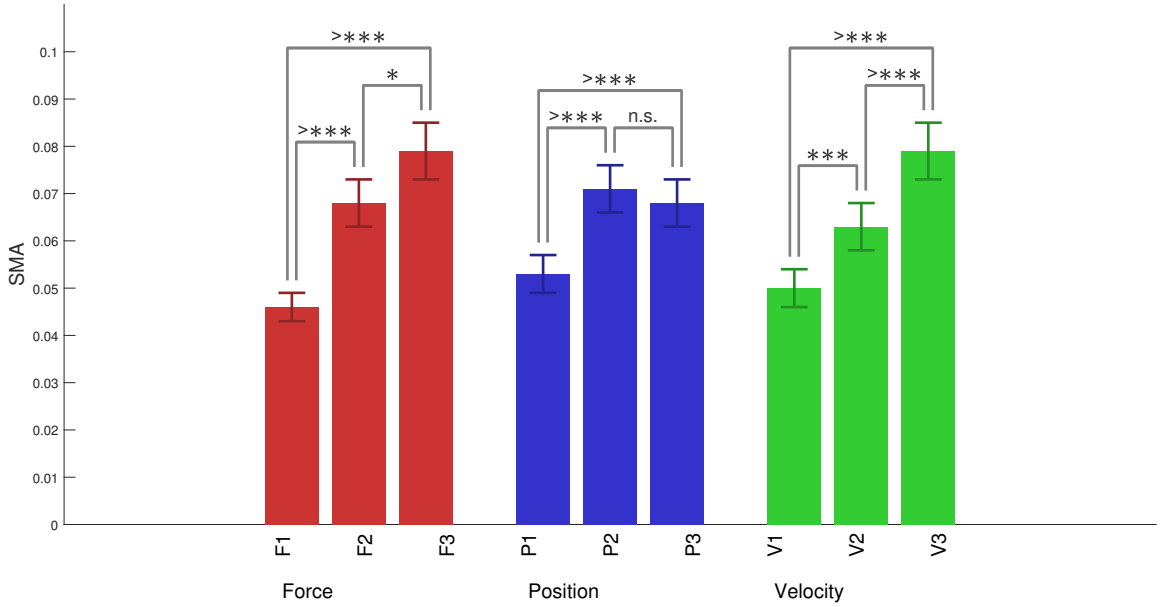

Figure 3.7: Comparisons among mean SMA values for the TRIM. P2 and P3 were not significantly different. Asterisks denote statistical significance (* p <0.05; ** p <0.01; *** p <0.001) whereas "n.s." is written above non-significant comparisons. Error bars represent standard deviation.

3.2.1.2 ADL's Statistical Results

For ADLs 1 and 2, there were fewer feature and muscle combinations that had significant differences for the force levels, when compared to the flexion–extension results.

For ADL1, which consisted in lowering and raising arm above horizontal, there were not significant differences between force levels, except for ISPI. Anatomically, the ISPI contributes to shoulder rotation [65]. It was expected that it would play an essential role in such kind of motions. On the other hand, significant differences between velocity levels were found for all the muscles.

For ADL2, significant differences between velocity levels were found for all the muscles. No statistically significant differences were found between force levels for either SMA or SMV.

3.2.1.3 Discussion

As expected, accelerometer features differed across motion factors. Overall, the impact of the motion factors on the accelerometer signals was strong especially for the velocity factor, where all

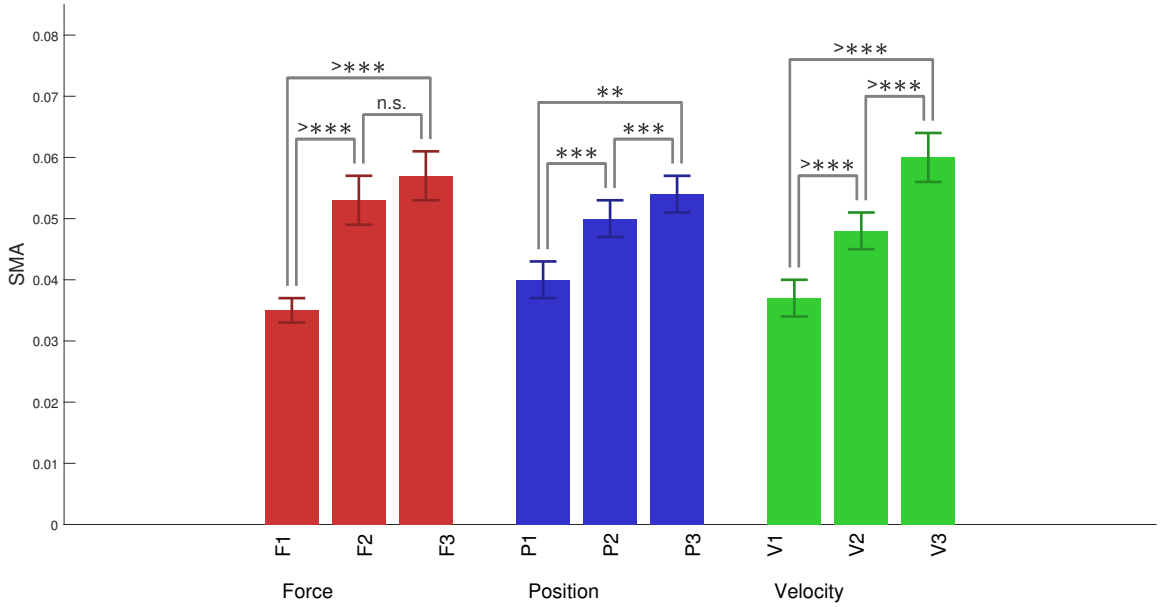

Figure 3.8: Comparisons among mean SMA values for the LD. F2 and F3 were not significantly different. Asterisks denote statistical significance (* p <0.05; ** p <0.01; *** p <0.001) whereas "n.s." is written above non-significant comparisons. Error bars represent standard deviation.

of the muscles showed significant mean differences. Velocity levels influenced accelerometer signals in a more consistent manner compared to force. In contrast, EMG signals have been found to be more influenced by force levels than by velocity levels [97]. The faster velocities and higher forces were represented by the highest values of SMA and SMV. This result was anticipated based on the increased intensity of the chosen tasks. The velocity impact on accelerometer signals was consistent for both ADL motions and flexion–extension movements. This suggests that accelerometer features may be robust if used to detect intended velocity during both simple and complex tasks. In future studies, more velocity levels could be tested. The post-hoc tests revealed that the feature values were significantly higher in P2 and P3 than P1. However, not all the muscles showed statistically significant mean differences between position categories. In addition, force impacted accelerometer signals for ADL motions in a less consistent manner compared to the basic elbow flexion–extension motion. This was expected, as the ADL motions involved more complex movements. These findings suggest that the accelerometer sensors are sensitive to the increase in joint velocity, interaction force and have a mild sensitivity to limb position changes.

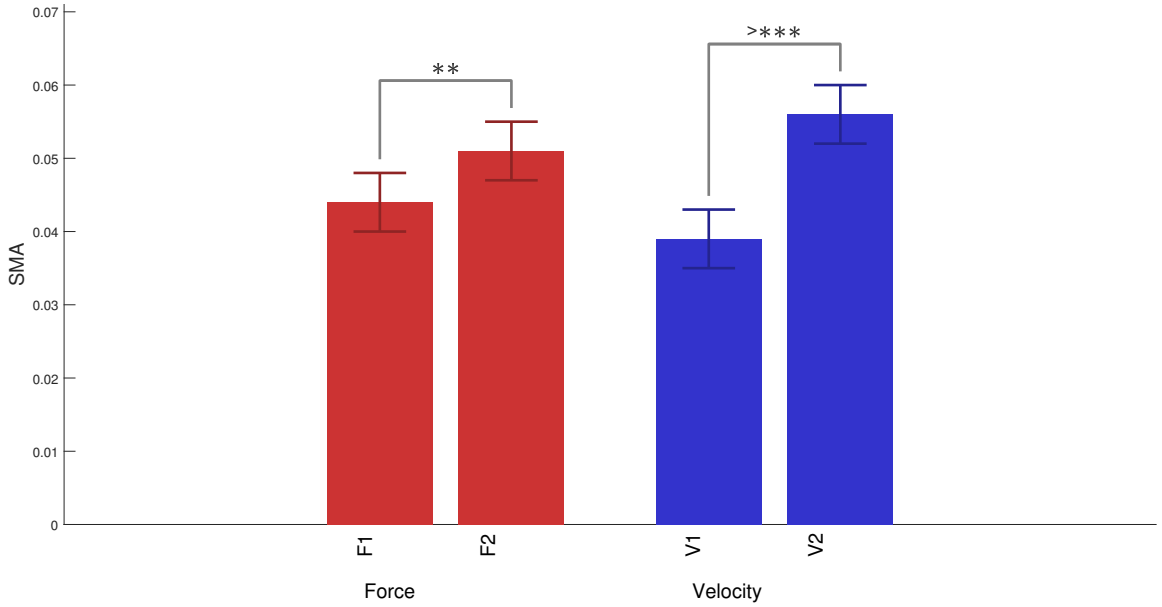

Figure 3.9: Comparisons among mean SMA values for the ISPI in two force levels. Asterisks denote statistical significance (* p <0.05; ** p <0.01; *** p <0.001). Error bars represent standard deviation.

In conclusion, we demonstrated that accelerometer data varied differently with categories of motion factors. Therefore, they contain potentially complementary information that should be useful for motion intention detection techniques. The relationship is explored further and used to determine intended arm motion in Chapter 4.

Chapter 4

Motion Characteristic Classification and Applications

Previous studies have demonstrated the impact of motion characteristics, such as limb position, interaction force, and velocity, on muscle activation [97]. In the previous chapter, it was demonstrated that motion characteristics, or factors that affect motion, have a significant impact on accelerometer signals as well. Depending on the motion factor (position, force, velocity) and motion type (elbow flexion–extension or ADLs), various feature values changed for differing muscles. In this Chapter, the achieved insight is used to classify levels of motion characteristics by incorporating ACC signals with muscle activation data. The results of motion characteristic classification and further applications are described below.

4.1 Classification

EMG and ACC features extracted from the database collected in the previous study [97] were used in MATLAB to train three types of classifiers, LDA, SVM, and DT Ensemble using an AdaBoost boosting algorithm [89], to detect classes of motion factors.

Separate models were trained and evaluated for four different motion groups: standard movements (elbow flexion-extension and isometric exercises), ADL1 (lowering and raising arm above horizontal), ADL2 (moving the hand to mouth), and both ADLs (observations from ADL 1 and

ADL 2 were combined). For the standard movements, three position classes (P1, P2, P3) were determined. As well, three force classes (0 N, +22 N, -22 N) were classified. With respect to the velocity factor, motions were classified into three classes (stationary (0°/s), slow, fast) or two classes (stationary, moving). For the ADL trial groups, these motions were separated into two force classes (11 N, 22 N), or two velocity classes (slow, fast). Data were separated by type of motion to train separate models, because the force levels introduced during standard movements were different from the ones introduced during ADLs [97]. In addition, arm position was not a controlled variable during ADLs.

The input of the classifiers consisted of predictors (feature values from the various muscles measured), and labels corresponding to motion factor levels. Two sets of predictors were developed from the feature vectors. The first one was formed by the EMG feature values (11) for all available muscles (15), and the second contained all EMG features plus the ACC feature values (2). A feature-level fusion approach [120] was employed to form the second set, by concatenating each feature vector to create a single feature vector of 13 features.

Native MATLAB functions, `fitcdiscr`, `fitcecoc`, and `fitensemble` were used to generate the LDA, SVM and DT Ensemble classifiers, respectively (see Appendix A for MATLAB scripts). The method for checking the classifier accuracy is outlined in the following section.

4.2 Model Evaluation

A leave-one-subject-out (LOSO) cross-validation technique was used to estimate the accuracy of each classification model [121]. Accordingly, all the trials from one subject were excluded and used as a testing set, while the trials from the remaining subjects were used as the training set. The classifier outputs were compared to the trial labels (that represented what the subject was actually doing at the time of the respective trial) and the number of correct predictions was used to calculate an accuracy score for each subject. This process was then repeated for each left-out subject and the accuracies were averaged across all iterations to obtain a metric for each model.

Once this process was finished, a statistical analysis was performed in order to identify the best classification methods. The accuracies scores of each subject obtained position, force and velocity

classification were averaged to obtain overall accuracies for each sensing modality (EMG data only, or combined EMG and ACC data) and classification model (LDA, SVM, DT Ensemble). This was done to allow for a general comparison of each method. The statistical analysis was performed using SPSS software to determine if the obtained accuracies showed significant differences between groups. A tree-by-two repeated measures ANOVA with a Bonferroni correction [119] was performed on the accuracies to compare means across classification methods. The process was repeated for each of the motion groups (standard movements, ADL1, ALD2, and both ADLs). The accuracies of the classification models as well as the results of the statistical analysis are demonstrated in the next section.

4.3 Results

4.3.1 Position

The three classifiers were first trained with data from the standard movements to determine the position (P1, P2, P3) of the arm. As it can be seen in Figure 4.1, despite the very diverse training data with varied force levels and velocity levels, position could be determined with less than 25% error with the LDA (78.70%) and SVM (83.02%) classifiers. The accuracy of the DT Ensemble classifier was lower in this case, at 73.45%. The accuracies of the SVM and DT Ensemble remained the same when ACC were incorporated in the classification, but the accuracy of the LDA classifier increased by 3%.

The average accuracy results of each sensor modality during position classification can be seen in Fig. 4.2. A statistically significant difference in accuracy was found between the two modalities, although the overall improvement was small (about 1%). The average accuracy results for each classifier during position classification can be seen in Fig. 4.3. There was not any significant difference between the LDA and SVM classifiers but a significant difference was found for the Decision Tree Ensemble classifier, whose performance was worse in this case.

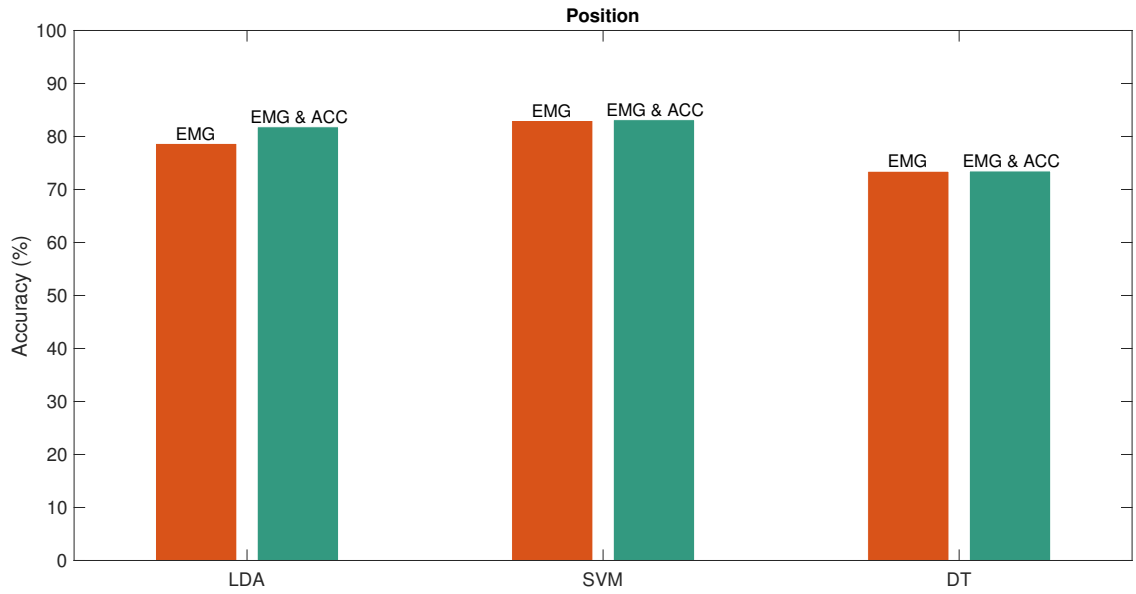

Figure 4.1: Classification accuracies of the trained models identifying positions during standard movements.

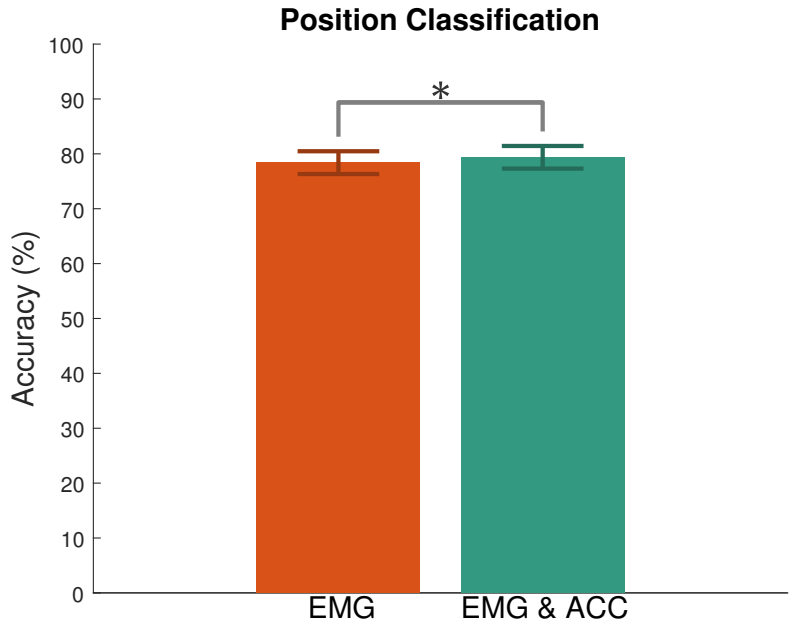

Figure 4.2: Mean position classification accuracies of each sensor modality during standard movements. Asterisks denote statistical significance (* p <0.05; ** p <0.01; *** p <0.001). Error bars represent standard deviation.

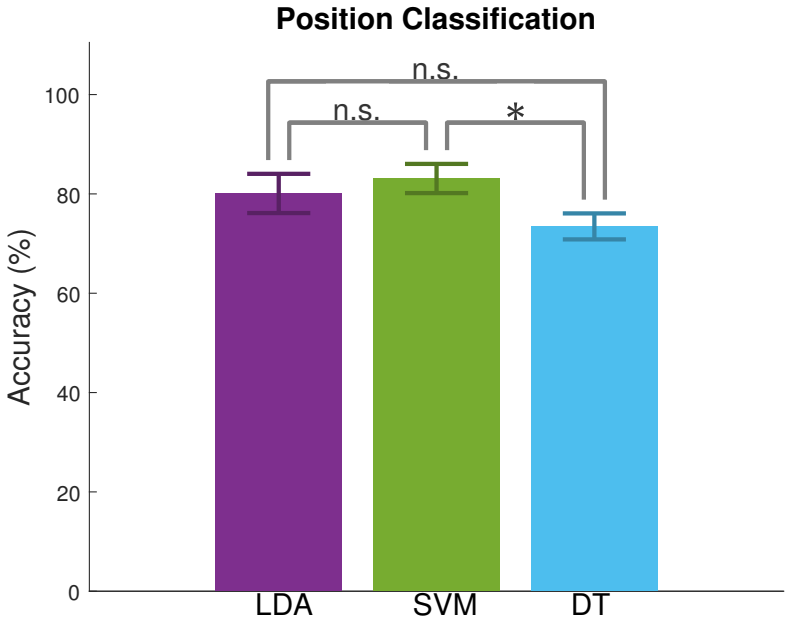

Figure 4.3: Mean position classification accuracies of each classifier during standard movements. Asterisks denote statistical significance (* p <0.05; ** p <0.01; *** p <0.001) whereas "n.s." is written above non-significant comparisons. Error bars represent standard deviation.

4.3.2 Force

The results of force classification during standard movements are shown in Figure 4.4. The accuracies were lower for LDA (73.77%) and SVM (74.54%) but a small increase in accuracy was observed with the DT Ensemble classifier (75.92%). Using this classifier, interaction with the environment could be determined with less than 25% error when arm position and velocity varied. Again, incorporating ACC data in the classification did not make much difference, but the LDA classifier improved by 4%.

The average accuracy results of each sensor modality during force classification can be seen in Fig. 4.5. A statistically significant difference in accuracy was found between the two modalities. This indicated that EMG & ACC showed better classification accuracy. The average accuracy results of each classifier during force classification can be seen in Fig. 4.6. The three classifiers were found to perform at the same level, showing no statistically significant difference between means.

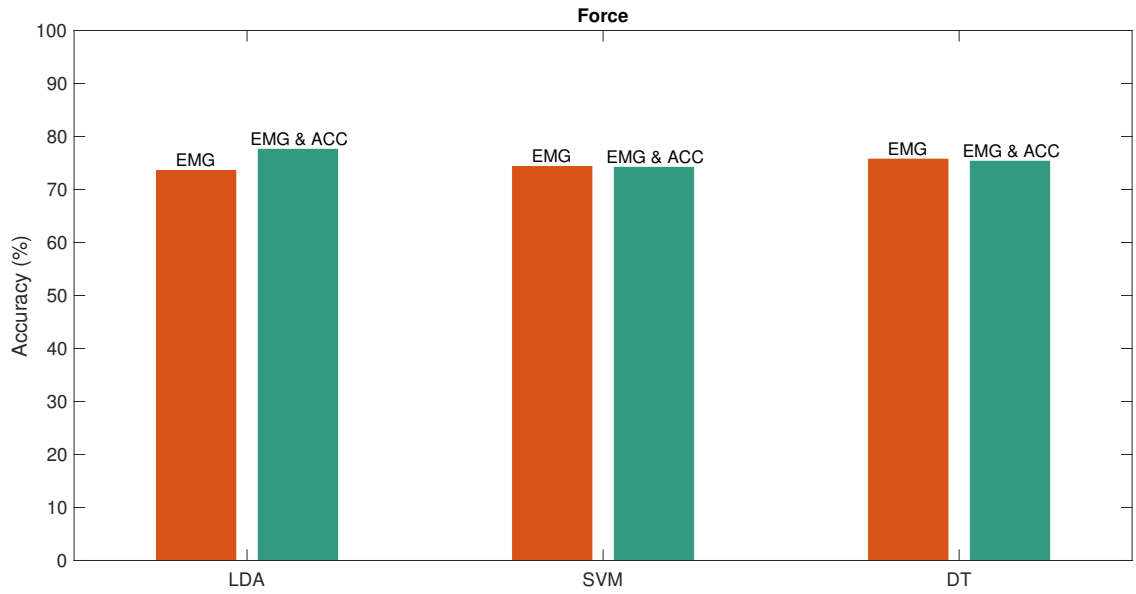

Figure 4.4: Classification accuracies of the trained models identifying force levels during standard movements.

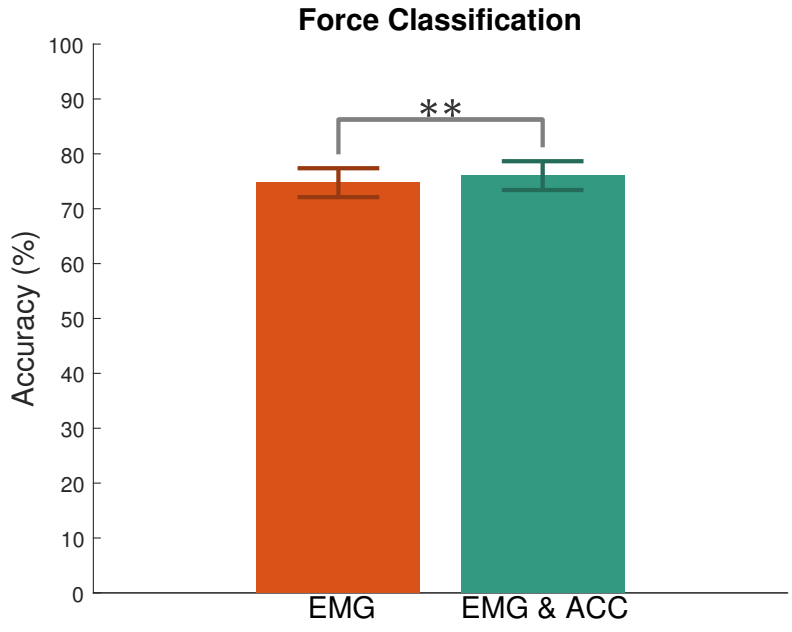

Figure 4.5: Mean force classification accuracies of each sensor modality during standard movements. Asterisks denote statistical significance (* p <0.05; ** p <0.01; *** p <0.001). Error bars represent standard deviation.

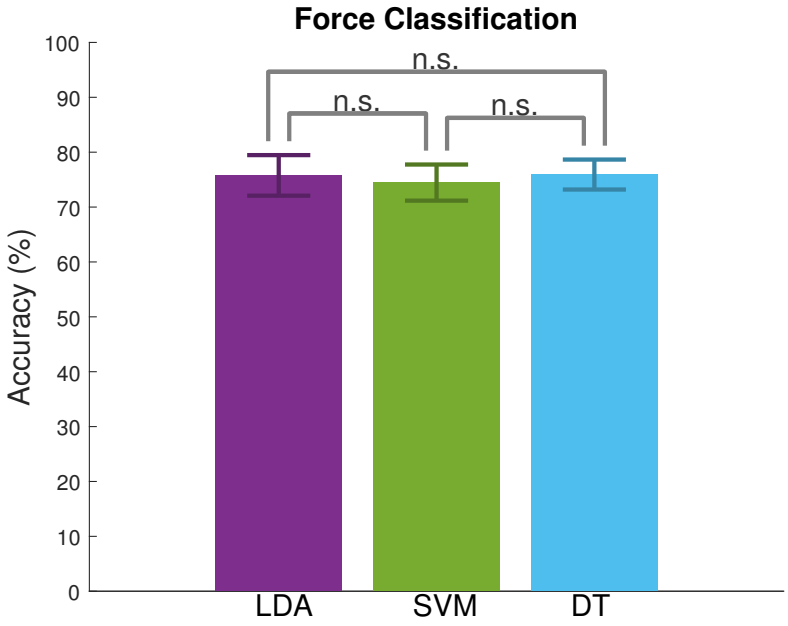

Figure 4.6: Mean force classification accuracies of each classifier during standard movements. "n.s." is written above non-significant comparisons. Error bars represent standard deviation.

4.3.3 Velocity (3 classes)

The three classifier types were very poor at determining velocity (stationary, slow, fast) during standard movements, as shown in Figure 4.7. However, augmenting the predictor vector with ACC features reduced the classification error. The accuracy of LDA increased from 43.98% to 58.33%, SVM increased from 47.22% to 52.50% and DT Ensemble classifier increased from 49.84% to 62.03%. Poor discrimination of velocity classes was expected, as these classes were the goal velocities at which the participants were instructed to move. During the experiment, the actual joint rotation and hand speeds varied between and within participants, even though the subjects were instructed to perform motions over consistent durations [97]. The average accuracy results of each sensor modality during velocity classification can be seen in Fig. 4.8. A statistically significant difference in accuracy was found between the two modalities, indicating that EMG & ACC showed better classification accuracy than EMG. The average accuracy results of each classifier during velocity classification can be seen in Fig. 4.9. The three classifiers had a similar performance, showing no statistically significant difference between means.

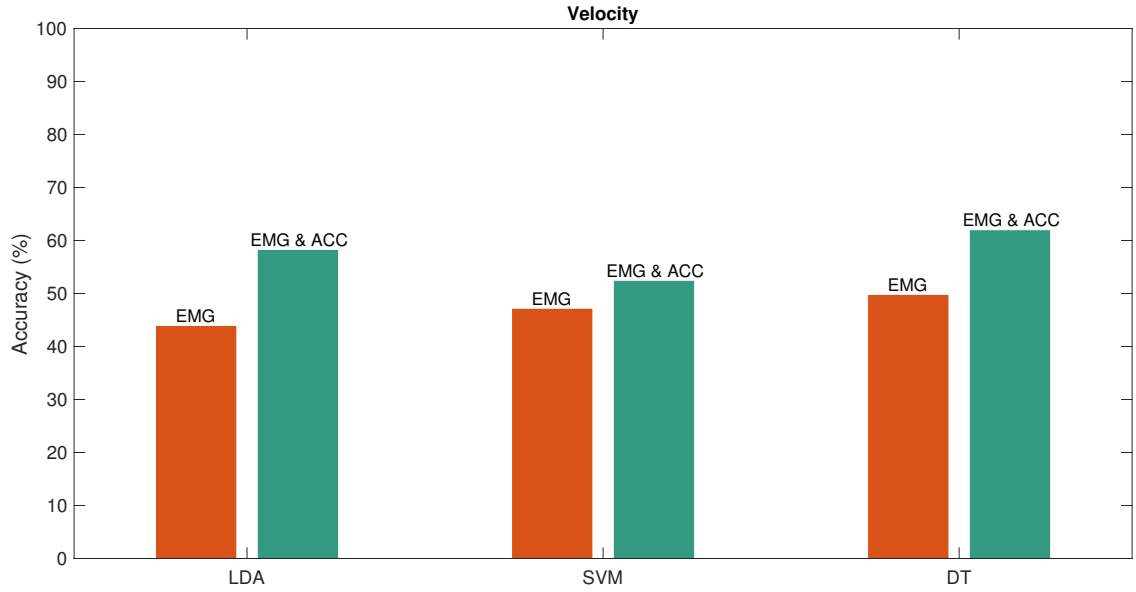

Figure 4.7: Classification accuracies of the trained models identifying 3 velocity levels during standard movements.

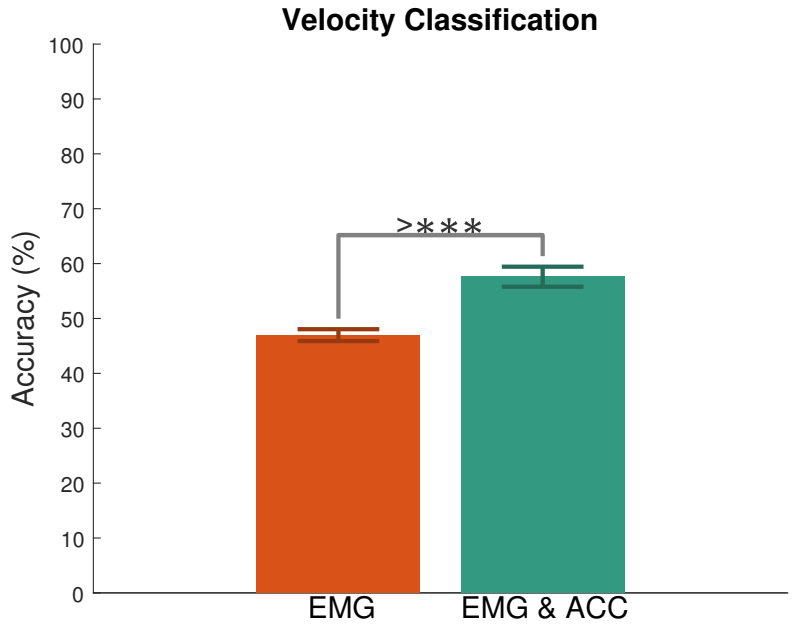

Figure 4.8: Mean velocity classification (3 classes) accuracies of each sensor modality during standard movements. Asterisks denote statistical significance (* p <0.05; ** p <0.01; *** p <0.001). Error bars represent standard deviation.

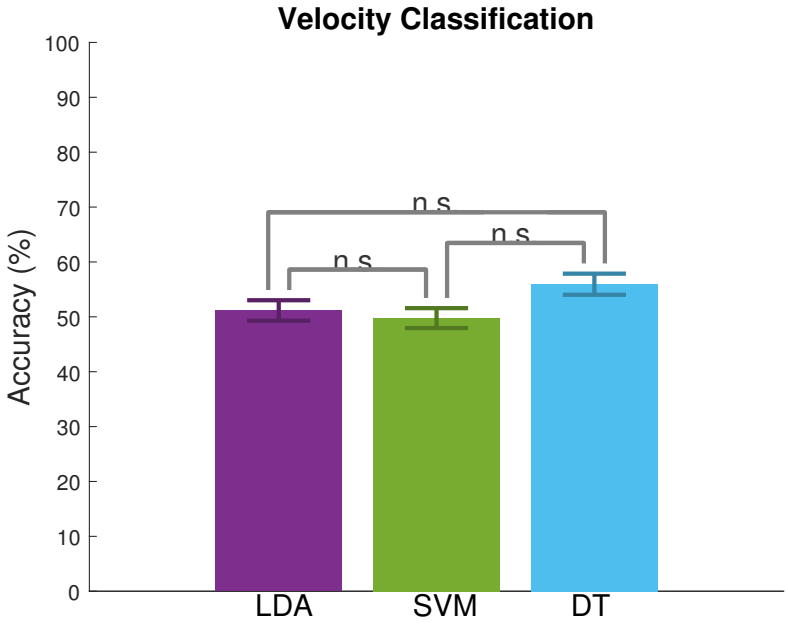

Figure 4.9: Mean velocity classification accuracies of each classifier during standard movements. "n.s." is written above non-significant comparisons. Error bars represent standard deviation.

4.3.4 Velocity (2 classes)

It was noted that the classification accuracies considerably increased when only two velocity levels (stationary, moving) were classified, as shown in Figure 4.10. The accuracy of velocity classification during standard movements increased up to 91% with the DT Ensemble classifier. The average accuracy results of each sensor modality during velocity classification (2 classes) can be seen in Fig. 4.11. A statistically significant difference in accuracy was found between the two modalities, indicating that EMG & ACC had a better performance than EMG. The average accuracy results of each classifier during velocity classification (2 classes) can be seen in Fig. 4.12. Statistically significant differences were found between the DT Ensemble and the other two classifiers, indicating that the DT Ensemble classifier showed a better accuracy.

4.3.5 ADL 1 Force

The results of training classifiers to detect force levels during ADL 1 are shown in Figure 4.13. Force classification was worse for ADL 1 motions than the standard movements. This was expected as

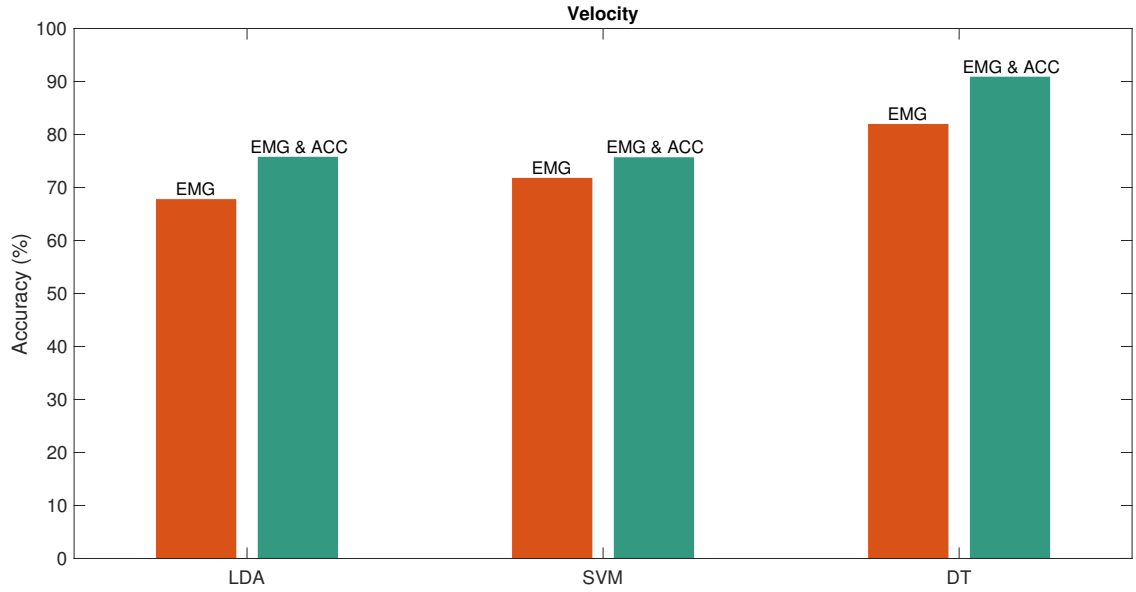

Figure 4.10: Classification accuracies of the trained models identifying 2 velocity levels during standard movements.

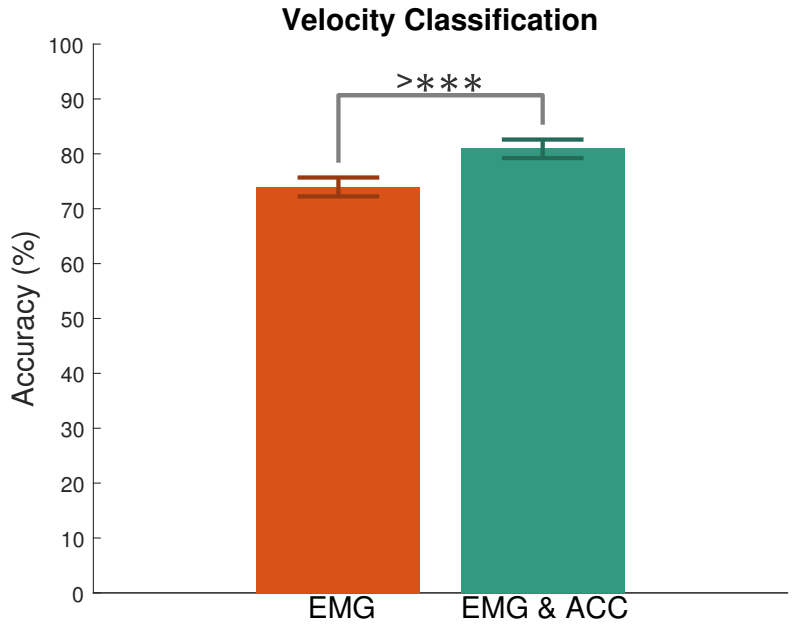

Figure 4.11: Mean velocity classification (2 classes) accuracies of each sensor modality during standard movements. Asterisks denote statistical significance (* p <0.05; ** p <0.01; *** p <0.001). Error bars represent standard deviation.

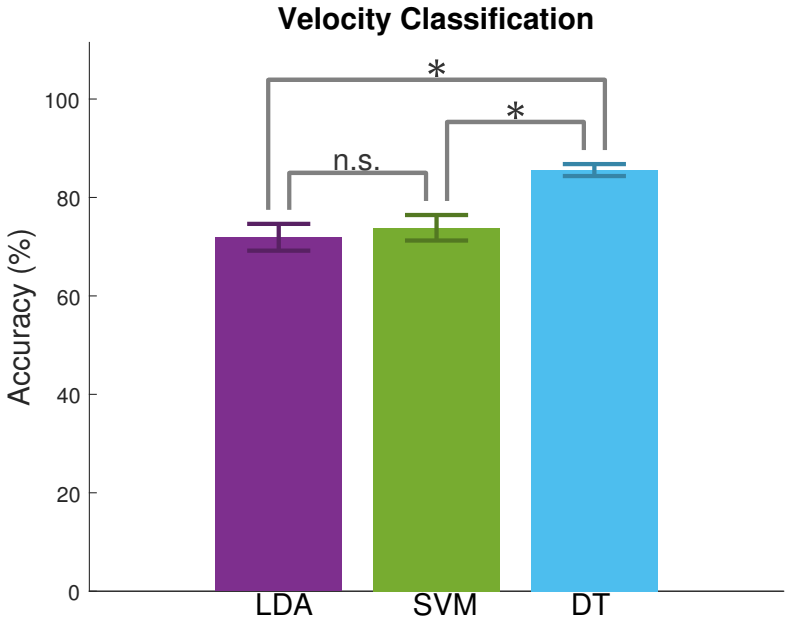

Figure 4.12: Mean velocity classification (2 classes) accuracies of each classifier during standard movements. Asterisks denote statistical significance (* p <0.05; ** p <0.01; *** p <0.001) whereas "n.s." is written above non-significant comparisons. Error bars represent standard deviation.

the motions in the ADL 1 group were more complex; thus, there was more variation in the torques experienced at the elbow [97]. Plus, the difference between force levels (11 N and 22 N) for ADLs was smaller compared to the force levels (0 N, +22 N, -22 N). When trained using ACC data, the LDA classifier had a higher accuracy (4% higher). However, no statistically significant difference in overall accuracy was found between the two sensor modalities, as it can be seen in Fig.4.14. Similarly, no statistically significant differences were found between the accuracies of the 3 classifiers, as it can bee seen in Fig.4.15. Neither classifier performed significantly better or worse than the others with comparable accuracies.

4.3.6 ADL 1 Velocity

The accuracies of velocity classification were modest during ADL 1, as can be seen in Figure 4.16, but increased considerably when ACC data were used. The accuracy of LDA improved from 56.25% to 66.70% and DT Ensemble improved from 53.13 to 78.12%. The average accuracy results

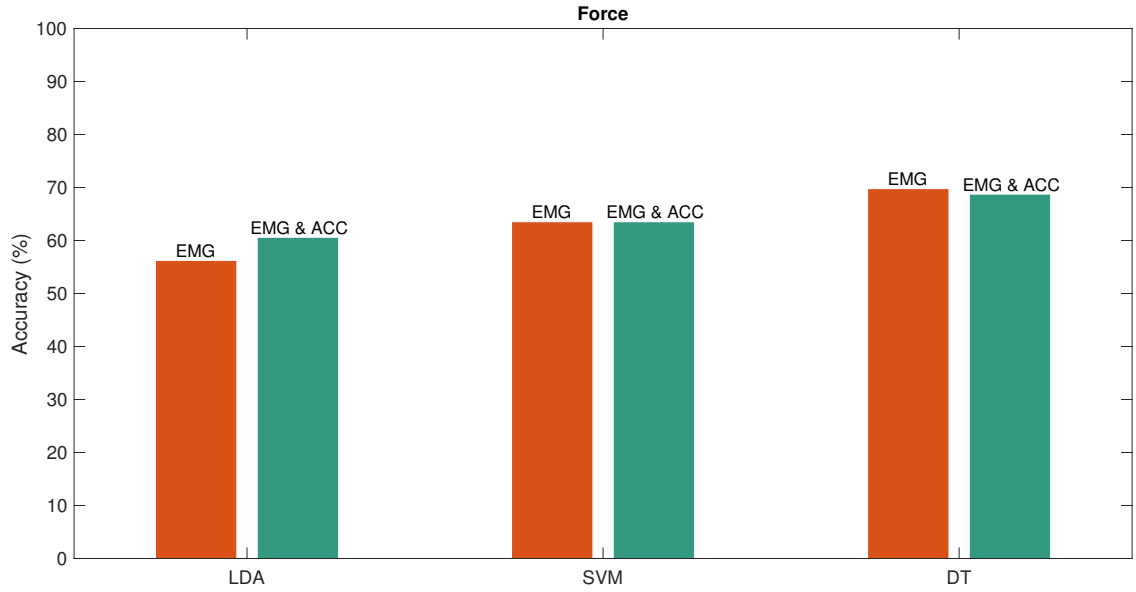

Figure 4.13: Classification accuracies of the trained models identifying force levels during ADL1.

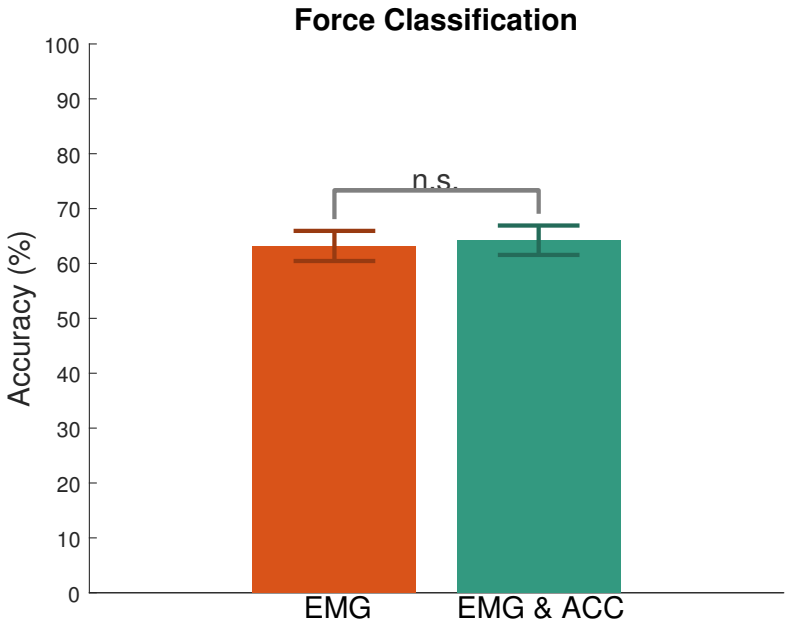

Figure 4.14: Mean force classification accuracies of each sensor modality during ADL1 motions. "n.s." is written above non-significant comparisons. Error bars represent standard deviation.

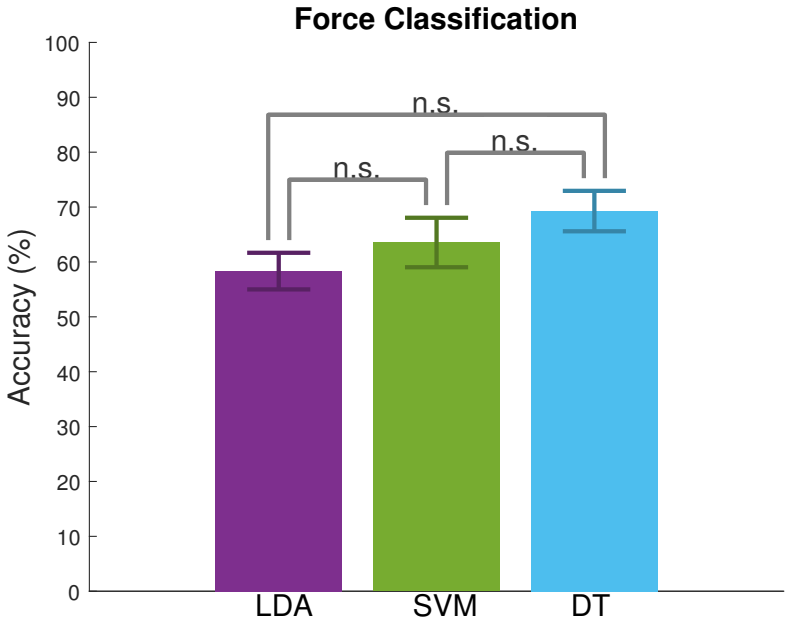

Figure 4.15: Mean force classification accuracies of each classifier during ADL1 motions. "n.s." is written above non-significant comparisons. Error bars represent standard deviation.

of each sensor modality during velocity classification can be seen in Fig. 4.17.

A statistically significant difference in accuracy was found between the two sensor modalities, which can be observed by the increase in performance when ACC data were used. The average accuracy results of each classifier during velocity classification can be seen in Fig. 4.18. A statistically significant difference was observed between the SVM and DT Ensemble classifiers, meaning that the DT Ensamble performed significantly better than SVM.

4.3.7 ADL 2 Force

The results of force classification during ADL 2 are shown in Figure 4.19. Again, force classification was worse than the flexion–extension movements. This was also expected due to the complexity of the movements. When trained using ACC data, the LDA, SVM, and DT Ensemble achieved accuracies of 60.42%, 60.41%, and 64.60%, respectively. The average accuracy results of each sensor modality during force classification are shown in Fig. 4.20. No statistically significant difference in accuracy was found between the two sensor modalities during ADL2. In addition, there were not any statistically significant differences between the accuracies of the 3 classifiers, as

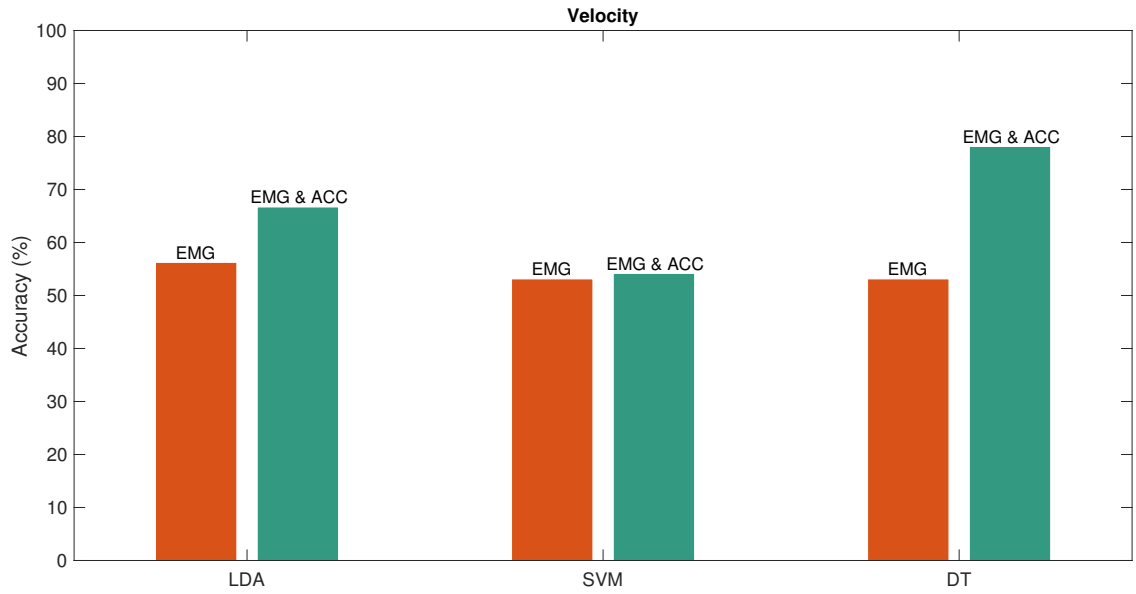

Figure 4.16: Classification accuracies of the trained models identifying velocity levels during ADL1.

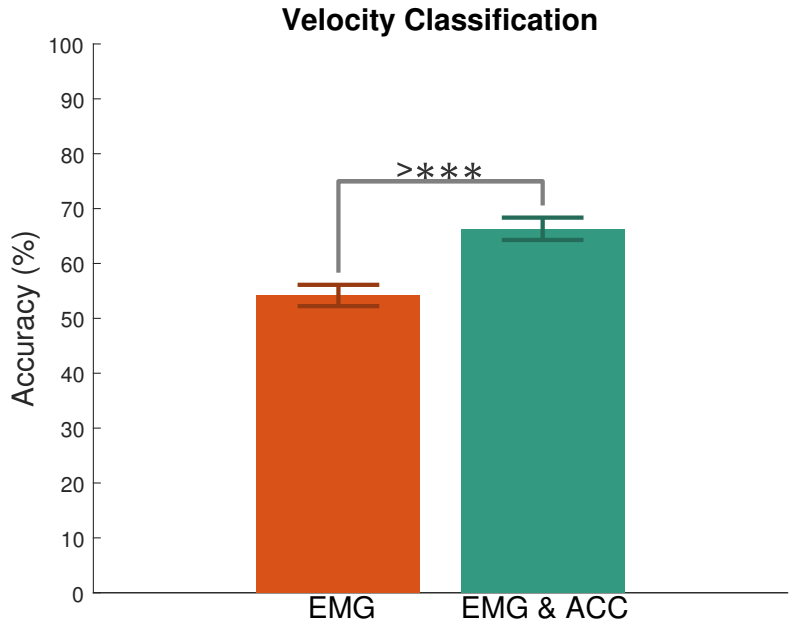

Figure 4.17: Mean velocity classification accuracies of each sensor modality during ADL1 motions. Asterisks denote statistical significance (* p <0.05; ** p <0.01; *** p <0.001). Error bars represent standard deviation.

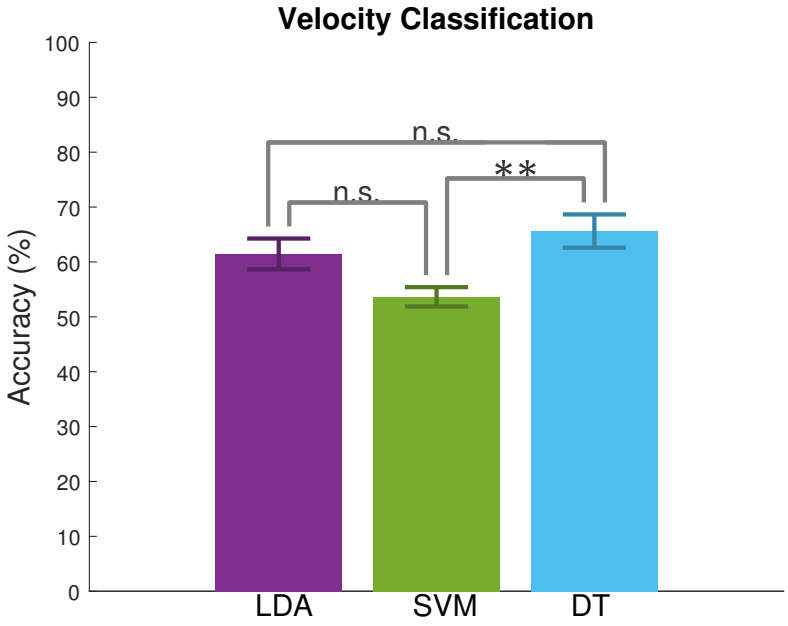

Figure 4.18: Mean velocity classification accuracies of each classifier during ADL1 motions. Asterisks denote statistical significance (* p <0.05; ** p <0.01; *** p <0.001), whereas "n.s." is written above non-significant comparisons. Error bars represent standard deviation.

shown in Fig. 4.21. Neither classifier performed significantly better or worse than the others with comparable accuracies.

4.3.8 ADL 2 Velocity

Very modest results were observed for velocity classification, as can bee seen in Figure 4.22. When training the classification models with both EMG and ACC data, accuracies ranged from 53% to 68.75%. The average accuracy results of each sensor modality during velocity classification are shown in Fig. 4.23. No statistically significant difference in accuracy was found between the two sensor modalities during ADL2. In addition, there were not any statistically significant differences between the accuracies of the 3 classifiers, as shown in Fig. 4.24. Neither classifier performed significantly better or worse than the others with comparable accuracies.

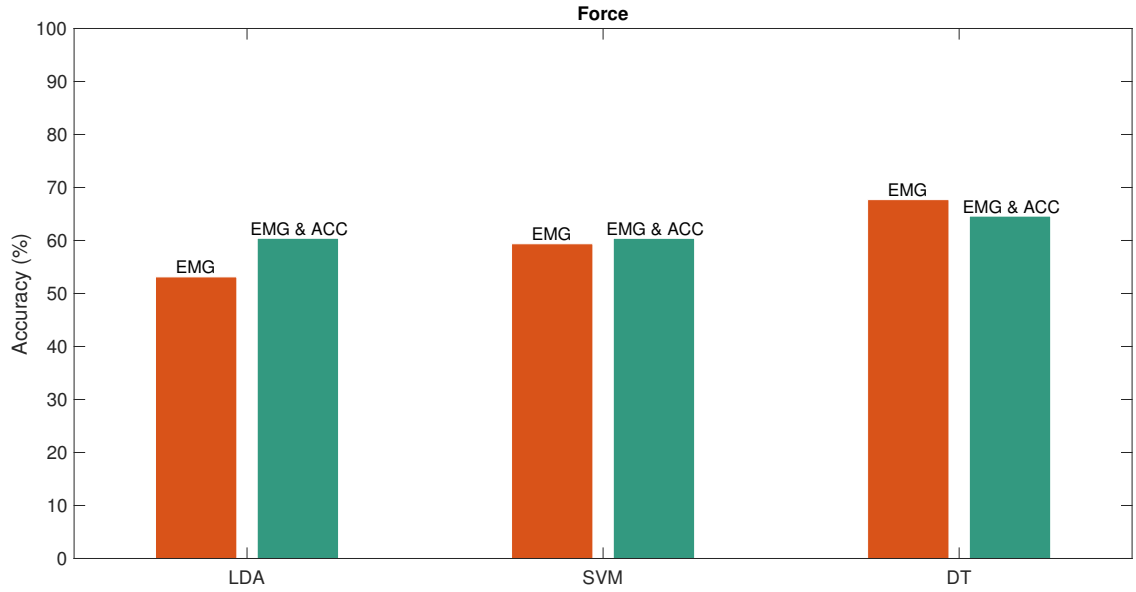

Figure 4.19: Classification accuracies of the trained models identifying force levels during ADL2.

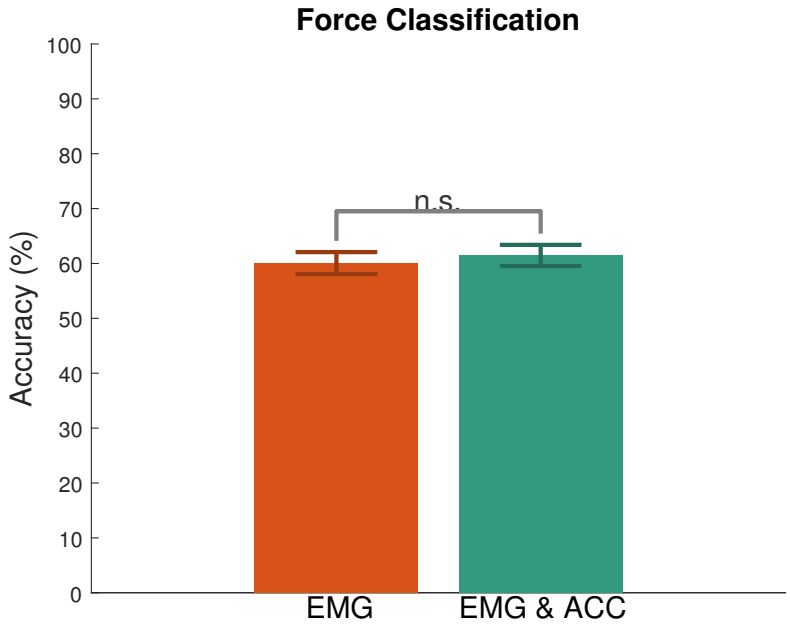

Figure 4.20: Mean force classification accuracies of each sensor modality during ADL2 motions. "n.s." is written above non-significant comparisons. Error bars represent standard deviation.

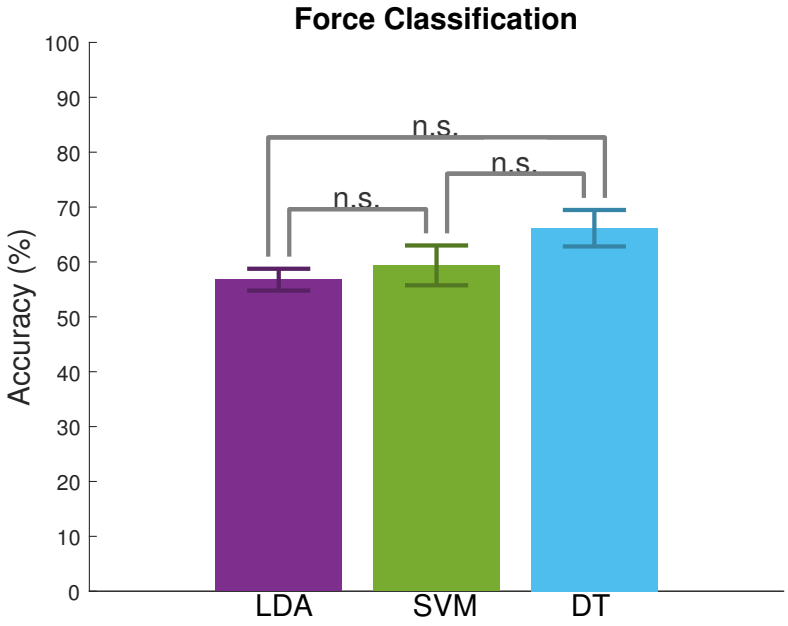

Figure 4.21: Mean force classification accuracies of each sensor classifier during ADL2 motions. "n.s." is written above non-significant comparisons. Error bars represent standard deviation.

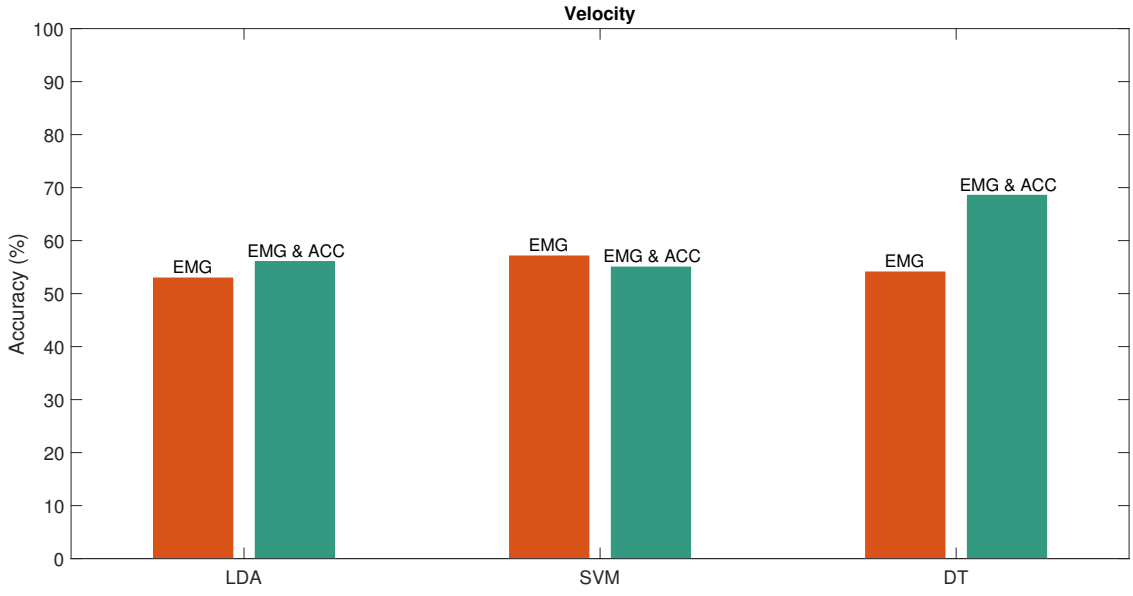

Figure 4.22: Classification accuracies of the trained models identifying velocity levels during ADL2.

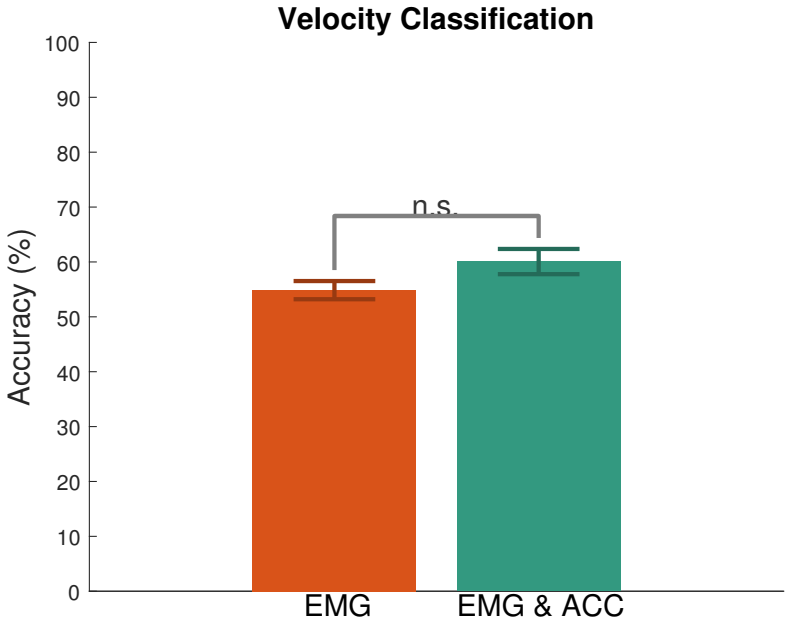

Figure 4.23: Mean velocity classification accuracies of each sensor modality during ADL2 motions. "n.s." is written above non-significant comparisons. Error bars represent standard deviation.

4.3.9 ADL 1 and ADL 2 Force

The last group included data from motions during both ADLs. The results of training classifiers to detect force levels are shown in Figure 4.25. Relatively low discrimination accuracies were observed. In addition, the accuracy of the LDA classifier decreased when ACC data were used. The average accuracy results of each sensor modality during force classification can be seen in Fig.4.26. A statistically significant difference in accuracy was found between the two sensor modalities, that indicated that EMG & ACC performed significantly worse. The average accuracy results of each classifier during force classification can be seen in Fig.4.27. A statistically significant difference between the accuracies of the LDA and DT Ensemble classifiers was found, indicating that performance of the LDA classifier was worse than the DT Ensemble.

4.3.10 ADL 1 and ADL 2 Velocity

The results of velocity classification during ADL 1 and ADL 2 are shown in Fig. 4.28. Low discrimination was also observed but the classification accuracies increased considerably when

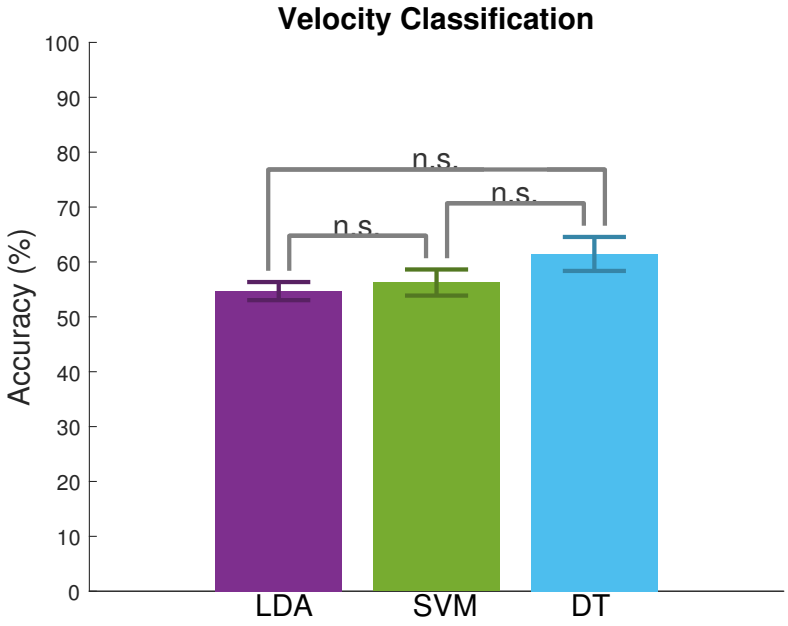

Figure 4.24: Mean velocity classification accuracies of each classifier during ADL2 motions. "n.s." is written above non-significant comparisons. Error bars represent standard deviation.

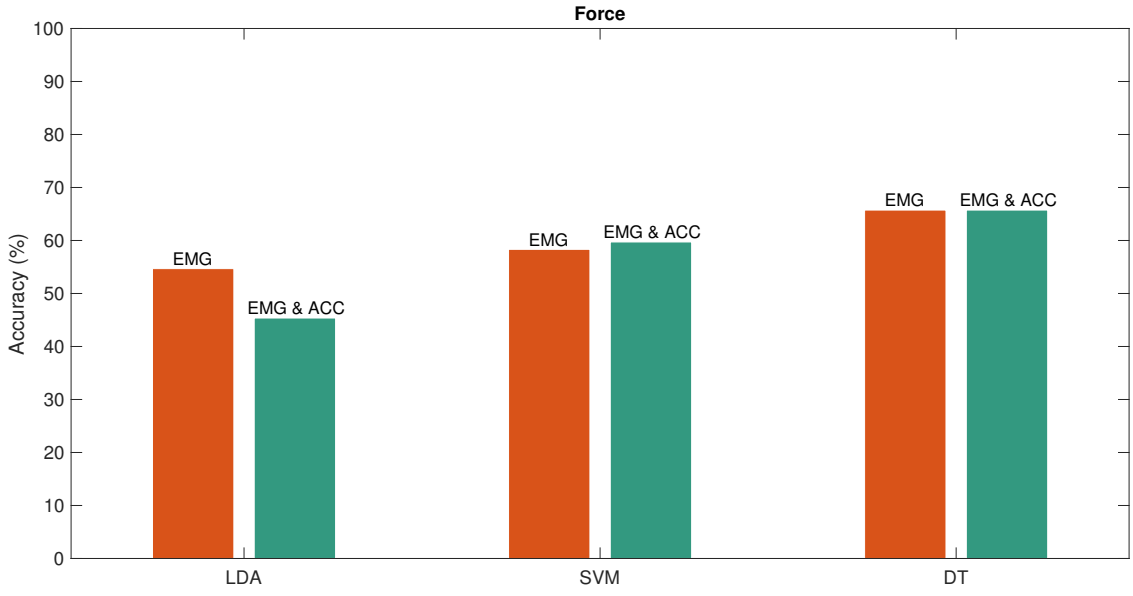

Figure 4.25: Classification accuracies of the trained models identifying force levels during both ADLs.

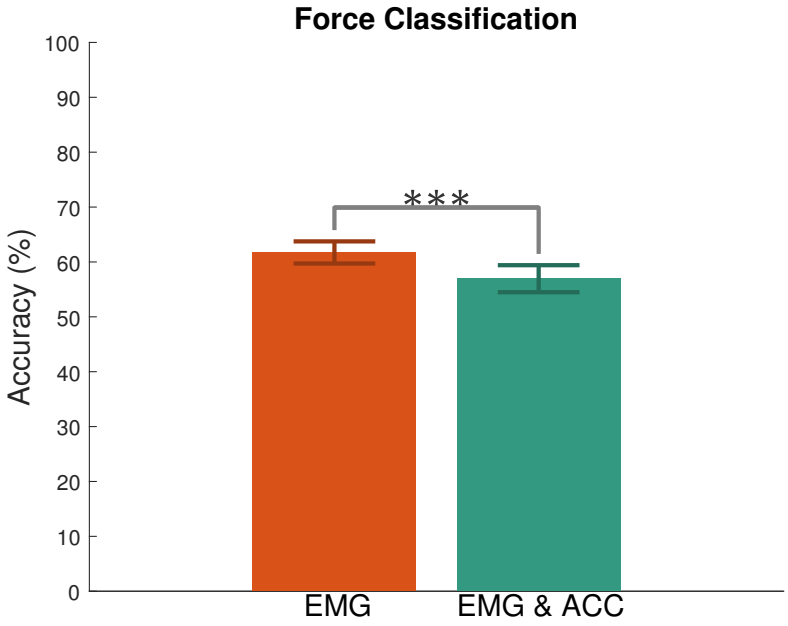

Figure 4.26: Mean force classification accuracies of each sensor modality during both ADLs. Asterisks denote statistical significance (* p <0.05; ** p <0.01; *** p <0.001). Error bars represent standard deviation.

ACC were used. The accuracy of LDA increased from 48.99% to 54.63%, SVM increased from 54.17% to 62.50% and DT Ensemble classifier increased from 62.50% to 72.22%. The average accuracy results of each sensor modality during velocity classification can be seen in Fig. 4.29.

A statistically significant difference in accuracy was found between the two modalities, indicating that EMG & ACC showed better classification accuracy than EMG. The average accuracy results of each classifier during velocity classification can be seen in Fig. 4.30. Statistically significant differences were found between the DT Ensemble and the other two classifiers, indicating that the DT Ensemble classifier showed a better accuracy.

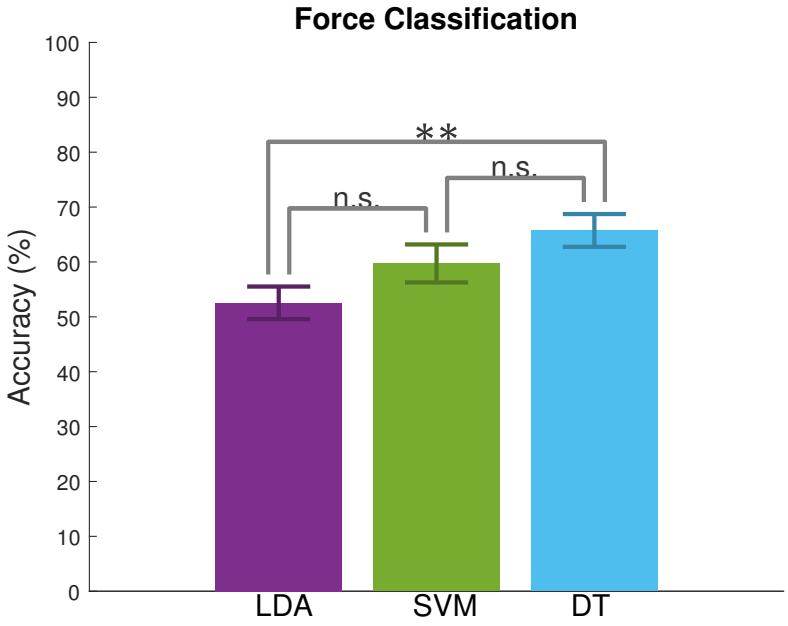

Figure 4.27: Mean force classification accuracies of each classifier during both ADLs. Asterisks denote statistical significance (* p <0.05; ** p <0.01; *** p <0.001), whereas "n.s." is written above non-significant comparisons. Error bars represent standard deviation.

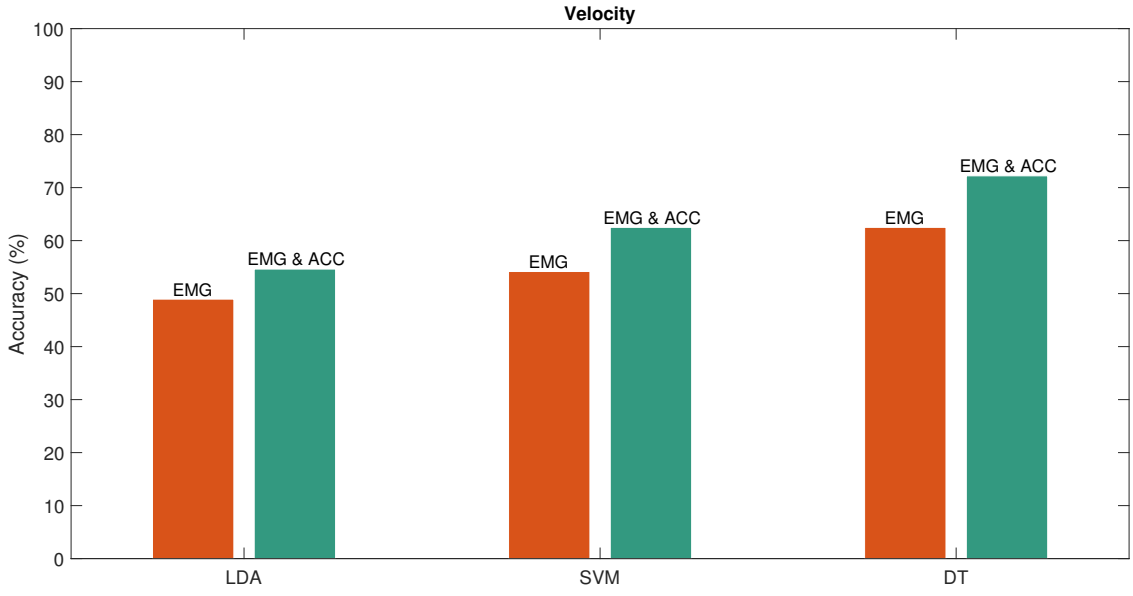

Figure 4.28: Classification accuracies of the trained models identifying velocity levels during both ADLs.

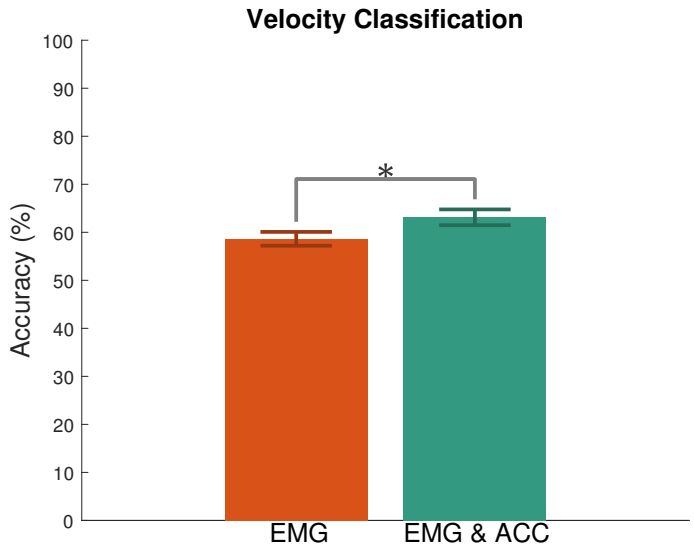

Figure 4.29: Mean velocity classification accuracies of each sensor modality during both ADLs. Asterisks denote statistical significance (* p <0.05; ** p <0.01; *** p <0.001). Error bars represent standard deviation.

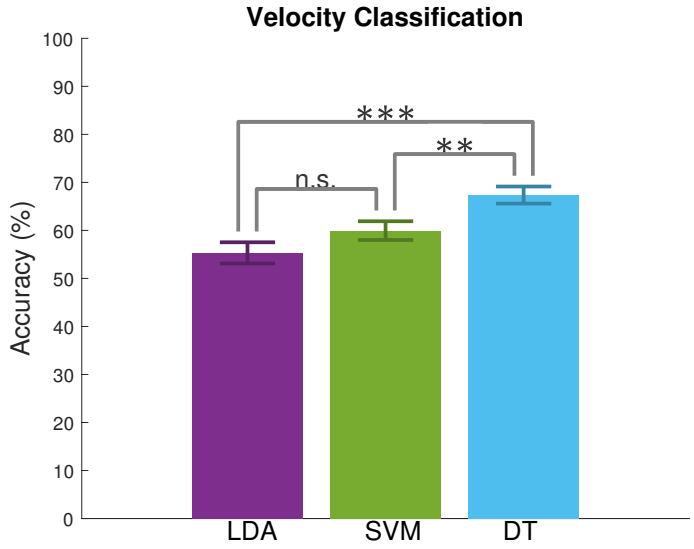

Figure 4.30: Mean velocity classification accuracies of each classifier during both ADLs. Asterisks denote statistical significance (* p <0.05; ** p <0.01; *** p <0.001), whereas "n.s." is written above non-significant comparisons. Error bars represent standard deviation.

4.4 Conclusion

This chapter presented the results of the implementation of motion characteristic classification using data collected from healthy subjects during the performance of several arm motions. EMG features, and a combination of EMG and ACC features, were fed into an LDA, SVM and DT Ensemble classifiers, which then detected categories of arm position, force levels, or movement.

As expected, it was observed that the combination of sensor modalities resulted in classifiers of a relatively higher accuracies. Consistent improvements were seen in velocity prediction. For instance, velocity classification (slow, fast) during ADL 1 was increased from 53.13% to 78.12% with a Decision Tree ensemble classifier using a boosting algorithm. In addition, the DT Ensemble classifier was capable of distinguishing velocity, between stationary and moving, during standard movements with less than 10% error (the maximum rate for a system classifying motions to be considered usable [60]). It was noted that the accuracy of the classifiers remained lower during ADLs than during standard movements. The poorer classification of motion characteristics for ADLs verifies that the control problem of using signals from wearable sensors to determine motion intention for ADLs is more complex than simple motions with limited movement [97].

The EMG & ACC sensor modality was identified to significantly improve the ability of the classification models to detect categories of arm position, force levels, and velocities during standard movements. However, including ACC information did not correspond with a consistent change in accuracy for identifying force levels during ADL1, ADL2, or the combination of ADL1 and ADL2 movements. It did increase the accuracy of velocity classification during AD1 and the combination of ADL1 and ADL2 movements. Furthermore, it was observed that, in most of the cases, none of the classification models performed better than the others. The main exception was the DT Ensemble classifier, which demonstrated a better ability to detect categories of velocities during standard movements and ADL1 movements.

Motion classifiers are commonly used to determine intended motion type such as wrist flexion–extension or grabbing objects [122]. In contrast, these results demonstrated that more information about intended motion can be determined wearable sensors. This is a potential way of improving the control of wearable mechatronic devices. Further applications of these findings are

discussed in the following chapter, along with the main conclusions and contributions from this work.

Chapter 5

Conclusions and Future Work

In this thesis, evidence that the inclusion of accelerometer information can significantly improve the classification scores was provided through an experimental evaluation. This is in line with previous studies employing sensor fusion. The use of accelerometers in EMG decoding was first proposed by Fougner et al. [18], who demonstrated that when data were collected under multiple limb positions, the use of accelerometers yielded a significant improvement in motion classification accuracy.

Accelerometer signals measured from 15 arm and shoulder muscles during motion trials were processed to extract relevant features. A statistical analysis was performed to quantify the way in which signal features varied depending on the motion factor (position, force, velocity) and motion type (standard movements or ADLs). We observed that the means of the features were significantly different across categories. This insight led to the inclusion of accelerometer features with muscle activation data in the training of classifiers to detect levels of motion characteristics.

It was demonstrated that a Decision Tree Ensemble classifier, trained with a combined set of EMG and ACC signal features, was capable of distinguishing isometric contractions from active motion during elbow flexion–extension with an accuracy of 91%. For comparison, a previous study distinguished motion from no motion with a classification error of 32.10%, using LDA and SVM models [97]. The approach presented in this study could be used to guide or tune the control models of a wearable mechatronic device.

It should be noted that gyroscope data were not used in these experiments. Given the relatively

higher power consumption of gyroscopes [123], it may be better to use EMG or ACC data when battery life and battery weight are critical factors, which applies for wearable mechatronic devices [9].

Importantly, there is yet no wearable sensor modality that can capture all aspects of human motor behaviour [123]. For instance, while accelerometers are sensitive to motion, they are not directly related to differences in force generation. Similarly, the relationship between muscle activation and motion is not straightforward.

Eventually, as more sensors capable of quantifying human motion and motor behaviour become available, a more comprehensive understanding of the relationships between sensor data and human motion will likely increase the accuracy of pattern recognition systems [123].

5.1 Contributions

The contributions of the work presented in this thesis are as follows:

- The observed effect of motion factors on accelerometer feature values led to the inclusion of information of this sensor modality into the motion intention detection. Even though other studies have already looked at the fusion of these sensors signals, this is the first time this type of fusion is used for motion characteristic classification, during upper limb movements. This work justifies the consideration of ACC signals as complementary inputs to a control system detecting intended elbow motion.
- A major contribution is the improvement of the performance of classification models when using combined ACC and EMG data.

5.2 Recommendations for Future Work

This section explains relevant topics for future work that can be done to effectively implement these methods during robot-assisted therapies. Suggested directions for future work are as follows:

- Perform feature reduction. The features employed in this study were selected as they are known to provide meaningful information. Nonetheless, feature reduction could be performed

to avoid redundant information and further improve the classification models [79].

- Implement sophisticated feature fusion techniques to improve the classifications methods. There are three main types of multi-sensor fusion: data-level fusion, decision-level fusion, and feature-level fusion [120]. During data-level fusion, data coming from multiple homogeneous sensors measuring the same physical phenomena are treated as a single dataset from which features are extracted. For its part, decision-level fusion refers to the process of selecting decisions coming from multiple sensors. Features coming from each sensor modality are classified separately and then, the outputs of these individual classifiers are combined using statistical methods to make a final decision [120]. In this work, feature-level fusion was implemented. During feature-level fusion, feature matrices from each sensor modality are joined into a single multi-dimensional feature vector from which the classification is made. The main drawback of this technique is that, in most cases, feature reduction algorithms are required to find an optimal feature vector. Further research should explore the effects of these fusion levels on the classification performance of motion characteristic classifiers.

- Repeat the study with data from subjects with a musculoskeletal injury or going through the process of rehabilitation. Investigate differences in EMG and ACC features between subjects with and without an injury. Since the movements of subjects with an injury may be more constrained during ADLs, it is expected that fewer significant differences in ACC features would be observed, since these are indicators of gross motion and movement intensity [118]. Thus, a reduction in the classification performance might also be observed.

- Alternative applications. The methods developed in this study can also be used on other problems; not only upper-limb devices. They can be used on other joints, such as the knee.

The purpose of this thesis was to implement motion detection classification models using accelerometer and EMG-based sensor fusion. The main objective of this work was to increase the accuracy of motion intention detection. In this sense, improved accuracies were achieved. Further work developing more strategies for using sensor fusion techniques to achieve better motion intention detection will be able to promote long term adoption of wearable mechatronic devices during rehabilitation.

References

[1] G. . D. Collaborators, I. Incidence, and Prevalence, "Global, regional, and national incidence, prevalence, and years lived with disability for 328 diseases and injuries for 195 countries, 1990-2016: A systematic analysis for the Global Burden of Disease Study 2016," *The Lancet*, vol. 390, no. 10100, pp. 1211–1259, 2017.

[2] Canadian Institutes of Health Research and Institute of Musculoskeletal Health and Arthritis, "Institute of Musculoskeletal Health and Arthritis, Strategic Plan 2014-2018: Enhancing Musculoskeletal, Skin and Oral Health," pp. 1–26, 2014.

[3] A. D. Woolf and B. Pfleger, "Burden of major musculoskeletal conditions," *Bulletin of the World Health Organization*, vol. 81, no. 9, pp. 646–656, 2003.

[4] D. G. Hoy, E. Smith, M. Cross, L. Sanchez-Riera, F. M. Blyth, R. Buchbinder, A. D. Woolf, T. Driscoll, P. Brooks, and L. M. March, "Reflecting on the global burden of musculoskeletal conditions: Lessons learnt from the global burden of disease 2010 study and the next steps forward," *Annals of the Rheumatic Diseases*, vol. 74, no. 1, pp. 4–7, 2015.

[5] H. S. Lo and S. Q. Xie, "Exoskeleton robots for upper-limb rehabilitation: State of the art and future prospects," *Medical Engineering and Physics*, vol. 34, no. 3, pp. 261–268, 2012.

[6] K. E. Wilk, L. C. Macrina, E. L. Cain, J. R. Dugas, and J. R. Andrews, "Rehabilitation of the Overhead Athlete's Elbow," *Sports Health*, vol. 4, no. 5, pp. 404–414, 2012.

[7] I. Fusaro, S. Orsini, S. Stignani Kantar, T. Sforza, M. G. Benedetti, G. Bettelli, and R. Rotini, "Elbow rehabilitation in traumatic pathology," *Musculoskeletal Surgery*, vol. 98, no. SUPPL. 1, pp. 95–102, 2014.

[8] S. Bassett, "The assessment of patient adherence to physiotherapy rehabilitation," *New Zealand journal of physiotherapy*, vol. 31, no. 2, pp. 60–66, 2003.

[9] T. Desplenter, *Development of Digital Control Systems for Wearable Mechatronic Devices: Applications in Musculoskeletal Rehabilitation of the Upper Limb*. PhD thesis, 2018.

[10] P. S. Lum, C. G. Burgar, P. C. Shor, M. Majmundar, and M. Van der Loos, "Robot-assisted movement training compared with conventional therapy techniques for the rehabilitation of upper-limb motor function after stroke," *Archives of Physical Medicine and Rehabilitation*, vol. 83, no. 7, pp. 952–959, 2002.

[11] B. T. Volpe, D. Lynch, A. Rykman-Berland, M. Ferraro, M. Galgano, N. Hogan, and H. I. Krebs, "Intensive sensorimotor arm training mediated by therapist or robot improves hemiparesis in patients with chronic stroke," *Neurorehabilitation and Neural Repair*, vol. 22, no. 3, pp. 305–310, 2008.

[12] S. Page, V. Hill, and S. White, "Portable Upper Extremity Robotics is as Efficacious as Upper Extremity Rehabilitative Therapy," *Clinical Rehabilitation*, vol. 27, no. 6, pp. 494–503, 2013.

[13] H. T. Peters, S. J. Page, and A. Persch, "Giving Them a Hand: Wearing a Myoelectric Elbow-Wrist-Hand Orthosis Reduces Upper Extremity Impairment in Chronic Stroke," *Archives of Physical Medicine and Rehabilitation*, vol. 98, no. 9, pp. 1821–1827, 2017.

[14] T. Desplenter, A. Kyrylova, T. K. Stanbury, A. Escoto, S. Chinchalkar, and A. L. Trejos, "A wearable mechatronic brace for arm rehabilitation," *5th IEEE RAS/EMBS International Conference on Biomedical Robotics and Biomechatronics*, pp. 491–496, 2014.

[15] C. J. De Luca, "The use of surface electromyography in biomechanics," *Journal of Applied Biomechanics*, vol. 13, no. 2, pp. 135–163, 1997.

[16] R. A. Gopura, D. S. Bandara, K. Kiguchi, and G. K. Mann, "Developments in hardware systems of active upper-limb exoskeleton robots: A review," *Robotics and Autonomous Systems*, vol. 75, pp. 203–220, 2016.

[17] R. N. Khushaba, A. Al-Timemy, S. Kodagoda, and K. Nazarpour, "Combined influence of forearm orientation and muscular contraction on EMG pattern recognition," *Expert Systems with Applications*, vol. 61, pp. 154–161, 2016.

[18] A. Fougner, E. Scheme, A. D. Chan, K. Englehart, and Ø. Stavdahl, "Resolving the limb position effect in myoelectric pattern recognition," *IEEE Transactions on Neural Systems and Rehabilitation Engineering*, vol. 19, no. 6, pp. 644–651, 2011.

[19] N. Gebruers, S. Truijen, S. Engelborghs, G. Nagels, R. Brouns, and P. P. De Deyn, "Actigraphic measurement of motor deficits in acute ischemic stroke," *Cerebrovascular Diseases*, vol. 26, no. 5, pp. 533–540, 2008.

[20] A. Godfrey, A. K. Bourke, G. M. Ólaighin, P. van de Ven, and J. Nelson, "Activity classification using a single chest mounted tri-axial accelerometer," *Medical Engineering and Physics*, vol. 33, no. 9, pp. 1127–1135, 2011.

[21] D. M. Karantonis, M. R. Narayanan, M. Mathie, N. H. Lovell, and B. G. Celler, "Implementation of a real-time human movement classifier using a triaxial accelerometer for ambulatory monitoring," *IEEE Transactions on Information Technology in Biomedicine*, vol. 10, no. 1, pp. 156–167, 2006.

[22] A. Mannini and A. M. Sabatini, "Machine learning methods for classifying human physical activity from on-body accelerometers," *Sensors*, vol. 10, no. 2, pp. 1154–1175, 2010.

[23] D. Rand, J. J. Eng, P. F. Tang, J. S. Jeng, and C. Hung, "How active are people with stroke?: use of accelerometers to assess physical activity.," *Stroke; a journal of cerebral circulation*, vol. 40, no. 1, pp. 163–168, 2009.

[24] B. F. Morrey, "Anatomy and biomechanics of the elbow joint.," *Instructional course lectures*, vol. 35, no. 4, pp. 59–68, 1986.

[25] C. Shirota, J. Jansa, J. Diaz, S. Balasubramanian, S. Mazzoleni, N. A. Borghese, and A. Melendez-Calderon, "On the assessment of coordination between upper extremities: Towards a common language between rehabilitation engineers, clinicians and neuroscientists," *Journal of NeuroEngineering and Rehabilitation*, vol. 13, no. 1, pp. 1–14, 2016.

[26] J. C. MacDermid, J. I. Vincent, L. Kieffer, A. Kieffer, J. Demaiter, and S. MacIntosh, "A Survey of Practice Patterns for Rehabilitation Post Elbow Fracture," *The Open Orthopaedics Journal*, vol. 6, no. 1, pp. 429–439, 2012.

[27] L. Q. Zhang, J. Son, H. S. Park, S. H. Kang, Y. Lee, and Y. Ren, "Changes of shoulder, elbow, and wrist stiffness matrix post stroke," *IEEE Transactions on Neural Systems and Rehabilitation Engineering*, vol. 25, no. 7, pp. 844–851, 2017.

[28] S. J. Chinchalkar and M. Szekeres, "Rehabilitation of elbow trauma," *Hand Clinics*, vol. 20, no. 4, pp. 363–374, 2004.

[29] J. Kristensen and F.-M. Andy, "Resistance training in musculoskeletal rehabilitation: a systematic review," *British Journal of Sports Medicine*, vol. 46, pp. 719–726, 2012.

[30] A. Marinelli, G. Bettelli, E. Guerra, M. Nigrisoli, and R. Rotini, "Mobilization brace in post-traumatic elbow stiffness," *Musculoskeletal Surgery*, vol. 94, no. SUPP, 2010.

[31] T. Walters-Salas, "The challenge of patient adherence," *Bariatric Nursing and Surgical Patient Care*, vol. 7, no. 4, p. 186, 2012.

[32] L. O'brien, "Adherence to therapeutic splint wear in adults with acute upper limb injuries: A systematic review," *Hand Therapy*, vol. 15, no. 1, pp. 3–12, 2010.

[33] J. Mehrholz, M. Pohl, K. J, and B. Elsner, "Electromechanical and robot-assisted arm training for improving activities of daily living, arm function, and arm muscle strength after stroke," *The Cochrane database of systematic reviews*, vol. 2015, no. 11, p. CD006876, 2015.

[34] S. L. Wolf, P. A. Thompson, D. M. Morris, D. K. Rose, C. J. Winstein, E. Taub, C. Giuliani, and S. L. Pearson, "The EXCITE trial: Attributes of the Wolf Motor Function Test in patients with subacute stroke," *Neurorehabilitation and Neural Repair*, vol. 19, no. 3, pp. 194–205, 2005.

[35] J. I. Vincent, J. C. Macdermid, G. J. King, and R. Grewal, "Linking of the Patient Rated Elbow Evaluation (PREE) and the American Shoulder and Elbow Surgeons - Elbow questionnaire (pASES-e) to the International Classification of Functioning Disability and Health (ICF) and hand core sets," *Journal of Hand Therapy*, vol. 28, no. 1, pp. 61–68, 2015.

[36] S. H. Roy, M. S. Cheng, J. Moore, G. De Luca, S. H. Nawab, and C. J. De Luca, "A Combined sEMG and Accelerometer System for Monitoring Functional Activity in Stroke," *IEEE Transactions on Neural Systems and Rehabilitation Engineering*, vol. 17, no. 6, pp. 585–594, 2009.

[37] M. H. Rahman, M. Saad, J. P. Kenné, and P. S. Archambault, "Nonlinear Sliding Mode Control Implementation of an Upper Limb Exoskeleton Robot to Provide Passive Rehabilitation Therapy," in *Lecture Notes in Computer Science (including subseries Lecture Notes in Artificial Intelligence and Lecture Notes in Bioinformatics)*, pp. 52–62, Springer, Berlin, Heidelberg, 2012.

[38] R. Colombo, F. Pisano, S. Micera, A. Mazzone, C. Delconte, M. Chiara Carrozza, P. Dario, and G. Minuco, "Robotic techniques for upper limb evaluation and rehabilitation of stroke patients," *IEEE Transactions on Neural Systems and Rehabilitation Engineering*, vol. 13, no. 3, pp. 311–324, 2005.

[39] M. S. Erden and A. Billard, "End-point impedance measurements across dominant and nondominant hands and robotic assistance with directional damping," *IEEE Transactions on Cybernetics*, vol. 45, no. 6, pp. 1146–1157, 2015.

[40] N. Hogan, H. I. Krebs, J. Charnnarong, P. Srikrishna, and A. Sharon, "MIT-MANUS: A Workstation for Manual Therapy and Training," in *IEEE International Workshop on Robot and Human Communication*, pp. 161–165, 1992.

[41] R. Loureiro, F. Amirabdollahian, M. Topping, B. Driessen, and W. Harwin, "Upper Limb Robot Mediated Stroke Therapy—GENTLEs Approach," *Autonomous Robots*, vol. 15, pp. 35–51, 2003.

[42] G. Fazekas, M. Horvath, and A. Toth, "A novel robot training system designed to supplement upper limb physiotherapy of patients with spastic hemiparesis," *International Journal of Rehabilitation Research*, vol. 29, no. 3, pp. 251–254, 2006.

[43] P. Maciejasz, J. Eschweiler, K. Gerlach-Hahn, A. Jansen-Troy, and S. Leonhardt, "A survey on robotic devices for upper limb rehabilitation," *Journal of NeuroEngineering and Rehabilitation*, 2014.

[44] T. Proietti, V. Crocher, A. Roby-Brami, and N. Jarrasse, "Upper-limb robotic exoskeletons for neurorehabilitation: A review on control strategies," *IEEE Reviews in Biomedical Engineering*, vol. 9, pp. 4–14, 2016.

[45] A. Basteris, A. F., N. S.M., B. J.H., P. G.B., and S. A.H.A., "Training modalities in robot-mediated upper limb rehabilitation in stroke: A framework for classification based on a systematic review," *Journal of NeuroEngineering and Rehabilitation*, vol. 11, no. 1, pp. 1–15, 2014.

[46] R. Looned, J. Webb, Z. G. Xiao, and C. Menon, "Assisting drinking with an affordable BCI-controlled wearable robot and electrical stimulation: A preliminary investigation," *Journal of NeuroEngineering and Rehabilitation*, vol. 11, no. 1, pp. 1–13, 2014.

[47] T. Morizono, T. Komiya, and M. Higashi, "Study on a Wearable Elbow Joint Capable of Mechanical Adjustment of Stiffness," pp. 552–557, 2009.

[48] T. Ripel, J. Krejsa, and J. Hrbáček, "Patient Activity Measurement in Active Elbow Orthosis," in *Mechatronics 2013*, (Cham), pp. 817–824, Springer International Publishing, 2014.

[49] S. Schulz, C. Pylatiuk, I. Gaiser, and M. Reischl, "Design of a Hybrid Powered Upper Limb Orthisis," *IFMBE Proceedings*, vol. 25, no. 9, pp. 468–471, 2009.

[50] I. Vanderniepen, R. Van Ham, M. Van Damme, R. Versluys, and D. Lefeber, "Orthopaedic rehabilitation: A powered elbow orthosis using compliant actuation," *2009 IEEE International Conference on Rehabilitation Robotics, ICORR 2009*, pp. 172–177, 2009.

[51] T. Wilps, R. A. Kaufmann, S. Yamakawa, and J. R. Fowler, "Elbow Biomechanics: Bony and Dynamic Stabilizers," *Journal of Hand Surgery*, vol. 45, no. 6, pp. 528–535, 2020.

[52] D. Copaci, F. Martin, L. Moreno, and D. Blanco, "SMA Based Elbow Exoskeleton for Rehabilitation Therapy and Patient Evaluation," *IEEE Access*, vol. 7, pp. 31473–31484, 2019.

[53] T. Wojtara, F. Alnajjar, S. Shimoda, and H. Kimura, "Muscle synergy stability and human balance maintenance," *Journal of NeuroEngineering and Rehabilitation*, vol. 11, no. 1, pp. 1–9, 2014.

[54] C. Disselhorst-Klug, T. Schmitz-Rode, and G. Rau, "Surface electromyography and muscle force: Limits in sEMG-force relationship and new approaches for applications," *Clinical Biomechanics*, vol. 24, pp. 225–235, mar 2009.

[55] G. Kamen and D. A. Gabriel, *Essentials of Electromyography*. 2009.

[56] H. J. Hermens, B. Freriks, C. Disselhorst-Klug, and G. Rau, "Development of recommendations for SEMG sensors and sensor placement procedures," *Journal of Electromyography and Kinesiology*, vol. 10, pp. 361–374, 2000.

[57] J. L. Nielsen, S. Holmgaard, N. Jiang, K. B. Englehart, D. Farina, and P. A. Parker, "Simultaneous and proportional force estimation for multifunction myoelectric prostheses using mirrored bilateral training," *IEEE Transactions on Biomedical Engineering*, vol. 58, no. 3 PART 1, pp. 681–688, 2011.

[58] D. Farina, "Interpretation of the surface electromyogram in dynamic contractions," *Exercise and Sport Sciences Reviews*, vol. 34, no. 3, pp. 121–127, 2006.

[59] M. Asghari Oskoei and H. Hu, "Myoelectric control systems-A survey," *Biomedical Signal Processing and Control*, vol. 2, no. 4, pp. 275–294, 2007.

[60] M. Hakonen, H. Piitulainen, and A. Visala, "Current state of digital signal processing in myoelectric interfaces and related applications," *Biomedical Signal Processing and Control*, vol. 18, pp. 334–359, 2015.

[61] D. R. Bueno and L. Montano, "An optimized model for estimation of muscle contribution and human joint torques from sEMG information," *Proceedings of the Annual International Conference of the IEEE Engineering in Medicine and Biology Society, EMBS*, no. 2, pp. 3364–3367, 2012.

[62] D. A. Funk, K. N. An, B. F. Morrey, and J. R. Daube, "Electromyographic analysis of muscles across the elbow joint.," *Journal of orthopaedic research : official publication of the Orthopaedic Research Society*, vol. 5, no. 4, pp. 529–538, 1987.

[63] S. Guo, M. Pang, B. Gao, H. Hirata, and H. Ishihara, "Comparison of sEMG-based feature extraction and motion classification methods for upper-limb movement," *Sensors (Switzerland)*, vol. 15, no. 4, pp. 9022–9038, 2015.

[64] Z. O. Khokhar, Z. G. Xiao, and C. Menon, "Surface EMG pattern recognition for real-time control of a wrist exoskeleton," *BioMedical Engineering Online*, vol. 9, pp. 1–17, 2010.

[65] K. Kiguchi and Y. Hayashi, "Motion estimation based on EMG and EEG signals to control wearable robots," *Proceedings - 2013 IEEE International Conference on Systems, Man, and Cybernetics, SMC 2013*, pp. 4213–4218, 2013.

[66] T. K. Koo and A. F. Mak, "Feasibility of using EMG driven neuromusculoskeletal model for prediction of dynamic movement of the elbow," *Journal of Electromyography and Kinesiology*, vol. 15, no. 1, pp. 12–26, 2005.

[67] T. Lenzi, S. M. M. De Rossi, N. Vitiello, and M. C. Carrozza, "Intention-based EMG control for powered exoskeletons," *IEEE Transactions on Biomedical Engineering*, vol. 59, no. 8, pp. 2180–2190, 2012.

[68] F. P. Kendall, *Muscles: Testing and Function With Posture and Pain*. Philadelphia, PA: American Physical Therapy Association, Inc, 5th ed., 2005.

[69] F. H. Netter, *Atlas of human anatomy*. Philadelphia: Saunders/Elsevier, 5th ed., 2011.

[70] R. Snell, *Clinical anatomy by regions*. Philadelphia: Lippincott Williams & Wilkins, 8th ed., 2008.

[71] E. J. Rechy-Ramirez and H. Hu, "Bio-signal based control in assistive robots: a survey," *Digital Communications and Networks*, vol. 1, no. 2, pp. 85–101, 2015.

[72] F. Ryser, T. Bützer, J. P. Held, O. Lambercy, and R. Gassert, "Fully embedded myoelectric control for a wearable robotic hand orthosis," in *IEEE International Conference on Rehabilitation Robotics*, pp. 615–621, 2017.

[73] J. Wang, L. Tang, and J. E Bronlund, "Surface EMG Signal Amplification and Filtering," *International Journal of Computer Applications*, vol. 82, no. 1, pp. 15–22, 2013.

[74] J. R. Potvin and S. H. Brown, "Less is more: High pass filtering, to remove up to 99% of the surface EMG signal power, improves EMG-based biceps brachii muscle force estimates," *Journal of Electromyography and Kinesiology*, vol. 14, no. 3, pp. 389–399, 2004.

[75] P. W. Hodges and B. H. Bui, "A comparison of computer-based methods for the determination of onset of muscle contraction using electromyography," *Electroencephalography and clinical Neurophysiology*, pp. 511–519, 1996.

[76] J. H. Abbink, A. Van Der Bilt, and H. W. Van Der Glas, "Detection of onset and termination of muscle activity in surface electromyograms," *Journal of Oral Rehabilitation*, vol. 25, no. 5, pp. 365–369, 1998.

[77] B. Hudgins, P. Parker, and R. N. Scott, "A New Strategy for Multifunction Myoelectric Control," *IEEE Transactions on Biomedical Engineering*, vol. 40, no. 1, pp. 82–94, 1993.

[78] M. A. Oskoei and H. Hu, "Support vector machine-based classification scheme for myoelectric control applied to upper limb," *IEEE Transactions on Biomedical Engineering*, vol. 55, no. 8, pp. 1956–1965, 2008.

[79] A. Phinyomark, P. Phukpattaranont, and C. Limsakul, "Feature reduction and selection for EMG signal classification," *Expert Systems with Applications*, vol. 39, no. 8, pp. 7420–7431, 2012.

[80] K. Englehart and B. Hudgins, "A Robust, Real-Time Control Scheme for Multifunction Myoelectric Control," *IEEE Transactions on Biomedical Engineering*, vol. 50, no. 7, pp. 848–854, 2003.

[81] M. Zecca, S. Micera, M. C. Carrozza, and P. Dario, "Control of multifunctional prosthetic hands by processing the electromyographic signal," *Critical Reviews in Biomedical Engineering*, vol. 30, no. 4-6, pp. 459–485, 2002.

[82] L. J. Hargrove, G. Li, K. B. Englehart, and B. S. Hudgins, "Principal components analysis preprocessing for improved classification accuracies in pattern-recognition-based myoelectric control," *IEEE Transactions on Biomedical Engineering*, vol. 56, no. 5, pp. 1407–1414, 2009.

[83] R. James, G., Witten, D., Hastie, T., Tibshirani, *An Introduction to Statistical Learning with Applications in R.* 2013.

[84] F. AlOmari and G. Liu, "Analysis of extracted forearm sEMG signal using LDA, QDA, K-NN classification algorithms," *Open Automation and Control Systems Journal*, vol. 6, no. 1, pp. 108–116, 2014.

[85] K. S. Kim, H. H. Choi, C. S. Moon, and C. W. Mun, "Comparison of k-nearest neighbor, quadratic discriminant and linear discriminant analysis in classification of electromyogram signals based on the wrist-motion directions," *Current Applied Physics*, vol. 11, no. 3, pp. 740–745, 2011.

[86] M. A. Hearst, S. T. Dumais, E. Osuna, J. Platt, and B. Scholkopf, "Support vector machines," *IEEE Intelligent Systems and their Applications*, vol. 13, no. 4, pp. 18–28, 1998.

[87] F. Amirabdollahian and M. L. Walters, "Application of support vector machines in detecting hand grasp gestures using a commercially off the shelf wireless myoelectric armband," *IEEE International Conference on Rehabilitation Robotics*, pp. 111–115, 2017.

[88] S. Patel, R. Hughes, T. Hester, J. Stein, M. Akay, J. G. Dy, and P. Bonato, "A novel approach to monitor rehabilitation outcomes in stroke survivors using wearable technology," *Proceedings of the IEEE*, vol. 98, no. 3, pp. 450–461, 2010.

[89] Y. Freund and R. E. Schapire, "A Decision-Theoretic Generalization of On-Line Learning and an Application to Boosting," *Journal of Computer and System Sciences*, vol. 55, no. 1, pp. 119–139, 1997.

[90] R. E. Schapire, *Explaining AdaBoost*, pp. 37–52. Berlin, Heidelberg: Springer Berlin Heidelberg, 2013.

[91] A. A. Lima, R. M. Araujo, F. A. D. Santos, V. H. Yoshizumi, F. K. De Barros, D. H. Spatti, L. H. Liboni, and M. E. Dajer, "Classification of Hand Movements from EMG Signals using Optimized MLP," *Proceedings of the International Joint Conference on Neural Networks*, vol. 2018-July, pp. 14–15, 2018.

[92] E. Scheme and K. Englehart, "Electromyogram pattern recognition for control of powered upper-limb prostheses: State of the art and challenges for clinical use," *Journal of Rehabilitation Research and Development*, vol. 48, no. 6, pp. 643–660, 2011.

[93] E. Farago and A. L. Trejos, *Development of an EMG-based Muscle Health Model for Elbow Trauma Patients*. PhD thesis, Western University, 2018.

[94] N. Jiang, S. Dosen, K. R. Muller, and D. Farina, "Myoelectric control of artificial limbsis there a need to change focus?," *IEEE Signal Processing Magazine*, vol. 29, no. 5, pp. 148–152, 2012.

[95] T. Lorrain, N. Jiang, and D. Farina, "Influence of the training set on the accuracy of surface EMG classification in dynamic contractions for the control of multifunction prostheses," *Journal of NeuroEngineering and Rehabilitation*, vol. 8, no. 1, p. 25, 2011.

[96] D. Yang, W. Yang, Q. Huang, and H. Liu, "Classification of Multiple Finger Motions during Dynamic Upper Limb Movements," *IEEE Journal of Biomedical and Health Informatics*, vol. 21, no. 1, pp. 134–141, 2017.

[97] T. Stanbury and A. L. Trejos, *Dynamic Calibration of EMG Signals for Control of a Wearable Elbow Brace*. PhD thesis, Western University, 2018.

[98] K. H. Park, H. I. Suk, and S. W. Lee, "Position-independent decoding of movement intention for proportional myoelectric interfaces," *IEEE Transactions on Neural Systems and Rehabilitation Engineering*, vol. 24, no. 9, pp. 928–939, 2016.

[99] S. C. F. A. von Werder and C. Disselhorst-Klug, "The role of biceps brachii and brachioradialis for the control of elbow flexion and extension movements," *Journal of Electromyography and Kinesiology*, vol. 28, pp. 67–75, 2016.

[100] D. W. Franklin, G. Liaw, T. E. Milner, R. Osu, E. Burdet, and M. Kawato, "Endpoint stiffness of the arm is directionally tuned to instability in the environment," *Journal of Neuroscience*, vol. 27, no. 29, pp. 7705–7716, 2007.

[101] M. Farooq and A. A. Khan, "Effects of shoulder rotation combined with elbow flexion ondiscomfort and EMG activity of ECRB muscle," *International Journal of Industrial Ergonomics*, vol. 44, no. 6, pp. 882–891, 2014.

[102] R. Merletti, M. Aventaggiato, A. Botter, A. Holobar, H. Marateb, and T. M. M. Vieira, "Advances in surface EMG: recent progress in detection and processing techniques.," *Critical reviews in biomedical engineering*, vol. 38, no. 4, pp. 305–345, 2010.

[103] J. Hashemi, E. Morin, P. Mousavi, and K. Hashtrudi-Zaad, "Enhanced dynamic EMG-force estimation through calibration and PCI modeling," *IEEE Transactions on Neural Systems and Rehabilitation Engineering*, vol. 23, no. 1, pp. 41–50, 2015.

[104] J.-H. Song, J.-W. Jung, and Z. Bien, "Robust EMG Pattern Recognition to Muscular Fatigue Effect for Human-Machine Interaction BT - MICAI 2006: Advances in Artificial Intelligence," (Berlin, Heidelberg), pp. 1190–1199, Springer Berlin Heidelberg, 2006.

[105] N. A. Dimitrova and G. V. Dimitrov, "Interpretation of EMG changes with fatigue: Facts, pitfalls, and fallacies," *Journal of Electromyography and Kinesiology*, vol. 13, no. 1, pp. 13–36, 2003.

[106] D. K. Kumar, S. P. Arjunan, and G. R. Naik, "Measuring increase in synchronization to identify muscle endurance limit," *IEEE Transactions on Neural Systems and Rehabilitation Engineering*, vol. 19, no. 5, pp. 578–587, 2011.

[107] G. Venugopal, M. Navaneethakrishna, and S. Ramakrishnan, "Extraction and analysis of multiple time window features associated with muscle fatigue conditions using sEMG signals," *Expert Systems with Applications*, vol. 41, no. 6, pp. 2652–2659, 2014.

[108] D. Blana, T. Kyriacou, J. M. Lambrecht, and E. K. Chadwick, "Feasibility of using combined EMG and kinematic signals for prosthesis control: A simulation study using a virtual reality environment," *Journal of Electromyography and Kinesiology*, vol. 29, pp. 21–27, 2016.

[109] N. Popovic, S. Williams, T. Schmitz-rode, and C. Disselhorst-klug, "Robot-based methodology for a kinematic and kinetic analysis of unconstrained , but reproducible upper extremity movement," vol. 42, pp. 1570–1573, 2009.

[110] A. Albu-Schäffer and G. Hirzinger, "Cartesian impedance control techniques for torque controlled light-weight robots," *Proceedings - IEEE International Conference on Robotics and Automation*, vol. 1, no. May, pp. 657–663, 2002.

[111] C. E. Boettcher, K. A. Ginn, and I. Cathers, "Standard maximum isometric voluntary contraction tests for normalizing shoulder muscle EMG," *Journal of Orthopaedic Research*, vol. 26, no. 12, pp. 1591–1597, 2008.

[112] E. Scheme, B. Lock, L. Hargrove, W. Hill, U. Kuruganti, and K. Englehart, "Motion normalized proportional control for improved pattern recognition-based myoelectric control," *IEEE Transactions on Neural Systems and Rehabilitation Engineering*, vol. 22, no. 1, pp. 149–157, 2014.

[113] B. Knorr, R. Hughes, and D. Sherrill, "Quantitative Measures of Functional Upper Limb Movement in Persons after Stroke," in *IEEE 2nd International EMBS Conference on Neural Engineering*, (Arlington), 2005.

[114] A. Phinyomark, C. Limsakul, and P. Phukpattaranont, "A novel feature extraction for robust EMG pattern recognition," *Journal of Computing*, vol. 1, no. 1, 2009.

[115] W. Xiao and Y. Lu, "Daily Human Physical Activity Recognition Based on Kernel Discriminant Analysis and Extreme Learning Machine," *Mathematical Problems in Engineering*, 2015.

[116] F. Bianchi, S. J. Redmond, M. R. Narayanan, S. Cerutti, B. G. Celler, and N. H. Lovell, "Falls event detection using triaxial accelerometry and barometric pressure measurement," *Proceedings of the 31st Annual International Conference of the IEEE Engineering in Medicine and Biology Society: Engineering the Future of Biomedicine, EMBC 2009*, pp. 6111–6114, 2009.

[117] S. Jeran, A. Steinbrecher, and T. Pischon, "Prediction of activity-related energy expenditure using accelerometer-derived physical activity under free-living conditions : a systematic review," *Nature Publishing Group*, no. December 2015, pp. 1187–1197, 2016.

[118] S. D. Bersch, D. Azzi, R. Khusainov, I. E. Achumba, and J. Ries, "Sensor data acquisition and processing parameters for human activity classification," *Sensors*, vol. 14, no. 3, pp. 4239–4270, 2014.

[119] R. A. Armstrong, "When to use the Bonferroni correction," *Ophthalmic & physiological optics*, vol. 34, pp. 502–508, 2014.

[120] R. Gravina, P. Alinia, H. Ghasemzadeh, and G. Fortino, "Multi-sensor fusion in body sensor networks: State-of-the-art and research challenges," *Information Fusion*, vol. 35, pp. 1339–1351, 2017.

[121] J. Chiang, Z. J. Wang, and M. J. McKeown, "A hidden Markov, multivariate autoregressive (HMM-mAR) network framework for analysis of surface EMG (sEMG) data," *IEEE Transactions on Signal Processing*, vol. 56, no. 8 II, pp. 4069–4081, 2008.

[122] B. A. Lock, K. Englehart, and B. Hudgins, "Real-time myoelectric control in a virtual environment to relate usability vs. accuracy," *Proceedings of the 2005 MyoElectric Controls/Powered Prosthetics Symposium*, no. May 2014, pp. 17–20, 2005.

[123] M. S. Totty and E. Wade, "Muscle Activation and Inertial Motion Data for Noninvasive Classification of Activities of Daily Living," *IEEE Transactions on Biomedical Engineering*, vol. 65, no. 5, pp. 1069–1076, 2018.

Appendix A

MATLAB Code

A.1 Filtering Data Code

```
function [filtsignal] = accfilter_trigno(rawsignal)
fs=1.481481e+002;  %ACC Sampling frequency: 1.481481e+002
%EMG Sampling frequency 1.925926e+003
filtsignal=rawsignal;
%4th order Butterworth band-pass filter with cut-off frequencies of
   0.2 and 15 Hz
[b,a]=butter(4,[0.2/(fs/2),15/(fs/2)]);
filtsignal = filtfilt(b,a,filtsignal);
%notch filterwear
wo = 60/(fs/2);
bw = wo/10;
[b,a] = iirnotch(wo,bw);
% fvtool(b,a);
filtsignal = filtfilt(b,a,filtsignal);
```

A.2 Processing ACC Data Code

```
numstart=0;
for i=numstart:24
%% assigning variables
subNum = i; % set as subject currently being processed
numReps = 3;

startTrial = 1;
numTrials = 38; % ONLY THE 38 trials, no need to normalize
timeOffsetRepStartT = zeros(numReps, numTrials);
timeOffsetRepEndT = zeros(numReps, numTrials);
offset = 26; % offset of trigno to get to real time move 2 seconds
   back, kuka to real time 28 seconds back, between is 26 seconds
[offsetK, offsetKTimezone] = getKOffset(subNum); % time offset of Kuka
   , specific for subject
offsetKTimezone = offsetKTimezone{1,1};

%% get time offsets
% run assign variables section first
fileName = strcat('D:\Data\S',int2str(subNum),'\Trigno\
   EMGRecTimestamps.xlsx');
[numT, txtT, rawT] = xlsread(fileName,'B1:C40');
timestampFileT = datetime(strcat(txtT(:,1),txtT(:,2)),'InputFormat','
   yyyy/MM/ddHH:mm:ss.SSSSSSS');
timestampFileT.TimeZone = offsetKTimezone; %-4:00 for S1, S2, -3:00 S3
   ,
timestampFileT.Format = 'yyyy/MM/dd HH:mm:ss.SSSSSSS';

%load KUKA timestamps
name1=['D:\Data\Processing\S',int2str(subNum),'\timesStartK.csv'];
```

```
25 name2=['D:\Data\Processing\S',int2str(subNum),'\timesEndK.csv'];
26 TimeStartKFilename = csvread(name1);
27 TimeEndKFilename = csvread(name2);
28
29 timeRepStartFromKfile = TimeStartKFilename;
30 timestampRepStartFromKfile = datetime(timeRepStartFromKfile,'
      ConvertFrom','epochtime');
31 timestampRepStartFromKfile.TimeZone = '+00:00';
32 timestampRepStartFromKfile.Format = 'yyyy/MM/dd HH:mm:ss.SSSSSSS';
33
34 timeRepEndFromKfile = TimeEndKFilename;
35 timestampRepEndFromKfile = datetime(timeRepEndFromKfile,'ConvertFrom',
      'epochtime');
36 timestampRepEndFromKfile.TimeZone = '+00:00';
37 timestampRepEndFromKfile.Format = 'yyyy/MM/dd HH:mm:ss.SSSSSSS';
38
39 for trial=startTrial:(startTrial - 1 + numTrials)
40         for rep=1:numReps
41             tempTimeOffsetStart = (timestampRepStartFromKfile(rep,
                  trial)-seconds(offsetK)) - (timestampFileT(trial));
42             timeOffsetRepStartT(rep,trial) = seconds(duration(
                  tempTimeOffsetStart));
43
44             tempTimeOffsetEnd = (timestampRepEndFromKfile(rep,trial)-
                  seconds(offsetK)) - (timestampFileT(trial));
45             timeOffsetRepEndT(rep,trial) = seconds(duration(
                  tempTimeOffsetEnd));
46         end
47 end
```

```
48
49 matOffsetRepStartTEMG = round(timeOffsetRepStartT./(1/1925.926)) + 1;
50 matOffsetRepEndTEMG = round(timeOffsetRepEndT./(1/1925.926)) + 1;
51
52 % get Trigno data, save as separate reps
53 % run assign variables section first
54 for trial=startTrial:(startTrial - 1 + numTrials)
55        for rep=1:numReps
56         if(matOffsetRepStartTEMG(rep,trial)>1) %if offset is not
              negative
57             fileName = strcat('D:\Taylor Stanbury\Data\S',int2str(
                 subNum),'\Trigno\EMG',int2str(trial),'.csv');
58             dataTrigno = csvread(fileName,453,0);
59          if(matOffsetRepStartTEMG(rep,trial)&& matOffsetRepEndTEMG(rep
              ,trial)<length(dataTrigno)) %if offset is valid
60             l=length(dataTrigno(:,2)); %save length of EMG data
61             % load accelerometer data
62             acc1x=accfilter_trigno(dataTrigno(:,4)); %filter
63             acc1x=acc1x(1:(l/13)); %trim
64             acc1x=interp(acc1x,13); %interpolate
65             acc1y=accfilter_trigno(dataTrigno(:,6)); %filter
66             acc1y=acc1y(1:(l/13)); %trim
67             acc1y=interp(acc1y,13); %interpolate
68             acc1z=accfilter_trigno(dataTrigno(:,8)); %filter
69             acc1z=acc1z(1:(l/13)); %trim
70             acc1z=interp(acc1z,13); %interpolate
71             acc2x=accfilter_trigno(dataTrigno(:,12)); %filter
72             acc2x=acc2x(1:(l/13)); %trim
73             acc2x=interp(acc2x,13); %interpolate
```

```
74          acc2y=accfilter_trigno(dataTrigno(:,14)); %filter
75          acc2y=acc2y(1:(l/13)); %trim
76          acc2y=interp(acc2y,13); %interpolate
77          acc2z=accfilter_trigno(dataTrigno(:,16)); %filter
78          acc2z=acc2z(1:(l/13)); %trim
79          acc2z=interp(acc2z,13); %interpolate
80          acc3x=accfilter_trigno(dataTrigno(:,20)); %filter
81          acc3x=acc3x(1:(l/13)); %trim
82          acc3x=interp(acc3x,13); %interpolate
83          acc3y=accfilter_trigno(dataTrigno(:,22)); %filter
84          acc3y=acc3y(1:(l/13)); %trim
85          acc3y=interp(acc3y,13); %interpolate
86          acc3z=accfilter_trigno(dataTrigno(:,24)); %filter
87          acc3z=acc3z(1:(l/13)); %trim
88          acc3z=interp(acc3z,13); %interpolate
89          acc4x=accfilter_trigno(dataTrigno(:,28)); %filter
90          acc4x=acc4x(1:(l/13)); %trim
91          acc4x=interp(acc4x,13); %interpolate
92          acc4y=accfilter_trigno(dataTrigno(:,30)); %filter
93          acc4y=acc4y(1:(l/13)); %trim
94          acc4y=interp(acc4y,13); %interpolate
95          acc4z=accfilter_trigno(dataTrigno(:,32)); %filter
96          acc4z=acc4z(1:(l/13)); %trim
97          acc4z=interp(acc4z,13); %interpolate
98          acc5x=accfilter_trigno(dataTrigno(:,36)); %filter
99          acc5x=acc5x(1:(l/13)); %trim
100         acc5x=interp(acc5x,13); %interpolate
101         acc5y=accfilter_trigno(dataTrigno(:,38)); %filter
102         acc5y=acc5y(1:(l/13)); %trim
```

```
103             acc5y=interp(acc5y,13); %interpolate
104             acc5z=accfilter_trigno(dataTrigno(:,40)); %filter
105             acc5z=acc5z(1:(l/13)); %trim
106             acc5z=interp(acc5z,13); %interpolate
107             acc6x=accfilter_trigno(dataTrigno(:,44)); %filter
108             acc6x=acc6x(1:(l/13)); %trim
109             acc6x=interp(acc6x,13); %interpolate
110             acc6y=accfilter_trigno(dataTrigno(:,46)); %filter
111             acc6y=acc6y(1:(l/13)); %trim
112             acc6y=interp(acc6y,13); %interpolate
113             acc6z=accfilter_trigno(dataTrigno(:,48)); %filter
114             acc6z=acc6z(1:(l/13)); %trim
115             acc6z=interp(acc6z,13); %interpolate
116             acc7x=accfilter_trigno(dataTrigno(:,52)); %filter
117             acc7x=acc7x(1:(l/13)); %trim
118             acc7x=interp(acc7x,13); %interpolate
119             acc7y=accfilter_trigno(dataTrigno(:,54)); %filter
120             acc7y=acc7y(1:(l/13)); %trim
121             acc7y=interp(acc7y,13); %interpolate
122             acc7z=accfilter_trigno(dataTrigno(:,56)); %filter
123             acc7z=acc7z(1:(l/13)); %trim
124             acc7z=interp(acc7z,13); %interpolate
125             acc8x=accfilter_trigno(dataTrigno(:,60)); %filter
126             acc8x=acc8x(1:(l/13)); %trim
127             acc8x=interp(acc8x,13); %interpolate
128             acc8y=accfilter_trigno(dataTrigno(:,62)); %filter
129             acc8y=acc8y(1:(l/13)); %trim
130             acc8y=interp(acc8y,13); %interpolate
131             acc8z=accfilter_trigno(dataTrigno(:,64)); %filter
```

```
132             acc8z=acc8z(1:(l/13)); %trim
133             acc8z=interp(acc8z,13); %interpolate
134             acc9x=accfilter_trigno(dataTrigno(:,68)); %filter
135             acc9x=acc9x(1:(l/13)); %trim
136             acc9x=interp(acc9x,13); %interpolate
137             acc9y=accfilter_trigno(dataTrigno(:,70)); %filter
138             acc9y=acc9y(1:(l/13)); %trim
139             acc9y=interp(acc9y,13); %interpolate
140             acc9z=accfilter_trigno(dataTrigno(:,72)); %filter
141             acc9z=acc9z(1:(l/13)); %trim
142             acc9z=interp(acc9z,13); %interpolate
143             acc10x=accfilter_trigno(dataTrigno(:,76)); %filter
144             acc10x=acc10x(1:(l/13)); %trim
145             acc10x=interp(acc10x,13); %interpolate
146             acc10y=accfilter_trigno(dataTrigno(:,78)); %filter
147             acc10y=acc10y(1:(l/13)); %trim
148             acc10y=interp(acc10y,13); %interpolate
149             acc10z=accfilter_trigno(dataTrigno(:,80)); %filter
150             acc10z=acc10z(1:(l/13)); %trim
151             acc10z=interp(acc10z,13); %interpolate
152             acc11x=accfilter_trigno(dataTrigno(:,84)); %filter
153             acc11x=acc11x(1:(l/13)); %trim
154             acc11x=interp(acc11x,13); %interpolate
155             acc11y=accfilter_trigno(dataTrigno(:,86)); %filter
156             acc11y=acc11y(1:(l/13)); %trim
157             acc11y=interp(acc11y,13); %interpolate
158             acc11z=accfilter_trigno(dataTrigno(:,88)); %filter
159             acc11z=acc11z(1:(l/13)); %trim
160             acc11z=interp(acc11z,13); %interpolate
```

```
161             acc12x=accfilter_trigno(dataTrigno(:,92)); %filter
162             acc12x=acc12x(1:(l/13)); %trim
163             acc12x=interp(acc12x,13); %interpolate
164             acc12y=accfilter_trigno(dataTrigno(:,94)); %filter
165             acc12y=acc12y(1:(l/13)); %trim
166             acc12y=interp(acc12y,13); %interpolate
167             acc12z=accfilter_trigno(dataTrigno(:,96)); %filter
168             acc12z=acc12z(1:(l/13)); %trim
169             acc12z=interp(acc12z,13); %interpolate
170             acc13x=accfilter_trigno(dataTrigno(:,100)); %filter
171             acc13x=acc13x(1:(l/13)); %trim
172             acc13x=interp(acc13x,13); %interpolate
173             acc13y=accfilter_trigno(dataTrigno(:,102)); %filter
174             acc13y=acc13y(1:(l/13)); %trim
175             acc13y=interp(acc13y,13); %interpolate
176             acc13z=accfilter_trigno(dataTrigno(:,104)); %filter
177             acc13z=acc13z(1:(l/13)); %trim
178             acc13z=interp(acc13z,13); %interpolate
179             acc14x=accfilter_trigno(dataTrigno(:,108)); %filter
180             acc14x=acc14x(1:(l/13)); %trim
181             acc14x=interp(acc14x,13); %interpolate
182             acc14y=accfilter_trigno(dataTrigno(:,110)); %filter
183             acc14y=acc14y(1:(l/13)); %trim
184             acc14y=interp(acc14y,13); %interpolate
185             acc14z=accfilter_trigno(dataTrigno(:,112)); %filter
186             acc14z=acc14z(1:(l/13)); %trim
187             acc14z=interp(acc14z,13); %interpolate
188             acc15x=accfilter_trigno(dataTrigno(:,116)); %filter
189             acc15x=acc15x(1:(l/13)); %trim
```

```
190             acc15x=interp(acc15x,13); %interpolate
191             acc15y=accfilter_trigno(dataTrigno(:,118)); %filter
192             acc15y=acc15y(1:(l/13)); %trim
193             acc15y=interp(acc15y,13); %interpolate
194             acc15z=accfilter_trigno(dataTrigno(:,120)); %filter
195             acc15z=acc15z(1:(l/13)); %trim
196             acc15z=interp(acc15z,13); %interpolate
197             acc16x=accfilter_trigno(dataTrigno(:,124)); %filter
198             acc16x=acc16x(1:(l/13)); %trim
199             acc16x=interp(acc16x,13); %interpolate
200             acc16y=accfilter_trigno(dataTrigno(:,126)); %filter
201             acc16y=acc16y(1:(l/13)); %trim
202             acc16y=interp(acc16y,13); %interpolate
203             acc16z=accfilter_trigno(dataTrigno(:,128)); %filter
204             acc16z=acc16z(1:(l/13)); %trim
205             acc16z=interp(acc16z,13); %interpolate
206             %get portion of Trigno data for specific rep, specific
                   trial
207             tempDataTrignoEMGRep = [
208             acc1x(matOffsetRepStartTEMG(rep,trial):matOffsetRepEndTEMG
                   (rep,trial)),...%BicepsBrachiiShortHead
209             acc1y(matOffsetRepStartTEMG(rep,trial):matOffsetRepEndTEMG
                   (rep,trial)),...
210             acc1z(matOffsetRepStartTEMG(rep,trial):matOffsetRepEndTEMG
                   (rep,trial)),...
211             acc2x(matOffsetRepStartTEMG(rep,trial):matOffsetRepEndTEMG
                   (rep,trial)),...%BicepsBrachiiLongHead
212             acc2y(matOffsetRepStartTEMG(rep,trial):matOffsetRepEndTEMG
                   (rep,trial)),...
```

```
213             acc2z(matOffsetRepStartTEMG(rep,trial):matOffsetRepEndTEMG
                    (rep,trial)),...
214             acc3x(matOffsetRepStartTEMG(rep,trial):matOffsetRepEndTEMG
                    (rep,trial)),...%Brachialis
215             acc3y(matOffsetRepStartTEMG(rep,trial):matOffsetRepEndTEMG
                    (rep,trial)),...
216             acc3z(matOffsetRepStartTEMG(rep,trial):matOffsetRepEndTEMG
                    (rep,trial)),...
217             acc4x(matOffsetRepStartTEMG(rep,trial):matOffsetRepEndTEMG
                    (rep,trial)),...%Brachioradialis
218             acc4y(matOffsetRepStartTEMG(rep,trial):matOffsetRepEndTEMG
                    (rep,trial)),...
219             acc4z(matOffsetRepStartTEMG(rep,trial):matOffsetRepEndTEMG
                    (rep,trial)),...
220             acc5x(matOffsetRepStartTEMG(rep,trial):matOffsetRepEndTEMG
                    (rep,trial)),...%TricepsBrachiiLongHead
221             acc5y(matOffsetRepStartTEMG(rep,trial):matOffsetRepEndTEMG
                    (rep,trial)),...
222             acc5z(matOffsetRepStartTEMG(rep,trial):matOffsetRepEndTEMG
                    (rep,trial)),...
223             acc6x(matOffsetRepStartTEMG(rep,trial):matOffsetRepEndTEMG
                    (rep,trial)),...%TricepsLateralHead
224             acc6y(matOffsetRepStartTEMG(rep,trial):matOffsetRepEndTEMG
                    (rep,trial)),...
225             acc6z(matOffsetRepStartTEMG(rep,trial):matOffsetRepEndTEMG
                    (rep,trial)),...
226             acc7x(matOffsetRepStartTEMG(rep,trial):matOffsetRepEndTEMG
                    (rep,trial)),...%TricepsMedialHead
227             acc7y(matOffsetRepStartTEMG(rep,trial):matOffsetRepEndTEMG
```

```
        (rep,trial)),...
228     acc7z(matOffsetRepStartTEMG(rep,trial):matOffsetRepEndTEMG
        (rep,trial)),...
229     acc8x(matOffsetRepStartTEMG(rep,trial):matOffsetRepEndTEMG
        (rep,trial)),...%PronatorTeres
230     acc8y(matOffsetRepStartTEMG(rep,trial):matOffsetRepEndTEMG
        (rep,trial)),...
231     acc8z(matOffsetRepStartTEMG(rep,trial):matOffsetRepEndTEMG
        (rep,trial)),...
232     acc9x(matOffsetRepStartTEMG(rep,trial):matOffsetRepEndTEMG
        (rep,trial)),...%Infraspinatus
233     acc9y(matOffsetRepStartTEMG(rep,trial):matOffsetRepEndTEMG
        (rep,trial)),...
234     acc9z(matOffsetRepStartTEMG(rep,trial):matOffsetRepEndTEMG
        (rep,trial)),...
235     acc10x(matOffsetRepStartTEMG(rep,trial):
        matOffsetRepEndTEMG(rep,trial)),...%AnteriorDeltoid
236     acc10y(matOffsetRepStartTEMG(rep,trial):
        matOffsetRepEndTEMG(rep,trial)),...
237     acc10z(matOffsetRepStartTEMG(rep,trial):
        matOffsetRepEndTEMG(rep,trial)),...
238     acc11x(matOffsetRepStartTEMG(rep,trial):
        matOffsetRepEndTEMG(rep,trial)),...%LateralDeltoid
239     acc11y(matOffsetRepStartTEMG(rep,trial):
        matOffsetRepEndTEMG(rep,trial)),...
240     acc11z(matOffsetRepStartTEMG(rep,trial):
        matOffsetRepEndTEMG(rep,trial)),...
241     acc12x(matOffsetRepStartTEMG(rep,trial):
        matOffsetRepEndTEMG(rep,trial)),...%PosteriorDeltoid
```

```
242             acc12y(matOffsetRepStartTEMG(rep,trial):
                   matOffsetRepEndTEMG(rep,trial)),...
243             acc12z(matOffsetRepStartTEMG(rep,trial):
                   matOffsetRepEndTEMG(rep,trial)),...
244             acc13x(matOffsetRepStartTEMG(rep,trial):
                   matOffsetRepEndTEMG(rep,trial)),...%ExtCarpiUlnaris
245             acc13y(matOffsetRepStartTEMG(rep,trial):
                   matOffsetRepEndTEMG(rep,trial)),...
246             acc13z(matOffsetRepStartTEMG(rep,trial):
                   matOffsetRepEndTEMG(rep,trial)),...
247             acc14x(matOffsetRepStartTEMG(rep,trial):
                   matOffsetRepEndTEMG(rep,trial)),...%ExtCarpiRadialis
248             acc14y(matOffsetRepStartTEMG(rep,trial):
                   matOffsetRepEndTEMG(rep,trial)),...
249             acc14z(matOffsetRepStartTEMG(rep,trial):
                   matOffsetRepEndTEMG(rep,trial)),...
250             acc15x(matOffsetRepStartTEMG(rep,trial):
                   matOffsetRepEndTEMG(rep,trial)),...%FlexCarpiUlnaris
251             acc15y(matOffsetRepStartTEMG(rep,trial):
                   matOffsetRepEndTEMG(rep,trial)),...
252             acc15z(matOffsetRepStartTEMG(rep,trial):
                   matOffsetRepEndTEMG(rep,trial)),...
253             acc16x(matOffsetRepStartTEMG(rep,trial):
                   matOffsetRepEndTEMG(rep,trial)),...%FlexCarpiRadialis
254             acc16y(matOffsetRepStartTEMG(rep,trial):
                   matOffsetRepEndTEMG(rep,trial)),...
255             acc16z(matOffsetRepStartTEMG(rep,trial):
                   matOffsetRepEndTEMG(rep,trial))];
256
```

```
257             saveTrignoEmgRepFilename = strcat('D:\S',int2str(subNum),'
                    \AccRepsFilt\ACCT',int2str(trial),'R',int2str(rep),'.
                    csv');
258             dlmwrite(saveTrignoEmgRepFilename,tempDataTrignoEMGRep,'
                    precision',16);
259           end
260           end
261         end
262 end
263 end
```

A.3 Average Feature Values

```
1  function [ ] = getAveFeats( sTrial,eTrial, openFold, saveFold,
       featName, subNumber)
2  %averages feature values of given feature for given subject
3  %   inputs are start and end trial, folder names, feature, subject
       number
4  %   average specified feature over trials for given subject, save csv
       file,
5  %   rows are trial, columns are muscle
6    clear ACCAveFeat ACCAveFeatAll
7     for trial = sTrial:eTrial
8         clear tempDataACCFeat ACCFeat
9         repsStartEnd = getSubReps(subNumber);
10        numRepsToAve = 0;
11        for rep=repsStartEnd(trial,1):repsStartEnd(trial,2)
12            numRepsToAve = numRepsToAve +1;
13            filename = strcat('D:\data\S',int2str(subNumber),'\',
```

```
                openFold,'\ACCFeatT',int2str(trial),'R',int2str(rep),
                featName,'.csv');
            tempDataACCFeat = csvread(filename);
            ACCFeat(numRepsToAve,:) = mean(tempDataACCFeat,1);
        end
        ACCAveFeat = mean(ACCFeat,1);
        ACCAveFeatAll(trial,:) = ACCAveFeat;
    end
    saveAveFeatAllTrial = strcat('D:\data\S',int2str(subNumber),'\',
       saveFold,'\',featName,'.csv');
    dlmwrite(saveAveFeatAllTrial,ACCAveFeatAll,'precision',16);
end
```

A.4 Classification Code

Adapted from [97].

```
numSubjects = 24;
numTrials = 38;

featNames = {'mav500_250'
    'ssc500_250'
    'wl500_250'
    'zc500_250'
    'rms500_250'
    'ar500_250'
    'ar500_250'
    'ar500_250'
    'ar500_250'
    'mnf500_250'
```

```
14      'mdf500_250'
15      'sma'
16      'svm'};
17
18  openFolders={'EMGMeanHudginsFeatOfNorm500_250'
19      'EMGMeanOskoeiFeatOfNorm500_250'
20      'EMGMeanFreqFeatOfNorm500_250'
21      'AccMeanFeat500_250'};
22
23  clear featuresAll
24  for subNum = 1:numSubjects
25      for feat = 1:size(featNames,1)
26          if feat < 5
27              folder = openFolders{1};
28          elseif feat < 10
29              folder = openFolders{2};
30          elseif feat < 12
31              folder = openFolders{3};
32          else
33              folder = openFolders{4};
34          end
35          filename = strcat('F:\Data\Processing\S',int2str(subNum),'\',
               folder,'\',featNames{feat},'.csv');
36          tempDataFeat = csvread(filename);
37
38          if feat < 6  % put in zeros for S7 M9, S9 M7 (unreliable data
               because of disconnecting sensor)
39              if subNum == 7
40                  tempDataFeat(:,9)=0;
```

```
41              elseif subNum == 9
42                  tempDataFeat(:,7)=0;
43              end
44
45              featuresAll(((subNum-1)*38 +1):subNum*38,((feat-1)*15 +1):
                    feat*15) = [tempDataFeat(:,1:7),tempDataFeat(:,9:16)];
46          elseif feat < 10
47              subFeat = feat - 5;
48              tempSubFeat(:,1:15) = [tempDataFeat(:,subFeat),
                    tempDataFeat(:,subFeat+4),tempDataFeat(:,subFeat+(2*4))
                    ,tempDataFeat(:,subFeat+(3*4)),tempDataFeat(:,subFeat
                    +(4*4)),tempDataFeat(:,subFeat+(5*4)),tempDataFeat(:,
                    subFeat+(6*4)),tempDataFeat(:,subFeat+(8*4)),
                    tempDataFeat(:,subFeat+(9*4)),tempDataFeat(:,subFeat
                    +(10*4)),tempDataFeat(:,subFeat+(11*4)),tempDataFeat(:,
                    subFeat+(12*4)),tempDataFeat(:,subFeat+(13*4)),
                    tempDataFeat(:,subFeat+(14*4)),tempDataFeat(:,subFeat
                    +(15*4))];
49
50              % put in zeros for S7 M9, S9 M7 (unreliable data because
                    of disconnecting sensor)
51              if subNum == 7
52                  tempSubFeat(:,8)=0; % data muscle 8 was already
                        excluded
53              elseif subNum == 9
54                  tempSubFeat(:,7)=0;
55              end
56
```

```
57              featuresAll(((subNum-1)*38 +1):subNum*38,((feat-1)*15 +1):
                    feat*15) = tempSubFeat;
58
59          else
60              % put in zeros for S7 M9, S9 M7 (unreliable data because
                    of disconnecting sensor)
61              if subNum == 7
62                  tempDataFeat(:,9)=0;
63              elseif subNum == 9
64                  tempDataFeat(:,7)=0;
65              end
66
67              featuresAll(((subNum-1)*38 +1):subNum*38,((feat-1)*15 +1):
                    feat*15) = [tempDataFeat(:,1:7),tempDataFeat(:,9:16)];
68          end
69      end
70  end
71  trial_labels = [
72  1,1,1,1,4,0,1,1,1
73  2,1,2,1,2,0,1,1,2
74  3,1,3,1,3,0,1,1,2
75  4,0,1,1,4,0,1,1,1
76  5,0,2,1,2,0,1,1,2
77  6,0,3,1,3,0,1,1,2
78  7,2,1,1,4,0,1,2,1
79  8,2,2,1,2,0,1,2,2
80  9,2,3,1,3,0,1,2,2
81  10,3,1,1,4,0,1,3,1
82  11,3,2,1,2,0,1,3,2
```

```
12,3,3,1,3,0,1,3,2
13,1,1,2,4,1,2,1,1
14,1,1,3,4,2,2,1,1
15,1,2,2,2,1,2,1,2
16,1,2,3,2,2,2,1,2
17,1,3,2,4,1,2,1,2
18,1,3,3,4,2,2,1,2
19,2,1,2,4,1,2,2,1
20,2,1,3,4,2,2,2,1
21,2,2,2,2,1,2,2,2
22,2,2,3,2,2,2,2,2
23,2,3,2,3,1,2,2,2
24,2,3,3,3,2,2,2,2
25,3,1,2,4,1,2,3,1
26,3,1,3,4,2,2,3,1
27,3,2,2,2,1,2,3,2
28,3,2,3,2,2,2,3,2
29,3,3,2,3,1,2,3,2
30,3,3,3,3,2,2,3,2
31,4,4,2,1,1,2,4,2
32,4,4,3,1,2,2,4,2
33,4,2,2,2,1,2,4,2
34,4,2,3,2,2,2,4,2
35,5,4,2,1,1,2,5,2
36,5,4,3,1,2,2,5,2
37,5,2,2,2,1,2,5,2
38,5,2,3,2,2,2,5,2
];

```

```
112 trials = [
113 1,1,0,0,0,1,1,0
114 2,1,0,0,0,1,1,0
115 3,1,0,0,0,1,1,0
116 4,0,0,0,0,1,0,0
117 5,0,0,0,0,1,0,0
118 6,0,0,0,0,1,0,0
119 7,1,0,0,0,1,0,0
120 8,1,0,0,0,1,0,0
121 9,1,0,0,0,1,0,0
122 10,1,0,0,0,1,0,0
123 11,1,0,0,0,1,0,0
124 12,1,0,0,0,1,0,0
125 13,1,0,0,1,1,1,0
126 14,1,0,0,1,1,1,0
127 15,1,0,0,1,1,1,0
128 16,1,0,0,1,1,1,0
129 17,1,0,0,1,1,1,0
130 18,1,0,0,1,1,1,1
131 19,1,0,0,1,1,0,0
132 20,1,0,0,1,1,0,0
133 21,1,0,0,1,1,0,0
134 22,1,0,0,1,1,0,0
135 23,1,0,0,1,1,0,0
136 24,1,0,0,1,1,0,0
137 25,1,0,0,1,1,0,0
138 26,1,0,0,1,1,0,0
139 27,1,0,0,1,1,0,0
140 28,1,0,0,1,1,0,0
```

```
29,1,0,0,1,1,0,0
30,1,0,0,1,1,0,0
31,0,1,0,0,1,0,1
32,0,1,0,0,1,0,1
33,0,1,0,0,1,0,1
34,0,1,0,0,1,0,1
35,0,0,1,0,1,0,1
36,0,0,1,0,1,0,1
37,0,0,1,0,1,0,1
38,0,0,1,0,1,0,1
];

muscles_feats_factors = zeros(13,15); %feature,muscle

clear predictors_v1
column = 1;
for feature = 1:13
    for muscle = 1:15
        if muscles_feats_factors(feature,muscle) == 1
            predictors_v1(:,column) =  featuresAll(:,(feature-1)*15 +
               muscle);
            column = column+1;
        end
    end

end

model = 'TEns'; % 'LDA' 'SVM'
trialSet=2; %trials, select flexion extension, ADLs etc
```

```
169 labelSet =7; %variable
170
171 clear predictors_v2
172 for sub = 1:numSubjects
173     trialCount = 1;
174     for trialCounter = 1:38
175         if trials(trialCounter,trialSet) == 1
176             predictors_v2((sub-1)*sum(trials(:,trialSet))+trialCount
                    ,:)= predictors_v1((sub-1)*38 + trialCounter,:);
177             trialCount = trialCount +1;
178         end
179     end
180 end
181
182 clear labels_v1
183 for sub = 1:numSubjects
184     trialCount = 1;
185     for trialCounter = 1:38
186         if trials(trialCounter,trialSet) == 1
187             labels_v1((sub-1)*sum(trials(:,trialSet))+trialCount,:)=
                    trial_labels(trialCounter,labelSet);
188             trialCount = trialCount +1;
189         end
190     end
191 end
192
193 clear predictors_full labels_full train_predictors train_labels
    test_predictors test_labels labels_mdl
194 clear Mdl
```

```
195 match= 0;
196 for sub = 1:numSubjects
197     sub
198     trials_per_sub = sum(trials(:,trialSet)); %select trials per
            subject(from 38trials)
199     predictors_full = predictors_v2;
200     labels_full = labels_v1;
201
202     train_predictors = predictors_full;
203     train_predictors((sub-1)*trials_per_sub+1:sub*trials_per_sub,:)
            =[];
204     train_labels = labels_v1;
205     train_labels((sub-1)*trials_per_sub+1:sub*trials_per_sub,:)=[];
206
207     test_predictors = predictors_full((sub-1)*trials_per_sub+1:sub*
            trials_per_sub,:); %predictors by trials
208     test_labels = labels_full((sub-1)*trials_per_sub+1:sub*
            trials_per_sub,1);
209
210     switch model
211         case 'LDA'
212             Mdl = fitcdiscr(train_predictors,train_labels);
213         case 'SVM'
214             Mdl = fitcecoc(train_predictors,train_labels);
215        case 'TEns' %decision tree ensemble using AdaBoost Multiclass
216            Mdl = fitensemble(train_predictors,train_labels,'AdaBoostM1
                ',300,'Tree'); %100 200MORE %M2 for multiclass
217
218     end
```

```
219
220     labels_mdl(:,sub) = predict(Mdl,test_predictors);
221
222    labels_result(sub) = sum(eq(labels_mdl(:,sub), test_labels)); %
          verify if predicted and test labels match
223
224     match= match+labels_result(sub);%alex test
225
226     A(sub) = labels_result(sub)/trials_per_sub; %accurate predicted
          labels divided by trials
227
228     cp = cvpartition(train_labels,'KFold',10);
229     cvmdl = crossval(Mdl,'CVPartition',cp);
230     CVErr(sub) = kfoldLoss(cvmdl);
231     a_cv(sub) = 1 - CVErr(sub);
232 end
233 Accuracy = (match/size(predictors_full,1))*100; %accuracy = match/N
       *100
```

Appendix B

Statistical Analysis Tables

B.1 Consolidated statistical analysis of ACC signals during flexion–extension motions

Muscle	Flexion–Extension		Level Mean			Std Error			Significance		
	Feature	Factor	L1	L2	L3	L1	L2	L3	L 1-2	L 1-3	L 2-3
BBS	SMA	Position	0.054	0.068	0.073	0.003	0.004	0.004	<0.001	<0.001	0.006
		Force	0.046	0.073	0.077	0.003	0.005	0.004	<0.001	<0.001	0.501
		Velocity	0.048	0.066	0.083	0.003	0.004	0.005	<0.001	<0.001	<0.001
	SMV	Position	0.036	0.046	0.049	0.002	0.003	0.003	<0.001	<0.001	0.006
		Force	0.031	0.048	0.052	0.002	0.003	0.003	<0.001	<0.001	0.296
		Velocity	0.032	0.044	0.055	0.002	0.003	0.003	<0.001	<0.001	<0.001
BBL	SMA	Position	0.054	0.067	0.072	0.003	0.004	0.004	<0.001	<0.001	0.003
		Force	0.045	0.070	0.077	0.002	0.004	0.005	<0.001	<0.001	0.157
		Velocity	0.047	0.064	0.081	0.003	0.004	0.005	<0.001	<0.001	<0.001
	SMV	Position	0.036	0.045	0.048	0.002	0.002	0.003	<0.001	<0.001	0.003
		Force	0.030	0.047	0.052	0.002	0.003	0.003	<0.001	<0.001	0.191
		Velocity	0.032	0.043	0.055	0.002	0.003	0.003	<0.001	<0.001	<0.001
BRA	SMA	Position	0.057	0.071	0.075	0.003	0.004	0.004	<0.001	<0.001	0.003
		Force	0.048	0.073	0.082	0.003	0.004	0.005	<0.001	<0.001	0.01

		Velocity	0.048	0.067	0.088	0.003	0.004	0.005	<0.001	<0.001	<0.001
	SMV	Position	0.038	0.047	0.050	0.002	0.002	0.003	0.001	0.001	0.001
		Force	0.032	0.049	0.054	0.002	0.003	0.003	<0.001	<0.001	0.037
		Velocity	0.032	0.045	0.058	0.002	0.003	0.003	<0.001	<0.001	<0.001
BRD	SMA	Position	0.064	0.078	0.079	0.003	0.004	0.004	<0.001	<0.001	0.908
		Force	0.059	0.080	0.082	0.003	0.005	0.005	<0.001	<0.001	0.990
		Velocity	0.044	0.073	0.103	0.003	0.004	0.006	<0.001	<0.001	<0.001
	SMV	Position	0.043	0.052	0.053	0.002	0.003	0.003	<0.001	<0.001	0.871
		Force	0.040	0.054	0.054	0.002	0.003	0.003	<0.001	<0.001	1.000
		Velocity	0.030	0.049	0.069	0.002	0.003	0.004	<0.001	<0.001	<0.001
TRILO	SMA	Position	0.055	0.074	0.071	0.003	0.004	0.004	0.002	0.002	0.001
		Force	0.046	0.071	0.083	0.003	0.004	0.005	<0.001	<0.001	0.002
		Velocity	0.054	0.065	0.081	0.003	0.004	0.005	0.001	<0.001	<0.001
	SMV	Position	0.037	0.050	0.048	0.002	0.003	0.003	<0.001	<0.001	0.367
		Force	0.031	0.048	0.056	0.002	0.003	0.003	<0.001	<0.001	0.001
		Velocity	0.037	0.044	0.055	0.002	0.003	0.003	0.002	<0.001	<0.001
TRILAT	SMA	Position	0.054	0.069	0.066	0.003	0.004	0.004	<0.001	<0.001	0.005
		Force	0.044	0.069	0.076	0.002	0.004	0.004	<0.001	<0.001	0.052
		Velocity	0.048	0.062	0.079	0.003	0.004	0.004	<0.001	<0.001	<0.001
	SMV	Position	0.036	0.047	0.044	0.002	0.003	0.003	<0.001	<0.001	0.004
		Force	0.030	0.046	0.052	0.002	0.003	0.003	<0.001	<0.001	0.033
		Velocity	0.033	0.041	0.053	0.002	0.003	0.003	<0.001	<0.001	<0.001
TRIM	SMA	Position	0.053	0.071	0.068	0.004	0.005	0.005	<0.001	<0.001	0.104
		Force	0.046	0.068	0.079	0.003	0.005	0.006	<0.001	<0.001	<0.011
		Velocity	0.050	0.063	0.079	0.004	0.005	0.006	0.001	<0.001	<0.001
	SMV	Position	0.035	0.047	0.045	0.003	0.003	0.003	<0.001	<0.001	0.114
		Force	0.030	0.045	0.052	0.002	0.004	0.004	<0.001	<0.001	0.012
		Velocity	0.033	0.042	0.053	0.003	0.003	0.004	0.001	<0.001	<0.001
ISPI	SMA	Position	0.026	0.035	0.035	0.002	0.003	0.003	<0.001	<0.001	0.925

		Force	0.028	0.031	0.037	0.002	0.003	0.003	0.012	<0.001	<0.001
		Velocity	0.025	0.032	0.040	0.002	0.003	0.003	<0.001	<0.001	<0.001
	SMV	Position	0.017	0.023	0.024	0.002	0.002	0.002	<0.001	<0.001	0.990
		Force	0.019	0.021	0.024	0.002	0.002	0.002	0.011	<0.001	0.001
		Velocity	0.016	0.021	0.026	0.001	0.002	0.002	<0.001	<0.001	<0.001
AD	SMA	Position	0.04	0.05	0.054	0.003	0.003	0.003	0.001	0.001	0.002
		Force	0.035	0.053	0.057	0.002	0.004	0.004	<0.001	<0.001	<0.001
		Velocity	0.037	0.048	0.060	0.003	0.003	0.004	<0.001	<0.001	<0.001
	SMV	Position	0.027	0.033	0.036	0.002	0.002	0.002	<0.001	<0.001	<0.001
		Force	0.024	0.035	0.037	0.002	0.002	0.002	0.011	<0.001	0.507
		Velocity	0.024	0.032	0.040	0.002	0.002	0.003	<0.001	<0.001	<0.001
LD	SMA	Position	0.042	0.054	0.055	0.003	0.004	0.004	<0.001	<0.001	0.990
		Force	0.037	0.054	0.061	0.003	0.004	0.004	<0.001	<0.001	0.043
		Velocity	0.038	0.050	0.063	0.003	0.004	0.004	<0.001	<0.001	<0.001
	SMV	Position	0.028	0.037	0.037	0.002	0.002	0.002	<0.001	<0.001	0.783
		Force	0.025	0.036	0.041	0.002	0.003	0.003	<0.001	<0.001	0.783
		Velocity	0.026	0.034	0.042	0.002	0.002	0.003	<0.001	<0.001	<0.001
PD	SMA	Position	0.038	0.050	0.050	0.003	0.003	0.003	<0.001	<0.001	1.000
		Force	0.036	0.047	0.056	0.002	0.003	0.004	<0.001	<0.001	0.001
		Velocity	0.036	0.046	0.057	0.002	0.003	0.004	<0.001	<0.001	<0.001
	SMV	Position	0.026	0.034	0.034	0.002	0.002	0.002	<0.001	<0.001	1.000
		Force	0.024	0.031	0.037	0.002	0.002	0.003	<0.001	<0.001	0.001
		Velocity	0.024	0.031	0.038	0.002	0.002	0.003	<0.001	<0.001	<0.001
ECU	SMA	Position	0.064	0.077	0.076	0.003	0.004	0.004	<0.001	<0.001	0.990
		Force	0.062	0.078	0.077	0.003	0.005	0.004	<0.001	0.001	0.990
		Velocity	0.045	0.069	0.104	0.003	0.004	0.005	<0.001	<0.001	<0.001
	SMV	Position	0.042	0.052	0.051	0.002	0.003	0.003	<0.001	<0.001	0.990
		Force	0.041	0.052	0.052	0.002	0.003	0.003	<0.001	<0.001	0.990

		Velocity	0.030	0.046	0.069	0.002	0.003	0.004	<0.001	<0.001	<0.001
ECR	SMA	Position	0.064	0.076	0.076	0.003	0.004	0.004	<0.001	<0.001	1.000
		Force	0.060	0.077	0.078	0.003	0.005	0.005	<0.001	<0.001	0.990
		Velocity	0.043	0.070	0.103	0.004	0.005	0.005	<0.001	<0.001	<0.001
	SMV	Position	0.042	0.051	0.051	0.002	0.003	0.003	<0.001	<0.001	1.000
		Force	0.040	0.052	0.052	0.002	0.003	0.003	<0.001	<0.001	1.000
		Velocity	0.029	0.046	0.069	0.002	0.003	0.004	<0.001	<0.001	<0.001
FCU	SMA	Position	0.062	0.077	0.077	0.003	0.004	0.004	<0.001	<0.001	1.000
		Force	0.062	0.078	0.076	0.003	0.005	0.005	<0.001	0.002	0.990
		Velocity	0.046	0.068	0.102	0.003	0.004	0.005	<0.001	<0.001	<0.001
	SMV	Position	0.042	0.052	0.052	0.002	0.003	0.003	<0.001	<0.001	1.000
		Force	0.042	0.053	0.051	0.002	0.003	0.003	<0.001	0.002	0.990
		Velocity	0.032	0.046	0.069	0.002	0.003	0.004	<0.001	<0.001	<0.001
FCR	SMA	Position	0.062	0.074	0.076	0.003	0.004	0.004	<0.001	<0.001	0.485
		Force	0.060	0.076	0.075	0.003	0.005	0.005	<0.001	<0.001	1.00
		Velocity	0.044	0.068	0.099	0.003	0.004	0.005	<0.001	<0.001	<0.001
	SMV	Position	0.041	0.050	0.051	0.002	0.003	0.003	<0.001	<0.001	0.701
		Force	0.040	0.051	0.050	0.002	0.003	0.003	<0.001	0.001	0.990
		Velocity	0.029	0.046	0.067	0.002	0.003	0.003	<0.001	<0.001	<0.001

B.2 Consolidated statistical analysis of ACC signals during ADL 1 motions

Muscle	ADL 1		Level Mean		Std Error		Significance
	Feature	Factor	L1	L2	L1	L2	L 1-2
BBS	SMA	Force	0.156	0.162	0.009	0.009	0.367
		Velocity	0.112	0.206	0.008	0.012	<0.001
	SMV	Force	0.102	0.106	0.006	0.006	0.323
		Velocity	0.074	0.134	0.005	0.008	<0.001

BBL	SMA	Force	0.147	0.154	0.009	0.010	0.274
		Velocity	0.107	0.195	0.008	0.013	<0.001
	SMV	Force	0.097	0.102	0.006	0.007	0.273
		Velocity	0.071	0.129	0.005	0.009	<0.001
BRA	SMA	Force	0.149	0.157	0.008	0.010	0.237
		Velocity	0.112	0.194	0.007	0.012	<0.001
	SMV	Force	0.098	0.103	0.006	0.006	0.244
		Velocity	0.074	0.128	0.005	0.008	<0.001
BRD	SMA	Force	0.143	0.149	0.008	0.010	0.432
		Velocity	0.109	0.183	0.008	0.011	<0.001
	SMV	Force	0.097	0.10	0.005	0.007	0.472
		Velocity	0.073	0.124	0.005	0.008	<0.001
TRILO	SMA	Force	0.143	0.152	0.009	0.009	0.184
		Velocity	0.106	0.189	0.008	0.012	<0.001
	SMV	Force	0.096	0.101	0.006	0.006	0.181
		Velocity	0.071	0.127	0.005	0.008	<0.001
TRILAT	SMA	Force	0.141	0.148	0.008	0.009	0.337
		Velocity	0.103	0.187	0.007	0.012	<0.001
	SMV	Force	0.093	0.097	0.006	0.006	0.301
		Velocity	0.068	0.122	0.005	0.008	<0.001
TRIM	SMA	Force	0.136	0.145	0.007	0.007	0.209
		Velocity	0.102	0.179	0.008	0.014	<0.001
	SMV	Force	0.089	0.095	0.007	0.007	0.181
		Velocity	0.067	0.117	0.005	0.009	<0.001
ISPI	SMA	Force	0.044	0.051	0.004	0.004	0.004
		Velocity	0.039	0.056	0.004	0.004	<0.001
	SMV	Force	0.029	0.034	0.002	0.003	0.004
		Velocity	0.026	0.037	0.002	0.003	<0.001
AD	SMA	Force	0.116	0.122	0.007	0.009	0.308

		Velocity	0.082	0.155	0.006	0.011	<0.001
	SMV	Force	0.077	0.081	0.005	0.006	0.309
		Velocity	0.055	0.104	0.004	0.007	<0.001
LD	SMA	Force	0.108	0.115	0.008	0.008	0.237
		Velocity	0.080	0.143	0.006	0.011	<0.001
	SMV	Force	0.072	0.077	0.005	0.006	0.178
		Velocity	0.053	0.096	0.004	0.007	<0.001
PD	SMA	Force	0.093	0.099	0.006	0.007	0.180
		Velocity	0.068	0.124	0.005	0.010	<0.001
	SMV	Force	0.062	0.066	0.004	0.005	0.178
		Velocity	0.046	0.082	0.003	0.006	<0.001
ECU	SMA	Force	0.149	0.155	0.008	0.010	0.392
		Velocity	0.106	0.198	0.008	0.010	<0.001
	SMV	Force	0.098	0.103	0.005	0.007	0.390
		Velocity	0.071	0.130	0.005	0.008	<0.001
ECR	SMA	Force	0.146	0.149	0.008	0.009	0.631
		Velocity	0.106	0.188	0.007	0.012	<0.001
	SMV	Force	0.099	0.101	0.005	0.007	0.584
		Velocity	0.072	0.129	0.005	0.008	<0.001
FCU	SMA	Force	0.144	0.152	0.008	0.010	0.296
		Velocity	0.104	0.191	0.007	0.012	<0.001
	SMV	Force	0.099	0.103	0.005	0.007	0.338
		Velocity	0.071	0.131	0.005	0.008	<0.001
FCR	SMA	Force	0.088	0.093	0.006	0.005	0.265
		Velocity	0.065	0.116	0.005	0.008	<0.001
	SMV	Force	0.059	0.062	0.004	0.004	0.357
		Velocity	0.043	0.078	0.003	0.005	<0.001

B.3 Consolidated statistical analysis of ACC signals during ADL 2 motions

Muscle	ADL 2		Level Mean		Std Error		Significance
	Feature	Factor	L1	L2	L1	L2	L 1-2
BBS	SMA	Force	0.076	0.08	0.005	0.005	0.343
		Velocity	0.061	0.095	0.005	0.006	<0.001
	SMV	Force	0.050	0.053	0.003	0.003	0.282
		Velocity	0.040	0.062	0.003	0.004	<0.001
BBL	SMA	Force	0.069	0.073	0.005	0.005	0.333
		Velocity	0.057	0.085	0.004	0.004	<0.001
	SMV	Force	0.046	0.048	0.003	0.003	0.336
		Velocity	0.038	0.056	0.003	0.003	<0.001
BRA	SMA	Force	0.075	0.081	0.005	0.005	0.194
		Velocity	0.062	0.094	0.004	0.006	<0.001
	SMV	Force	0.062	0.066	0.004	0.004	0.249
		Velocity	0.041	0.062	0.003	0.004	<0.001
BRD	SMA	Force	0.094	0.1	0.007	0.006	0.176
		Velocity	0.072	0.122	0.005	0.009	<0.001
	SMV	Force	0.062	0.066	0.004	0.004	0.207
		Velocity	0.048	0.081	0.004	0.006	<0.001
TRILO	SMA	Force	0.072	0.076	0.006	0.005	0.332
		Velocity	0.059	0.088	0.005	0.005	<0.001
	SMV	Force	0.047	0.050	0.004	0.003	0.296
		Velocity	0.039	0.058	0.004	0.004	<0.001
TRILAT	SMA	Force	0.069	0.073	0.005	0.005	0.276
		Velocity	0.056	0.086	0.005	0.005	<0.001
	SMV	Force	0.046	0.048	0.003	0.003	0.29
		Velocity	0.037	0.057	0.003	0.004	<0.001

TRIM	SMA	Force	0.068	0.072	0.006	0.006	0.374
		Velocity	0.055	0.085	0.005	0.005	<0.001
	SMV	Force	0.045	0.047	0.004	0.004	0.415
		Velocity	0.037	0.056	0.003	0.005	<0.001
ISPI	SMA	Force	0.034	0.036	0.006	0.006	0.350
		Velocity	0.029	0.041	0.003	0.004	<0.001
	SMV	Force	0.023	0.025	0.002	0.002	0.375
		Velocity	0.02	0.028	0.002	0.003	<0.001
AD	SMA	Force	0.054	0.057	0.004	0.004	0.276
		Velocity	0.044	0.067	0.004	0.004	<0.001
	SMV	Force	0.036	0.038	0.003	0.003	0.283
		Velocity	0.029	0.044	0.003	0.003	<0.001
LD	SMA	Force	0.052	0.055	0.004	0.004	0.258
		Velocity	0.043	0.064	0.004	0.005	<0.001
	SMV	Force	0.035	0.037	0.003	0.003	0.226
		Velocity	0.029	0.043	0.003	0.003	<0.001
PD	SMA	Force	0.048	0.051	0.004	0.004	0.230
		Velocity	0.040	0.059	0.004	0.004	<0.001
	SMV	Force	0.032	0.034	0.003	0.003	0.234
		Velocity	0.027	0.040	0.003	0.003	<0.001
ECU	SMA	Force	0.090	0.094	0.007	0.006	0.447
		Velocity	0.065	0.119	0.005	0.009	<0.001
	SMV	Force	0.060	0.062	0.004	0.004	0.431
		Velocity	0.043	0.079	0.003	0.006	<0.001
ECR	SMA	Force	0.089	0.092	0.006	0.005	0.515
		Velocity	0.066	0.115	0.005	0.007	<0.001
	SMV	Force	0.059	0.061	0.004	0.004	0.451
		Velocity	0.044	0.077	0.003	0.005	<0.001
FCU	SMA	Force	0.092	0.097	0.006	0.006	0.282

		Velocity	0.066	0.122	0.005	0.009	<0.001
	SMV	Force	0.061	0.064	0.004	0.004	0.304
		Velocity	0.044	0.081	0.003	0.006	<0.001
FCR	SMA	Force	0.088	0.093	0.006	0.005	0.265
		Velocity	0.065	0.116	0.005	0.005	<0.001
	SMV	Force	0.059	0.062	0.004	0.004	0.357
		Velocity	0.043	0.078	0.003	0.005	<0.001

Appendix C

Ethics Permissions and Approvals

C.1 Ethics Approval

Western Research

Date: 31 August 2020

To: Ana Luisa Trejos

Project ID: 109356

Study Title: Dynamic Calibration of EMG Signals

Application Type: Continuing Ethics Review (CER) Form

Review Type: Delegated

REB Meeting Date: October 2 2020

Date Approval Issued: 31/Aug/2020

REB Approval Expiry Date: 25/Aug/2021

LAPSE IN APPROVAL - 26/Aug/2020 - 31/Aug/2020

Dear Ana Luisa Trejos,

The Western University Research Ethics Board has reviewed the application. This study, including all currently approved documents, has been re-approved until the expiry date noted above.

REB members involved in the research project do not participate in the review, discussion or decision.

Western University REB operates in compliance with, and is constituted in accordance with, the requirements of the TriCouncil Policy Statement: Ethical Conduct for Research Involving Humans (TCPS 2); the International Conference on Harmonisation Good Clinical Practice Consolidated Guideline (ICH GCP); Part C, Division 5 of the Food and Drug Regulations; Part 4 of the Natural Health Products Regulations; Part 3 of the Medical Devices Regulations and the provisions of the Ontario Personal Health Information Protection Act (PHIPA 2004) and its applicable regulations. The REB is registered with the U.S. Department of Health & Human Services under the IRB registration number IRB 00000940.

Please do not hesitate to contact us if you have any questions.

Sincerely,

The Office of Human Research Ethics

Note: This correspondence includes an electronic signature (validation and approval via an online system that is compliant with all regulations).

VITA

Name:	José Alejandro López Molina
Post-secondary Education and Degrees:	Autonomous University of Aguascalientes Aguascalientes, Mexico 2012–2016 B.E., Biomedical Engineering
Honours and Awards:	CONACYT Scholarship-Master's Program
Related Work Experience:	Teaching Assistant *ECE 2240 – Electrical Laboratory* The University of Western Ontario 2019